Time Modulated Linear Arrays

Yizhen Tong

A Thesis Submitted to the University of Sheffield for the Degree of Doctor of Philosophy in Electronic and Electrical Engineering

The University of Sheffield

August 2013

In memory of my grandfather

Dedication

I would like to dedicate this thesis to my God, my parents, as well as my wife Alisa Zhang and her parents.

Have I not commanded you? Be strong and courageous. Do not be frightened, and do not be dismayed, for the Lord your God is with you wherever you go.

Joshua 1:9

The lord is my shepherd and I shall not want. Even though I walk through the valley of shadow of death, I will fear no evil, for you are with me; your rod and your staff, they comfort me.

Psalm 23: 1 and 4

Abstract

With increasing demand for modern technology in the communication systems, antenna arrays have attracted much interest in the areas of radio broadcasting, space communication, weather forecasting, radar and imaging. Antenna array with controlled low or ultralow sidelobes is of particular importance and it has been an on-going challenge for the antenna design engineers in the past few decades, as it requires a high dynamic range of excitations. Another desired feature provided by an antenna array is the ability to perform electronic beam steering and adaptive interference suppression.

These benefits can be achieved with the use of complicated feed network and expensive phase shifters and it can only found in the specialised military systems. Therefore this has motivated the research into the development of a simple and low cost system for the commercial applications.

The idea of time modulation was proposed to produce an antenna pattern with controlled low or ultralow sidelobe level, as well as achieving real time electronic beam scanning without the use of phase shifter. However, a fundamental problem of this concept is the generation of undesired harmonics or sidebands as they waste power.

This dissertation mainly focuses on the two important characteristics - pattern synthesis and multiple beams scanning of the time modulated antenna array and evaluates its potential application in the communication system.

The first main chapter of this research proposes two novel approaches to successfully suppress the sideband radiation and hence improve radiation efficiency. The following part of the study introduces a way of combining the electronic beam scanning with the controlled low or ultralow sidelobes and applies the null steering technique in the time modulated linear array. The final but most important attribute of this thesis is to propose the concept of time redundancy and evaluate the potential feasibility of employing smart antenna technology into the time modulated antenna array for a two-channel communication system, where individual adaptive beamforming can be performed to extract desired signal while suppressing interference from separate sources independently.

Acknowledgement

First of all I want to take this opportunity to express my genuine gratitude to my supervisor, as well as my mentor Dr. Alan Tennant, for guiding me into the appealing and fascinating world of wireless communication, particularly the antenna array system. I am grateful that he has not only provided me with excellent supervision, invaluable guidance and assistance, but also much patience, encouragement and all around support throughout the period of my study. It is my great honour to work with him and he is the most kind and wonderful supervisor that I have ever seen in my life.

A special thank to Dr. Jonathan Rigelsford and Dr. Lee Ford, for their valuable time of organising training sessions of the RF measurements and antenna radiation patterns. Thank you also to the Mr. Steve Marsden, the Staffs of Mechanical Workshop and all staffs in the Communication group for their technical assistance and support.

I am very grateful to all of my colleagues in the office, especially Dr. Huilai Liu, Dr. Lestor Low, Dr. Shaozhen Zhu, Dr. Hyung-Joo Lee, Dr. Luyi Liu, Dr. Lei Yu, Dr. Lei Zhang, Dr. Qiang Bai, Dr. Bo Peng, Mr. Hongzhe Shi and Mr. Yang Wang, for their practical and insightful discussion, constructive advice and outstanding assistance to the contribution of this thesis, as well as making me have a pleasant time at the university.

Much acknowledgement should be given to my beloved family members in China, for their consistent understanding, patience and faith in me during the past few years, especially my wife Alisa, thanks for her time of pray and providing me with encouragement, understanding and love all the time, I would not able to finish the thesis without their support, I love you all.

Finally, I wish to express my deepest gratitude to the almighty God, thanks for his everlasting love and continuous guidance in the course of my programme, and giving me the patience, strength, wisdom and great joy to complete this dissertation.

List of Acronyms

AF   Array Factor

AWGN   Additive White Gaussian Noise

BER   Bit Error Rate

BPSK   Binary Phase Shift Keying

DE   Differential Evolution Algorithm

DOA   Direction of Arrival

GA   Genetic Algorithm

LMS   Least Mean Square

PSO   Particle Swarm Optimization Algorithm

RF   Radio Frequency

SPST   Single Pole Single Throw

SPMT   Single Pole Multiple Throw

SIR   Signal to Interference Ratio

SINR   Signal Interference to Noise Ratio

SNR   Signal to Noise Ratio

SOI   Signal of Interest

SNOI   Signal Not of Interest

TM   Time Modulation

TMAA   Time Modulated Antenna Array

TMLA   Time Modulated Linear Array

List of Symbols

dB	Decibel
f	Frequency
λ	Wavelength
d	Element spacing between each array element
D	Directivity
$\mathbf{U_{max}}$	Maximum radiation intensity
$\mathbf{P_{rad}}$	Total radiated power
$\mathbf{P_{SB}}$	Sidebands power
$\mathbf{\eta_{SB}}$	Sidebands power in percentage
k	Propagation constant
m	Harmonic number
N	Number of elements
$\mathbf{\tau_{on}}$	Switching on time
$\mathbf{\tau_{off}}$	Switching off time
$\mathbf{T_o}$	Modulating time period
ω	Angular frequency
$\mathbf{\omega_o}$	Modulating angular frequency

Re Real part

Im Imaginary part

A_n Complex static weights

B_n Fixed complex static weights

a_{mn} Complex Fourier Series coefficients

w Array weights

Γ Reflection coefficient

υ Transmission coefficient

$d(t)$ Desired signals

$e(t)$ Errors signals

$y(t)$ Array output

$p(x)$ Gaussian probability distribution function

P_{BPSK} Probability of error or Bit Error Rate in BPSK signal

Contents

List of Publications

Journal Papers

[1] **Y. Tong and A. Tennant**, "Simultaneous control of sidelobe level and harmonic beam steering in time-modulated linear arrays," *IET Electronics Letters*, vol. 46, no. 3, pp. 200-202, February, 2010.

[2] **Y. Tong and A. Tennant**, "Reduced sideband levels in time-modulated arrays using half-power sub-arraying techniques", *IEEE Transactions on Antenna and Propagation*, vol. 59, no. 1, pp. 301-303, January, 2011.

[3] **Y. Tong and A. Tennant**, "Sideband level suppression in Time-modulated linear arrays using modified switching sequences and fixed bandwidth elements," *IET Electronics Letters*, vol. 48, no. 1, pp. 10-11, January, 2012.

[4] **Y. Tong and A. Tennant**, "A Two-Channel Time Modulated Linear Array With Adaptive Beamforming", *IEEE Transactions on Antenna and Propagation*, vol. 60, no. 1, pp.141-147, January, 2012.

Conference Papers

[1] **Y. Tong and A. Tennant**, "Beam Steering Techniques for Time-Switched Arrays", *IEEE Loughborough Antennas and Propagation Conference, Loughborough*, UK, pp. 233 – 236, 12 – 13 November, 2009.

[2] **Y. Tong and A. Tennant**, "Reduced sideband level in time-modulated linear array", *2010 Proceedings of the Fourth European Conference on Antennas and Propagation (EuCAP)*, Barcelona, Spain, pp. 1- 4, 12 – 16 April, 2010.

[3] **Y. Tong and A. Tennant**, "A Wireless Communication System Based on a Time-Modulated Array", *IEEE Loughborough Antennas and Propagation Conference, Loughborough*, UK, pp. 245 – 248, 8 – 9 November, 2010.

[4] **Y. Tong and A. Tennant**, "Low Sidelobe Level Harmonic Beam Steering Using Time-Modulated Linear Arrays", *IEEE Loughborough Antennas and Propagation Conference, Loughborough*, UK, pp. 249 – 252, 8 – 9 November, 2010.

[5] **Y. Tong and A. Tennant**, "Beam Steering and Adaptive Nulling of Low Sidelobe Level Time-Modulated Linear Array", *2011 Proceedings of the Fifth European Conference on Antennas and Propagation (EuCAP)*, Rome, Italy, pp. 948 - 951, 11 – 15 April, 2011.

[6] **Y. Tong and A. Tennant**, "Sidebands suppression in time-modulated linear arrays using directive element patterns", *IEEE Loughborough Antennas and Propagation Conference, Loughborough*, UK, pp. 1-4, 14 – 15 November, 2011.

[7] **Y. Tong and A. Tennant**, "Sideband Suppression in Time-Modulated Arrays Using Fixed Bandwidth Elements", *2012 Proceedings of the Sixth European Conference on Antennas and Propagation (EuCAP)*, Prague, Czech Republic, pp. 1 - 5, 26 – 30 March, 2012.

Chapter 1 Introduction

1.1 Overview

With the expansion of modern electronics technology, wireless communication has grown significantly over the past couple of decades. Antennas, which are used to transmit and receive radio waves in the free space, are gradually becoming one of the most essential components in the system. Therefore, antenna design has been studied extensively and widely used in various areas, ranging from mobile phones to medical treatment [1].

In certain cases, multiple antennas are integrated into an array to meet the requirement of long distance communication. An antenna array has the advantage of providing higher radiating directivity and gain over a single element, so it can be exploited to perform beam scanning or beam forming [2]. In order to achieve a better system performance, conventional antenna arrays should have a narrower beamwidth, lower sidelobe levels and fast tracking ability. These challenges have placed a rigorous requirement in the design of the feed network and tolerance control. However, as the introduction of an additional dimension – time into the antenna design, an antenna array is able to generate a radiation pattern with controlled sidelobe level and achieve real time electronic beam scanning simply through switching on-off array elements in a predetermined way. In fact, this technique, we called the Time Modulated Antenna Array (TMAA), provides more freedoms for the designer, since the parameter – time

can be controlled electronically, thus making it easier and more accurate to implement in reality.

The following section will briefly review the research background of time modulated antenna arrays and then discuss the difficulties and constraints that are present in the practical design. The outline of the thesis will be given at the end of this chapter.

1.2 Research Background

Some system specifications may demand an antenna array with a radiation pattern of sidelobe level less than -30dB to suppress signals from interfering receivers. Therefore, the most critical part will be how to calculate the excitation amplitudes and phase delays of each array element accurately in accord with the system requirements. The conventional technique is to apply a predefined current distributions to each array element so that the radiation pattern of the array will have a low or ultralow sidelobe levels (normally less than -30dB). Dolph-Chebyshev and Taylor [3-4] are the two most well-known distributions to be used among the various techniques.

With the advent of powerful modern computers, a variety of optimisation algorithms like Genetic Algorithm [5-8], Simulated Annealing [9-10] and Particle Swarm Optimisation [11-12] have found their broad applications in the pattern synthesis of the antenna array. However, the challenge is how we put these theoretical concepts into practice. For example, a 16 element uniform linear antenna array with -40dB sidelobe Taylor distribution requires the amplitude of excitation current from the

outer most to the central array element with a dynamic range from 0.122 to 1.0 [3].

For a -50dB sidelobe Taylor distribution, the dynamic range of excitation currents is

from 0.065 to 1.0 [4]. Therefore, the system requires a complicated hardware design

and a delicate error control, which are difficult to achieve from a practical point of

view.

A breakthrough occurred in the late 1950s, when Shanks and Bickmore [13]

originally proposed a theoretical model of a time modulated array antenna to produce

a beam pattern with low or ultralow sidelobe level. The physical system configuration

is that each radiating slot was individually controlled by ferrite switches which are

driven by a square wave generator. As a result, this new approach generates many

independent beam patterns corresponding to the multiples of the modulating

frequency. Moreover, the detecting system consists of a ranger of proper filters to

extract the desired output. The introduction of a fourth dimension - time can be used

to relax the design constraints and improve system performance. In 1961, Shanks

extended the analysis of time modulation into the real time electronic scanning

function [14], which has demonstrated a theoretical possibility of providing multiple

beams scanning at various angles.

In 1962, Kummer et al. [15] at the US Hughes Aircraft Company published a paper

on time modulation antenna array. An eight-element slot antenna array was designed

to obtain radiation patterns with ultralow sidelobes. Two sets of results were

considered in [15]: one is to reduce an initial static pattern with -30dB sidelobes to

-40dB through a time sequence, the other is to decrease an initial static pattern with

-13dB sidelobes directly to -39.5dB by a different time sequence. In [15], the experimental array was consisted of a corporate fed eight-element slot radiator which was connected to a diode switch. The time of switch was controlled by a programmed external circuitry. The second test assumes the antenna array with a uniform amplitude distribution, thus variable attenuators were not necessary to be used. Measurement results have shown that the sidelobe level of an array at the fundamental frequency can be reduced to nearly -40dB by periodically modulating the array element. Therefore, this proposed technique has great advantages over the conventional method, since the additional parameter - time is easier and more accurate to control instead of mechanical adjustment.

In 1962, Kummer et al. [16] performed another experiment to validate the theoretical idea of electronic beam scanning developed by Shanks [14], where a five-element and a twenty- element receiving array system were built. The measured array patterns illustrate that multiple beams scanning at different angles were achieved through periodically modulating the array elements on and off without the use of phase shifters. Two decades later, Lewis and Evins[17] introduced a new analytical way for reducing unwanted echoes that enter the radar. By means of Doppler Effect, the antenna array's phase centre can be shifted out of radar receiver's detecting range and the sidelobe of unwanted signal is suppressed. From another point of view, Lewis's proposed technique can be regarded as by periodically switching on and off the array elements. In 1985, Bickmore summarised the fundamental principles of time

modulated antenna array or TMAA based on the studies from many researchers [13-17] in the Microwave Scanning Antennas [18].

Generally, the utilisation of time in antenna design not only produces beam pattern with controlled sidelobes levels but can also perform simultaneous beam scanning operation. However, due to limitation of switching speed of RF switches and computing resources, these drawbacks restricted the historical development of time modulated antenna array in the old days.

As a result of rapid growth of electronic technology in recent years, the switching speed of the RF switches has improved significantly (modulation frequency must be much lower than the carrier frequency for the purpose of simple filtering process). In 2002, Yang [19] was the first to propose the application of an optimisation algorithm into the time modulated antenna array (TMMA) in an effort to suppress undesired harmonic levels introduced by time modulation process. In the following year, Yang [20] published another paper with the same optimisation technique for the power patterns synthesis in the TMMA.

In 2004, Yang [21] derived a mathematical formula for calculating the directivity and gain in various types of TMAAs and then validated the concept with experimental results. In addition, Tennant [22] applied the concept of time modulation to a two-element direction finding antenna array in 2007. As this topic became more and more popular in the recent years, many researchers started to explore other applications of TMAAs [23-30].

From the above discussion, it can be concluded that TMAA has two important characteristics: 1) sidelobe suppression - it relaxes the design constraint of the conventional system and has a great flexibility in the control of excitation currents; 2) electronic beam scanning - it generates multiple beams pointing at different angels without the use of phase shifters and dramatically reduces the system costs. However, the time modulation process produces harmonics or sidebands at the multiples of modulation frequency, this drawback results in parts of the power is redistributed into sidebands and it lowers the radiation directivity and gain at the fundamental frequency. In recent years, considerable efforts have been made to reduce undesired harmonic radiations of TMAAs using various types of optimisation algorithm, but so far no successful attempt has been made to combine the features of pattern synthesis and electronic beam scanning together. Furthermore, there has not got any exploration into the applications of TMAA in communication systems.

1.3 Original Contributions

The main innovations in thesis are summarised below:

a) Unlike using conventional optimisation algorithms to suppress sideband levels in the TMMAs, this thesis proposed an innovative and straightforward approach based on reducing the static element weights of the outer elements of a linear array using simple 3dB power dividers [31].

b) Proposed a new technique that utilises the fixed bandwidth of the radiating elements of the array to act as band-pass filters to suppress the out of band harmonics generated by the time-modulation process. The approach is combined with a new element switching sequence to reduce sideband radiation. This proposed method does not require the use of complicated optimisation procedures to generate the switching sequences and is applicable to synthesise beam patterns with any controlled sidelobe level [32].

c) Proposed a novel approach to combine electronic beam steering and low sidelobe levels operation in the time-modulated linear arrays. This technique relies solely on controlling the switching time of each array elements and does not require the use of additional amplitude weighting function [33].

d) Proposed a new technique based on a signal processing algorithm - Linearly Constrained Minimum Variance (LCMV) to form a deep null to attenuate interfering signals from degrading the system performance. This method does not need to use any phase shifters.

e) Proposed the concept of time redundancy – an efficient topology in terms of time utilization of the array elements.

f)   Proposed an innovative way to apply adaptive beamforming in the TMMAs

without the use of phase shifter and extend the analysis into a two-channel

commutation system in the presence of interference and noise [34].

1.4 Thesis Outline

This research work mainly focuses on the study of the two significant characteristics

of the TMMA: pattern synthesis and electronic beam scanning and evaluates the

feasibility of applying the proposed techniques in the communication system. The

thesis is outlined as follows:

In Chapter 2 three types of general antenna arrays: Binomial, Dolphy-Chebyshev and

Taylor arrays are described first to serve as a basic foundation. The underlying

principles of time modulated antenna array are introduced in the later chapter. The

core idea behind four-dimensional antenna array or TMAA is to periodically

switching on and off of the array element in a pre-described way through an external

programmed circuit, so that antenna radiation patterns can be controlled electronically.

This novel technique resolves the practical design concerns of using complicated feed

network, but at the price of sacrificing radiation efficiency at the fundamental

frequency.

In Chapter 3 two innovative techniques are proposed to minimise the power radiated

into harmonic patterns or sidebands. The first approach introduces a new array

topology based on simple 3dB power dividing networks, while the other utilises the

fixed bandwidth of a radiating element to act as bandpass filter to reduce the sideband levels of the harmonics.

Conventional phased antenna arrays have the capability of performing real electronic beam scanning by using costly phase shifter. Chapter 4 first investigates a way to realise multiple beam scanning without the use of phase shifters through periodically delaying the switching on time of each array element in a progressive manner. In the real application, some strong interfering signals may degrade the system performance, even though the beam pattern can produce a sidelobe level of -30dB. Hence the second part of this chapter implements Linearly Constrained Minimum Variance algorithms to steer a deep a null towards the direction of the interference while maintaining the main beam response.

From Chapter 4, we know that electronic beam scanning can be achieved through controlling each array element in a pre-defined manner, but this switching time scheme is inefficient. Chapter 5 proposed a new topology to exploit the redundancy of the conventional time sequence and apply the concept in a simple two-channel time modulated antenna array.

Having gained a solid understanding of the two important features of the TMAA, we will start to investigate its application in the wireless communication system. In the beginning of Chapter 6, it derives the mathematical model of the beamforming in a time modulated antenna array. Following that it exploits the feasibility of applying smart antenna technology of the time modulated antenna array in the wireless

communication system. Switched beam system of TMAA is first examined under various scenarios and then adaptive beamforming system of TMMA for a single output is introduced in the latter chapter. Finally analysis is extended to a two-channel adaptive beamforming scenario basing on the concept of time redundancy.

A summary of the research works undertaken along with the achievements made so far during the period of study are presented in Chapter 7. Later in the chapter we will discuss some possible works of the research can be done in the future.

References

[1] C. A. Balanis, Antenna Theory: analysis and design, Chapter 1: Antennas, 3rd edition, Wiley Interscience, 2005, pp. 1-24.

[2] L. C. Godara, "Applications of Antenna Arrays to Mobile Communications, Part I: Performance Improvement, Feasibility, and System Considerations", Proceedings of the IEEE, vol. 85, no. 7, July 1997, pp. 1031-1060.

[3] C. L. Dolph, "A Current Distribution for Broadside Arrays Which Optimizes the Relationship between Beam Width and Side-Lobe Level", Proceedings of the IRE, vol. 34, no. 6, June, 1946, pp. 335-348.

[4] T. T. Taylor, "Design of Line-Source Antennas for Narrow Beamwidth and Low Sidelobes", Transactions of the IRE Professional Group on Antennas and Propagation, vol. 3, no.1, January 1955, pp.16–28.

[5] K. K. Yan and Y. Lu, "Sidelobe reduction in array-pattern synthesis using genetic algorithm", IEEE Transactions on Antennas and Propagation, vol. 45, no. 7, July 1997, page 1117-1121.

[6] V. R. Mongon, W. A. Artuzi Jr., and J. R. Descardeci, "Tilt angle and side-lobe level control of microwave antenna arrays", Microwave Opt. Tech. Lett., vol. 33, no. 1, Apr. 2002, pp. 12-14.

[7] F. J. Ares, J. A. Rodriguez, E. Villanueva, and S. R. Rengarajan, "Genetic algorithms in the design and optimization of antenna array patterns", IEEE Transactions on Antennas and Propagation, vol. 47, no. 3, Mar. 1999, pp. 506-510.

[8] R. L. Haupt, "Thinned arrays using genetic algorithm", IEEE Transactions on Antennas and Propagation, vol. 42, no. 7, July 1994, pp. 993-999.

[9] V. Murino, A. Trucco and C. S. Regazzoni. "Synthesis of unequally spaced arrays by simulated annealing", IEEE Transactions on Signal Processing, vol. 44, no. 1, Jan.1996, pp. 119-122.

[10] G. Cardone, G. Cincotti and M. Pappalardo, "Design of wide-band arrays for low side-lobe level beam patterns by simulated annealing", IEEE Trans. Ultrason. Ferroelectr. Freq. Control., Aug. 2002, vol. 49, no. 8, pp. 1050-1059.

[11] M. M. Khodier and C. G. Christodoulou, "Linear array geometry synthesis with minimum sidelobe level and null control using particle swarm optimization", IEEE Trans. Antennas Propagat., Aug. 2005, vol. 53, no. 8, pp. 2674-2679.

[12] P. J. Bevelacqua and C. A. Balanis, "Minimum sidelobe levels for linear arrays", IEEE Trans. Antennas Propagat., Dec.2007, vol. 55, no. 12, pp. 3442-3449.

[13] H. E. Shanks and R. W. Bickmore, "Four-dimensional electromagnetic radiators", Canadian Journal of Physics, vol. 37, 1959, pp. 263-275.

[14] H. E. Shanks, "A new technique for electronic scanning," IEEE Transactions on Antennas and Propagation, vol. 9, no. 2, Mar., 1961, pp. 162–166.

[15] W. H. Kummer, A. T. Villeneuve, T. S. Fong, and F. G. Terrio, "Ultra-low sidelobes from time-modulated arrays", IEEE Transactions on Antenna and Propagation, vol. 11, no. 6, Nov., 1963, pp. 633-639.

[16] W. H. Kummer, A. T. Villeneuve and F. G. Terrio, "New antenna idea - Scanning without Phase Shifters," Electronics, vol. 36, March, 1963, pp. 27-32.

[17] B. L. Lewis and J. B. Evins, "A new technique for reducing radar response to signals entering antenna sidelobes", IEEE Transactions on Antennas and Propagation, vol. 31, no. 6, Nov.1983, pp. 993-996.

[18] R. W. Bickmore, Microwave Scanning Antennas, Chapter 4 - Time Versus Space in Antenna Theory, R. C. Hansen, vol. Ill, Peninsula Publishing, 1985.

[19] S. Yang, Y. B. Gan and A. Qing, "Sideband suppression in time-modulated linear arrays by the differential evolution algorithm", IEEE Antennas Wireless Propagation Letters, vol. 1, no. 1, 2002, pp. 173-175.

[20] S. Yang, Y. B. Gan and P. K. Tan, "A new technique for power-pattern synthesis in time-modulated linear arrays", IEEE Antenna Wireless Propagation Letters, vol. 2, no. 1, 2003, pp. 285-287.

[21] S. Yang, Y. B. Gan and P. K. Tan, "Evaluation of directivity and gain for time modulated linear antenna arrays", Microwave Opt. Technology Letter, vol. 42, no. 2, July 2004, pp.167-171.

[22] A. Tennant and B. Chambers, "A two-element time-modulated array with direction-finding properties", IEEE Antennas Wireless Propagation Letter, vol. 6, 2007, pp. 64–65.

[23] J. Fondevila, J. C. Bregains, F. Ares and E. Moreno, "Optimising uniformly excited linear arrays through time modulation", IEEE Antennas Wireless Propagation Letters, vol. 3, 2004, pp. 298-300.

[24] Y. Chen, S. Yang, G. Li and Z. Nie, "Adaptive nulling in time-modulated antenna arrays," 8th International Symposium on Antennas, Propagation and EM Theory, Kunming, China, Nov., 2008, pp. 713-716.

[25] J. C. Bregains, J. Fondevila, G. Franceschetti, and F. Ares, "Signal radiation and power losses of time-modulated arrays", IEEE Transactions on Antenna and Propagation, vol. 56, no. 6, June, 2008, pp. 1799-1804.

[26] L. Manica, P. Rocca, L. Poli, A. Massa, "Almost time-independent performance in time-modulated linear arrays," IEEE Antennas Wireless Propagation Letter, vol. 8, Aug., 2009, pp. 843-846.

[27] A. Basak, S. Pal, S. Das, A. Abraham and V. Snasel, "A modified Invasive Weed Optimization algorithm for time-modulated linear antenna array synthesis," IEEE Congress on Evolutionary Computation, July, 2010, pp. 1- 8.

[28] X. Huang, S. Yang, G. Li and Z. Nie, "A novel application for sum-difference pattern detection of signal direction using time-modulated linear arrays," International Symposium on Intelligent Signal Processing and Communication Systems, Chengdu, China, Dec., 2010, pp. 1-4.

[29] M. D'Urso, A. Iacono, A. Iodice and G. Franceschetti, "Optimizing uniformly excited time-modulated linear arrays", 2011 Proceedings of the Fifth European Conference on Antennas and Propagation (EuCAP), Rome, Italy,11 – 15 April, 2011, pp. 2082 – 2086.

[30] E. Aksoy and E. Afacan, "Calculation of Sideband Power Radiation in Time Modulated Arrays with Asymmetrically Positioned Pulses", IEEE Antennas and Wireless Propagation Letters, vol. 11, 2012, pp 133-136.

[31] Y. Tong and A. Tennant, "Reduced sideband levels in time-modulated arrays using half-power sub-arraying techniques", IEEE Transactions on Antenna and Propagation, vol. 59, no. 1, pp. 301-303, January, 2011.

[32] Y. Tong and A. Tennant, "Sideband level suppression in Time-modulated linear arrays using modified switching sequences and fixed bandwidth elements," IET Electronics Letters, vol. 48, no. 1, pp. 10-11, January, 2012.

[33] Y. Tong and A. Tennant, "Simultaneous control of sidelobe level and harmonic beam steering in time-modulated linear arrays," IET Electronics Letters, vol. 46, no. 3, pp. 200-202, February, 2010.

[34] Y. Tong and A. Tennant, "A Two-Channel Time Modulated Linear Array With Adaptive Beamforming", IEEE Transactions on Antenna and Propagation, vol. 60, no. 1, pp.141-147, January, 2012.

Chapter 2 Theoretical Background and Literature Review

2.1 Introduction

Nowadays, due to the widespread applications of the wireless communication systems, antenna design plays a more significant role in our daily life. A single-element antenna has a broad radiation pattern but with low directivity, in some applications which may demand much higher radiation energy in one certain direction to take account of long distance power loss.

An easy and convenient way to achieve a high directive radiation pattern is by grouping a number of radiators with different current excitations and phase delays together in a certain arrangement. This new configuration is regarded as an antenna array, so it can not only lead to greater gain but can also provide a important feature - scanning the main beam in any desired direction.

In this chapter, fundamental concepts of uniform and non-uniform amplitude linear arrays as well as the idea of beamforming technique will be presented. Subsequently, the theoretical background and methodology of time modulated linear arrays will be discussed later in the chapter.

2.2 Conventional Antenna Array

An antenna array is normally classified into three main categories: linear arrays, planar arrays and circular arrays [1-3] in terms of the elements geometrical arrangements. As a result of simple structure and a better physical demonstration, we only consider the case of linear array in the following thesis.

2.2.1 Uniform Amplitude and Spacing Linear Array

A uniform linear array is defined as an array of identical elements along a line with equal amplitudes and spacing [4], the generalised form of N-element antenna linear array is shown in Fig 2.1.
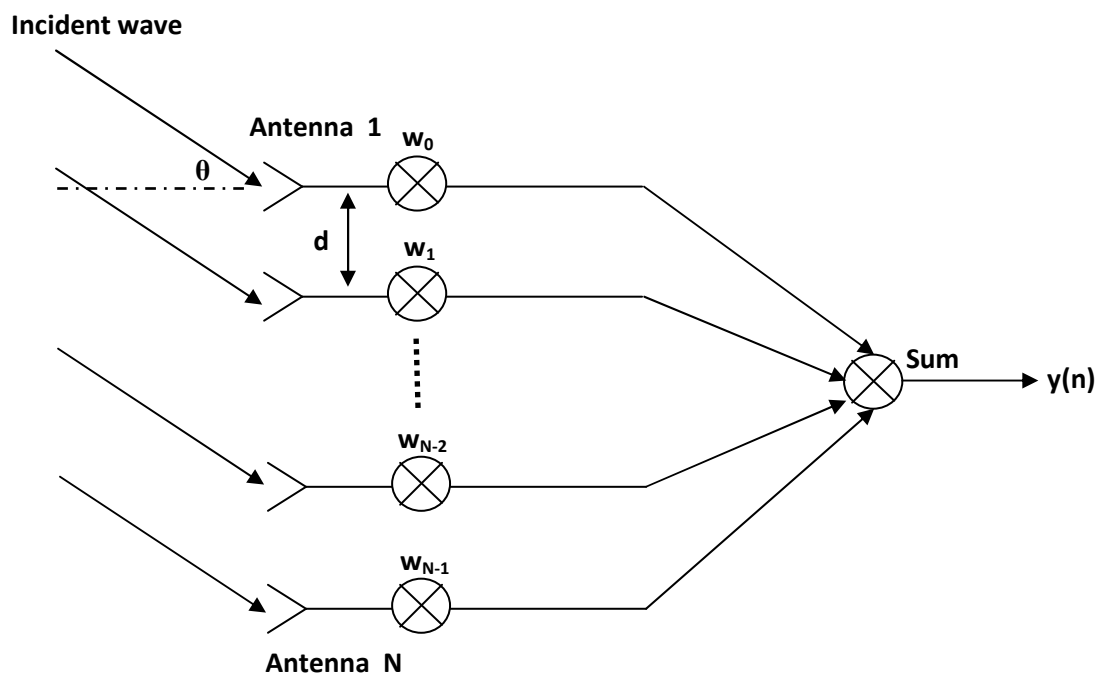

Fig 2.1. Uniform amplitude N-element linear array with equal spacing.

Let us assume each element is an isotropic source and the element spacing is a half wavelength. An incident wave impinges on the linear array, the total radiation pattern or array factor (AF) can be obtained by the summation of each individual element as given by [4]:

$$AF(\theta) = 1 + e^{j(kd\sin\theta+\beta)} + e^{j2(kd\sin\theta+\beta)} + \dots + e^{j(N-1)(kd\sin\theta+\beta)} = \sum_{n=0}^{N-1} e^{jn(kd\sin\theta+\beta)} \qquad (2.1)$$

where $k = 2\pi/\lambda$ is the propagation constant, β is the progressive phase delay between each array element and θ is the incident angle against the horizontal line. By multiplying both sides by $e^{j\Psi}$, the normalised array factor can be reduced to:

$$AF(\theta) = \frac{\sin(\frac{N}{2}\psi)}{N\sin(\frac{1}{2}\psi)} \qquad (2.2)$$

where $\Psi = kd\sin\theta + \beta$, the corresponding radiation pattern of the above equation is:
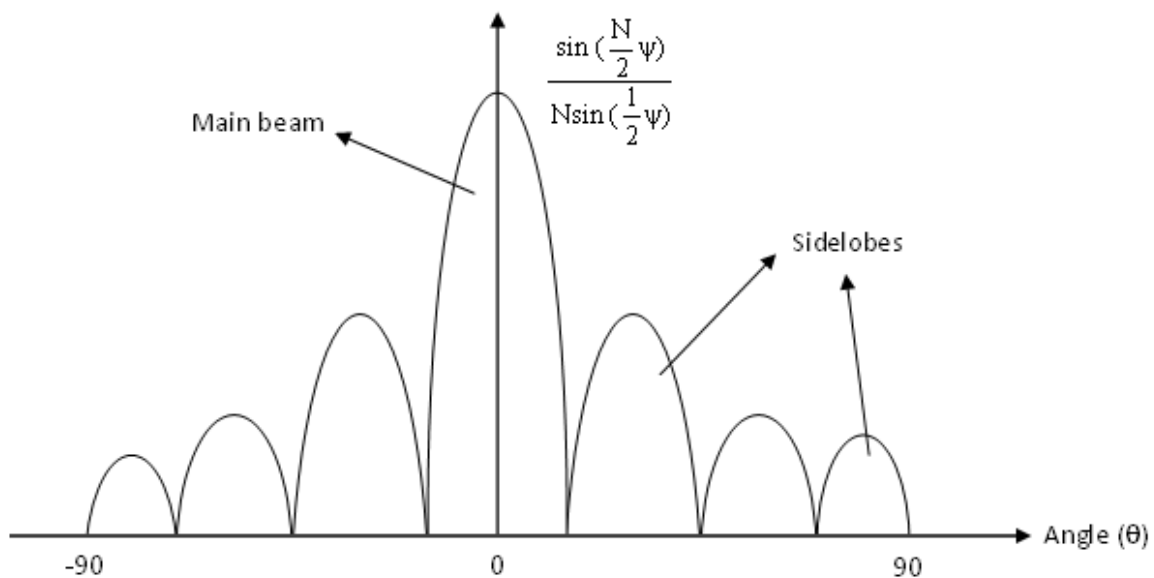

Fig 2.2. Corresponding radiation pattern of equation (2.2).

The maximum value occurs when $\Psi = 0$ or $\sin\theta = 0$ if all elements are in phase ($\beta = 0$), so $\theta = \pm n\pi$, where n is an integer. From Fig 2.2 it can be seen that maximum radiation is controlled by the phase delay β between each element. Some applications may require the antenna array to scan the main beam in any desired direction, particularly in a radar system. In order to accomplish this objective, the progressive phase delay is derived as: $\psi = kd\sin\theta + \beta$

= 0, thus β = -kdsinθ. In this thesis, all the numerical examples are simulated using MATLAB software, which is a matrix computing software designed for numerical modelling. An example of 10-element uniform amplitude phased array at an incident angle θ = 30$^{°}$ is shown in Fig 2.3:
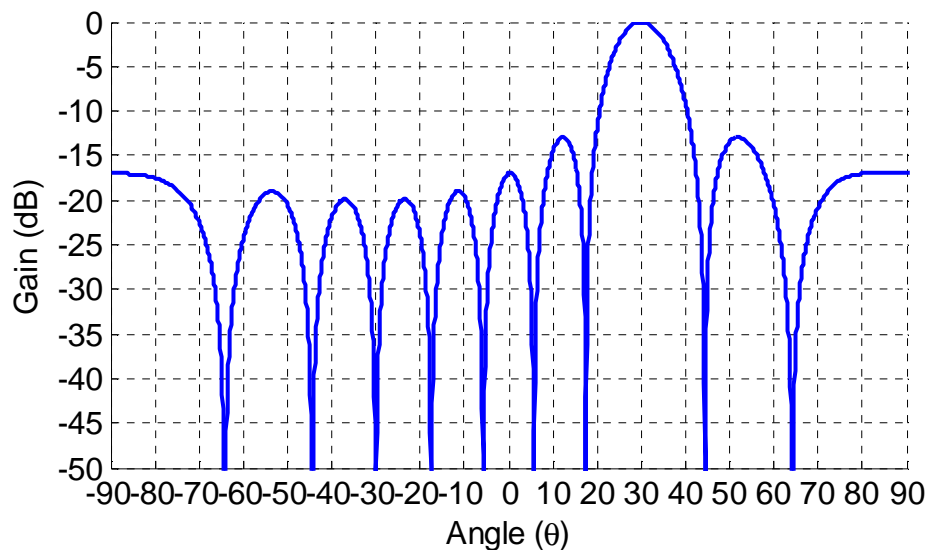

Fig 2.3. 10-element uniform amplitude phased array at θ = 30$^{°}$.

Therefore, a phased array is determined by the phase delay between each array element. This general concept lays the foundation for time modulated antenna array which will be discussed later.

2.2.2 Non-uniform Amplitude and uniform Spacing Linear Array

The uniform amplitude and spacing linear arrays was discussed in the previous section and the results has illustrated that a linear array with equal amplitude excitation produces a radiation pattern with a maximum sidelobe level of -13.5dB below the main beam. However, some systems may demand a much lower sidelobe levels -30dB or -40dB below the main beam to reduce the level of interference. In this section, we will examine three different types

of well-known antenna arrays: binomial, Dolph-Chebyshev and Taylor distribution. The array factor of a non-uniform amplitude linear array with half wavelength spacing can be written as:

$$AF(\theta) = w_0 1 + w_1 e^{j(kd\sin\theta+\beta)} + w_2 e^{j2(kd\sin\theta+\beta)} + \ldots + w_{N-1} e^{j(N-1)(kd\sin\theta+\beta)}$$

$$= \sum_{n=0}^{N-1} w_n e^{jn(kd\sin\theta+\beta)} \qquad (2.3)$$

where w_n represents the array element coefficients or array excitation amplitudes.

2.2.2.1 Binomial Linear Array

Stone [5] proposed the idea of reducing the sidelobe level by relating the array elements amplitudes according to the coefficients of a binomial series:

$$(1+x)^{n-1} = 1 + (n-1)x + \frac{(n-1)(n-2)}{2!}x^2 + \ldots \qquad (2.4)$$

where n is a discrete number from 1 to the given number of elements N. Considering an example of 16-element binominal array with half-wavelength spacing and zero phase delay between each element. The amplitude coefficients and resulting radiation pattern for a 16 elements Binomial array are shown as follows:

Element Number	1	2	3	4	5	6	7	8
Amplitude	0.0002	0.0023	0.0163	0.0707	0.2121	0.4667	0.7778	1.0000
Element Number	9	10	11	12	13	14	15	16
Amplitude	1.0000	0.7778	0.4667	0.2121	0.0707	0.0163	0.0023	0.0002

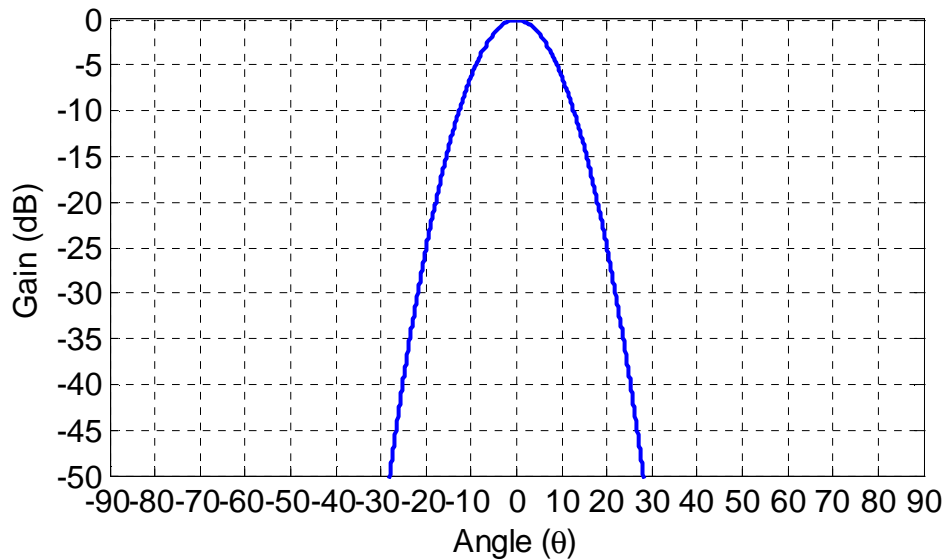Table 2.1. Amplitude coefficients of a 16-element binomial array.

Fig 2.4. Radiation pattern of 16-element binomial array with uniform spacing.

Thus, the array elements amplitudes are derived from the expansion of binomial series. Apart from the wide main beam, an ideal binomial array does not have any sidelobes. According to Table 2.1, binomial array requires a high dynamic range of excitation coefficients to produce the corresponding radiation pattern shown in Fig 2.4, so the feed network is difficult to fabricate in reality.

2.2.2.2 Dolph-Chebyshev Linear Array

It is often more preferable to have a radiation pattern with lower sidelobe levels (below -30dB) to attenuate the effect of interference, so another approach introduced by Dolph [6] and later developed by other researchers [7-10] to meet this criteria. The excitation coefficients in this type of array are determined by the Chebyshev polynomial, which is seen as a compromise approach between uniform and binomial linear arrays. There are a number of ways to obtain the amplitude coefficients of the Chebyshev array, but we will use the following technique [8] in this thesis:

$$w_n = \sum_{q=n}^{N} (-1)^{N-q}(z_0)^{2q-1} \frac{(q+N-2)!(2N-1)}{(q-n)!(q+n-1)!(N-q)!} \quad \text{for even number of elements } n = 1,2,\ldots N,$$

(2.5a)

$$w_n = \sum_{q=n}^{N+1} (-1)^{N-q+1}(z_0)^{2(q-1)} \frac{(q+N-2)!(2N)}{\varepsilon_n(q-n)!(q+n-2)!(N-q+1)!} \quad \text{for odd number of elements } n =$$

$1,2,\ldots N+1$, where $\varepsilon_n = 2$ for n =1; $\varepsilon_n = 1$ for $n \neq 1$. (2.6b)

where N is the number of elements, $z_o = 0.5 [(R_o + \sqrt{R_o^2 - 1})^{1/(N-1)} + (R_o - \sqrt{R_o^2 - 1})^{1/(N-1)}]$ and R_o is the voltage ratio of major to minor lobe of the radiation pattern. An example of 16-element Chebyshev array of -30dB maximum sidelobe levels with half-wavelength spacing is considered. The excitation coefficients and radiation pattern of a 16-element Chebyshev array are given in Table 2.2 and plotted in Fig 2.5 as follows:

Element Number	1	2	3	4	5	6	7	8
Amplitude	0.2910	0.3173	0.4557	0.6018	0.7424	0.8637	0.9528	1.0000
Element Number	9	10	11	12	13	14	15	16
Amplitude	1.0000	0.9528	0.8637	0.7424	0.6018	0.4557	0.3173	0.2910

Table 2.2. Excitation coefficients of 16-element Chebyshev array with -30dB maximum
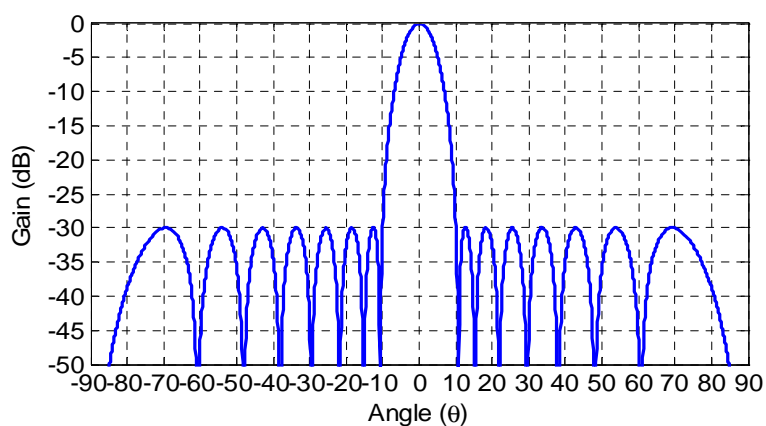
sidelobe levels.

Fig 2.5. Radiation pattern of 16-element Chebyshev array of -30dB maximum sidelobe levels.

A Chebyshev linear array is achieved by equating the amplitudes of each array element to the coefficients of Chebyshev polynomials. Although this approach effectively reduces the maximum sidelobe level to -30dB below the main beam, but the issue of non-continuous current distribution will become more apparent as the number of array elements increase to 20 in the design of feed network.

Element Number	1	2	3	4	5	6	7	8
Amplitude	**0.3256**	0.2856	0.3910	0.5046	0.6203	0.7315	0.8310	0.9124
Element Number	9	10	11	12	13	14	15	16
Amplitude	0.9701	1.0000	1.0000	0.9701	0.9124	0.8310	0.7315	0.6203
Element Number	17	18	19	20				
Amplitude	0.5046	0.3910	0.2856	**0.3256**				

Table 2.3. Excitation coefficients of 20-element Chebyshev array designed to produce -30dB maximum sidelobe levels.

2.2.2.3 Taylor Linear Array

In an effort to solve the problem of discontinuous current distribution occurred in the Chebyshev array as the number of element gets larger, another more advanced technique was introduced by Taylor [11]. Chebyshev distribution produces a radiation pattern with desired but constant minor lobe levels extended to infinity. However, Taylor's technique is able to generate a similar beam pattern but with steadily decayed sidelobes. The array excitation coefficients are expressed as [11]:

$$w_n = \frac{[(\bar{n}-1)!]^2}{(\bar{n}-1+m)!(\bar{n}-1-m)!} \prod_{n=1}^{\bar{n}-1} [1-(\frac{m}{u_n})^2] \qquad (2.7)$$

parameters $u_n = \begin{cases} \pm\pi\sigma\sqrt{A^2+(n-\frac{1}{2})^2} & 1 \le n < \bar{n} \\ \pm n\pi & \bar{n} \le n < \infty \end{cases}$ and $\sigma = \dfrac{\bar{n}}{\sqrt{A^2+(\bar{n}-\frac{1}{2})^2}}$,   where

$A = \dfrac{1}{\pi}\cosh^{-1}R$, $\bar{n}$ is the number of equal minor lobes chosen and R is the voltage ratio of

main beam to sidelobes. To examine the principles, we will use an example of a 16-element

Taylor linear array of half-wavelength inter-element spacing designed to produce of -30dB

sidelobe levels. The amplitudes of array elements and related radiation patterns are shown as:

Element Number	1	2	3	4	5	6	7	8
Amplitude	0.2596	0.3264	0.4466	0.5939	0.7386	0.8609	0.9509	1.0000
Element Number	9	10	11	12	13	14	15	16
Amplitude	1.0000	0.9509	0.8609	0.7386	0.5939	0.4466	0.3264	0.2596

Table 2.4. Excitation coefficients of 16-element Taylor array with -30dB maximum sidelobe
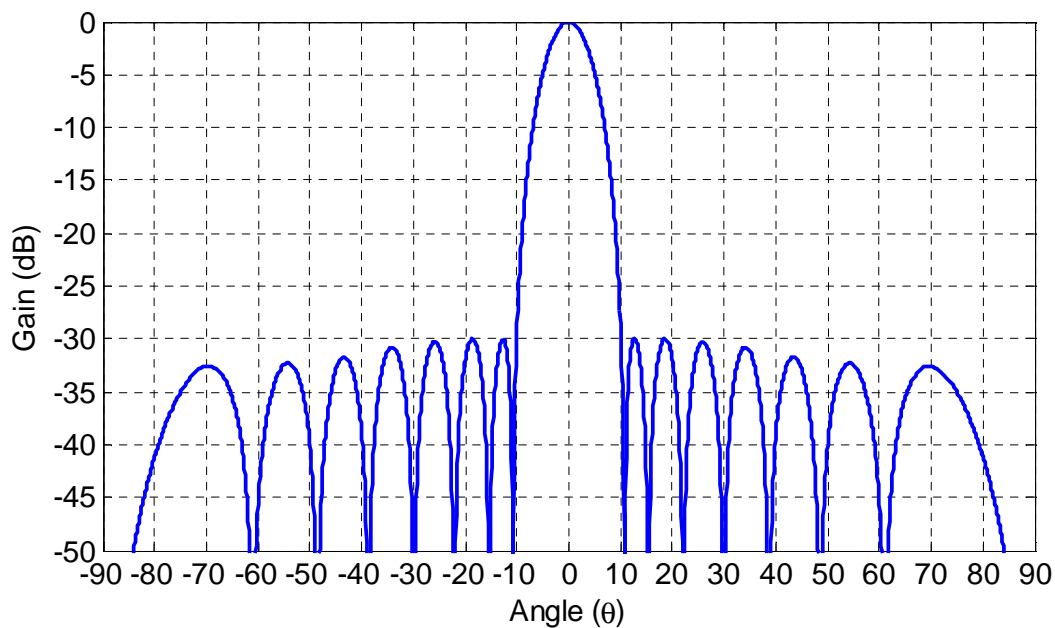levels when $\bar{n} = 5$.

Fig 2.6. Radiation pattern of 16-element Taylor array of -30dB maximum sidelobe levels.

with uniform spacing when $\bar{n} = 5$.

It can be noted from Fig 2.6 that Taylor distribution produces the desired radiation pattern with a maximum sidelobe level of -30dB, while the minor lobes outside the range of $\bar{n}$ decreases at a rate of sin(πu)/πu compared with Chebyshev array shown in Fig 2.5 [12]. The relative amplitudes of the array elements do not vary as the number of elements increases.

Element Number	1	2	3	4	5	6	7	8
Amplitude	**0.2559**	0.2992	0.3804	0.4882	0.6075	0.7232	0.8253	0.9083
Element Number	9	10	11	12	13	14	15	16
Amplitude	0.9682	1.0000	1.0000	0.9682	0.9083	0.8253	0.7232	0.6075
Element Number	17	18	19	20				
Amplitude	0.4882	0.3804	0.2992	**0.2559**				

Table 2.5. Amplitudes of 20-element Taylor linear array designed to produce a radiation pattern with a -30dB maximum sidelobe levels when $\bar{n} = 5$.

From the above discussion, we can conclude that pattern synthesis can be achieved by controlling the excitation coefficients of the array elements. The dynamic range of amplitude ratios from the outermost to the central element for a 16-element array under three different cases (binomial, Chebyshev and Taylor) are 1:0.0002, 1:0.2910 and 1:0.2596 respectively. Chebyshev and Taylor distributions are both widely used classic technique to produce a beam pattern with a controlled low or ultralow sidelobe levels (equal or less than -30dB), but Taylor array provides a smooth current distribution from the edge towards the centre as the number of elements increases.

2.2.3 Beamforming Basics

In a phased array system, beamforming is a spatial filtering technique that enhances radiation in one direction while rejecting unwanted signals from others. For a uniform linear array structure that is shown in Fig 2.1, a narrowband incident plane wave s(t) is transmitted from the far field source. Since the signal is arriving at the first element of the array has a delay compared to the second element, there is a progressive phase shift across the entire array. The array response a(θ) can be expressed in a complex vector form as:

$$a(\theta) = [1, e^{-jkd\sin\theta}, e^{-2jkd\sin\theta}, ..., e^{-j(N-1)kd\sin\theta}]^T \qquad (2.8)$$

where the superscript $[\cdot]^T$ represents transpose and θ is the direction of arrival angle of the signal. The transmitted signal s(t) from the far field source in the vector form is written as $s(t) = [s_0(t), s_1(t), s_2(t), ..., s_{N-1}(t)]^T$. Therefore, we denote the received signal x(t) as $x(t) = a(\theta)s(t)$.

The output y(t) is the summation of the signal received by individual element multiplied by a set of complex weights given by [13]:

$$y(t) = \sum_{n=0}^{N-1} w_n x_n(t) \qquad (2.9)$$

Denoting the array weights $w = [w_0^*, w_1^*, w_2^*, ..., w_{N-1}^*]^T$, where $(\cdot)^*$ represents the complex conjugate, the signal received from all the elements as $x(t) = [x_0(t), x_1(t), x_2(t), ..., x_{N-1}(t)]^T$, the output of the array becomes [13]:

$$y(t) = \mathbf{w}^H \mathbf{x}(t) = \mathbf{w}^H \mathbf{a}(\theta)s(t) \qquad (2.10)$$

where $(\cdot)^H$ is the complex conjugate transpose. A uniform amplitude linear array is regarded as a special case when $\mathbf{w} = [1, 1, 1, 1, 1, 1, 1, 1, 1, 1, 1, 1, 1, 1, 1, 1]^T$. For a non-uniform linear array, the array weights are normally determined by either the coefficients of binomial

expansion or Chebyshev polynomials coefficients. Therefore, various beam patterns can be designed by simply adjusting the proper array weights w according to the system specification. Understanding this basic characteristic is of great importance in studying the next topic.

2.3 Theoretical background of Time Modulated Linear Arrays

From the preceding analysis, two significant characteristics, pattern synthesis and real time electronic beam scanning, were accomplished by manipulating the excitation coefficients or the array weights of the array elements. For example, a 16-element Chebyshev linear array designed to generate -40dB maximum sidelobe levels has a normalised amplitude ratio of 0:1138 to 1 [8-9] from the 1st to the 8th element, while a 16-element Taylor linear array has a current distribution of 0.1216 to 1 [11-12]. Both of these techniques require a complicated feed network design. In addition, expensive digital phase shifters are essential components in a phased array system to achieve electronic beam steering. These can only be found in the specialised military system, so it has motivated the research into developing a simple and low cost array system for the commercial application.

In order to address the above concerns, an innovative idea of time modulation was firstly proposed by Shanks and Bickmore [14] in the late 1950s. A simple configuration of radiating slots, ferrite switches and square-wave generator was used to demonstrate the concept. In 1961, Shanks [15] applied this analysis into a phased array system and established a mathematical model of achieving electronic beam scanning property without the use of phase shifters. On the basis of this investigation, Kummer et al. [16] presented experimental results of an eight-element time modulated slot array at X band, it has shown that ultra-low sidelobe levels of -39.5dB below the main beam were achieved. In 1961, another measurement of a

twenty-element slotted array at X band was carried out by Kummer et al. [17] The experimental results verified the possibility of realising real time electronic beam steering by periodically modulating each array element. A few decades later, Lewis and Evins [18] extended the analysis to a radar system, and developed a theoretical model for reducing interference from entering the sidelobes of radar by moving the phase centre of the receiver array.

The essence of time-modulation is to periodically switch on and off each array element with a high speed RF switch for a prescribed period of time by an electronic control circuit so that the amplitude weighting functions of conventional antenna array can be synthesised in a time-average sense. By the virtue of periodic time modulation, harmonics or sidebands are generated at multiples of the switching frequency. Desired antenna patterns with controlled sidelobe levels can be obtained after proper filtering process. Sometimes harmonics are unwanted as they waste power, but there are applications in which such harmonic beams can be exploited to point in different directions.

Since each array element is connected to an RF switch and controlled by an external programmed circuit, the use of time as an additional parameter is more flexible and accurate to obtain the array weights compared with the conventional method. It not only relaxes the design constraint of feed network but also improves the system performance. In recent years, the concept of time modulated antenna arrays (TMMA) has been studied extensively by various researchers [19-36]. Much previous work has focused on exploring the potential applications of TMMA in many areas can be found in [37-49]. In this section, we will briefly introduce the fundamental principles of time modulated antenna array. Two important characteristics of TMAA as well as its potential applications in the communication system will be in the following few chapters.

2.3.1 Sideband Reduction

Referring to Fig 2.1, if a narrowband plane wave of an angular frequency ω impinges on the array at an angle of θ with respect to the broadside direction, the array factor of conventional linear array with uniform inter-element spacing is expressed as the sum of individual element:

$$AF(\theta,t) \;=\; e^{j\omega t} \sum_{n=0}^{N-1} w_n e^{jknd\sin\theta} \tag{2.11}$$

where the beampattern is expressed as a function of θ. Now let us assume the array weights w_n are a periodic function of time with a period T_0 much greater than the RF signal period $T=2\omega/\pi$. According to the mathematical definition, any periodic signal can be decomposed into the sum of infinite oscillating functions [50], so w_n can be represented in the Fourier series form as:

$$w_n(t) \;=\; \sum_{m=-\infty}^{\infty} a_{mn} e^{jm\omega_o t} \tag{2.12}$$

where $\omega_0 = 2\pi/T_0 \ll \omega$ is the angular modulation frequency and it is in the microwave range, since ω_0 closes to ω will cause serious interference between the carrier and fundamental frequency. The simplest way to realise time modulation is to periodically turn on and off one or more array elements through high speed RF switches, hence the array weights or weighting functions w_n are defined by:

$$w_n(t) \;=\; \begin{cases} 1 & 0 \le \tau_{non} < t < \tau_{noff} \le T_0 \\ 0 & \text{elsewhere} \end{cases} \tag{2.13}$$

where τ_{non} and τ_{noff} are the on and off time of the nth elements, T_0 is the switching period. Then equation (2.11) can be rearranged as:

$$AF(\theta,t) = e^{j\omega t}\sum_{n=0}^{N-1}w_n(t)\,e^{jknd\sin\theta} = \sum_{m=-\infty}^{\infty}e^{j(\omega+m\omega_o)t}\sum_{n=0}^{N-1}a_{mn}e^{jknd\sin\theta} \qquad (2.14)$$

where Fourier coefficients a_{mn} are given by:

$$a_{mn} = \frac{1}{T_0}\int_0^{T_o}w_n(t)e^{-jm\omega_o t}dt \qquad (2.15)$$

Substituting equation (2.13) into (2.15) leads to

$$
\begin{aligned}
a_{mn} &= \frac{1}{T_0}\int_{\tau_{non}}^{\tau_{noff}} e^{-jm\omega_o t}dt \\[2mm]
&= \frac{1}{T_0}\frac{1}{-jm\omega_o}[e^{-jm\omega_o t}]_{\tau_{non}}^{\tau_{noff}} \\[2mm]
&= \frac{1}{T_0}\frac{1}{-jm\omega_o}(e^{-jm\omega_o\tau_{noff}} - e^{-jm\omega_o\tau_{non}}) \\[2mm]
&= \frac{1}{2\pi/\omega_o}\frac{j}{m\omega_o}(e^{-jm2\pi\tau_{noff}} - e^{-jm2\pi\tau_{non}}) \\[2mm]
&= \frac{j}{2\pi m}(e^{-jm2\pi\tau_{noff}} - e^{-jm2\pi\tau_{non}}) \\[2mm]
&= \frac{j}{2\pi m}e^{-jm2\pi\tau_{non}}[e^{-jm2\pi(\tau_{noff}-\tau_{non})} - 1] \\[2mm]
&= \frac{j}{2\pi m}e^{-jm2\pi\tau_{non}}e^{-jm\pi(\tau_{noff}-\tau_{non})}[e^{-jm\pi(\tau_{noff}-\tau_{non})} - e^{jm\pi(\tau_{noff}-\tau_{non})}] \\[2mm]
&= \frac{j}{2\pi m}e^{-jm2\pi\tau_{non}}e^{-jm\pi(\tau_{noff}-\tau_{non})}(-2j\sin[m\pi(\tau_{noff}-\tau_{non})]) \\[2mm]
&= \frac{1}{\pi m}e^{-j\pi m(\tau_{noff}-\tau_{non}+2\tau_{non})}\sin[m\pi(\tau_{noff}-\tau_{non})] \\[2mm]
&= (\tau_{noff}-\tau_{non})\frac{\sin[m\pi(\tau_{noff}-\tau_{non})]}{m\pi(\tau_{noff}-\tau_{non})}\,e^{-j\pi m(\tau_{noff}+\tau_{non})}
\end{aligned}
\qquad (2.16)
$$

From equation (2.15), it can be noticed that one Fourier coefficient corresponds to one angular frequency with respect to ($\omega+m\omega_0$). Generally, the beampattern at the fundamental an angular frequency (when m=0) is of interest (when m=0), so the equation (2.14) reduces to:

$$AF(\theta,t) = e^{j\omega t}\sum_{n=0}^{N-1}a_{0n}e^{jknd\sin\theta} \qquad (2.17)$$

where

$$a_{0n} = \frac{1}{T_0}\int_{\tau_{non}}^{\tau_{noff}}w(t)e^{-j0\omega_o t}dt \qquad (2.18)$$

Substituting equation (2.13) into (2.18), we can acquire the Fourier coefficients at the fundamental frequency:

$$\begin{aligned}
a_{0n} &= \frac{1}{T_0}\int_{\tau_{non}}^{\tau_{noff}}e^{-j0\omega_o t}dt \\
&= \frac{1}{T_0}[1]_{\tau_{non}}^{\tau_{noff}} \\
&= \frac{\tau_{noff}-\tau_{non}}{T_0}
\end{aligned} \qquad (2.1)$$

It also can be emphasised that Fourier coefficients are simply the time average value of the modulated array elements. This implies that the array weights of a conventional antenna array are controlled by the Fourier coefficients at the fundament angular frequency, equation (2.17) simplifies to

$$AF(\theta,t) = e^{j\omega t}\sum_{n=0}^{N-1}\frac{(\tau_{noff}-\tau_{non})}{T_0}e^{jknd\sin\theta} \qquad (2.20)$$

The term $\frac{(\tau_{noff}-\tau_{non})}{T_0}$ in the time modulated linear array in equation (2.20) is the same as the static amplitude weights for a conventional array and it is determined by the effective on-time $(\tau_{off} - \tau_{on})$ of each array element. In fact, this technique allows conventional array amplitude weighting functions to be accomplished in a time-average sense at the fundamental frequency. Switching an element on for a given period of time corresponds to its excitation coefficients. For an example, if a particular array element has a relative amplitude weight of 0.5, then in

the time modulation scheme, the element would be turned on for a time which is equal to the half of the modulation period. In other words, any type of distribution functions such as Chebyshev and Taylor can be easily achieved through this technique.

The utilisation of time provides a more effective and precise way to synthesise patterns with controlled sidelobe level as well as relaxing the mechanical design constraint. A simple N-element time modulated linear array in the receive mode is illustrated in Fig 2.7.
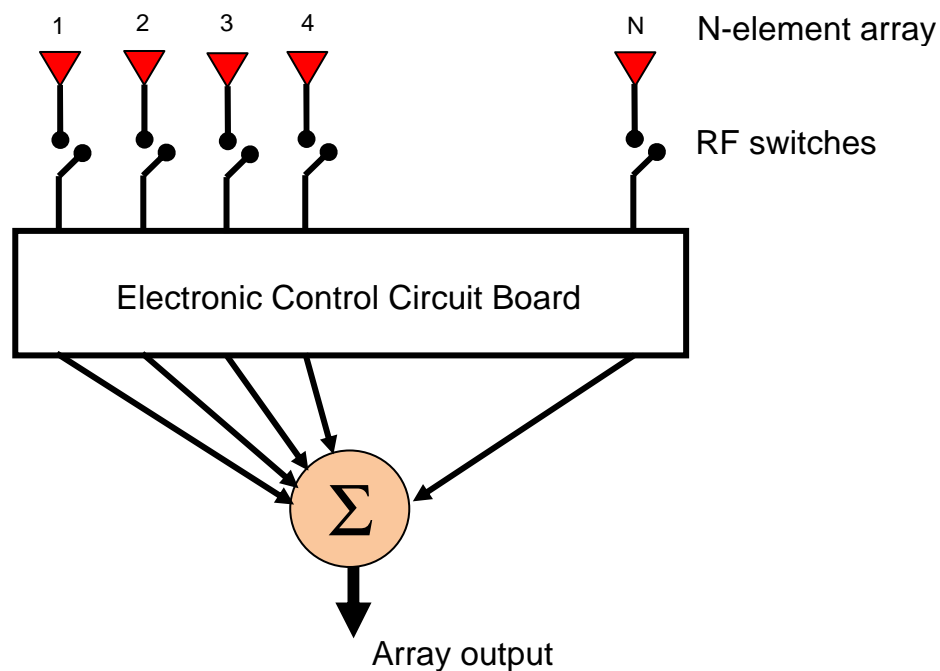

Fig 2.7. N-element time modulated linear array structure in the receive mode.

To aid the interpretation of the general concept, let us first examine a simple situation of a 16-element time modulated linear array, where all the elements are switched on for an entire switching period T_0 with a common starting time ($\tau_{non} = 0$). For simplicity, we will also assume a normalised switching period ($T_0=1$) and half wavelength inter-element spacing

(d=0.5λ). The time sequence of the array and corresponding radiation pattern at the

fundamental angular frequency are shown in Fig 2.8 and Fig 2.9 respectively.
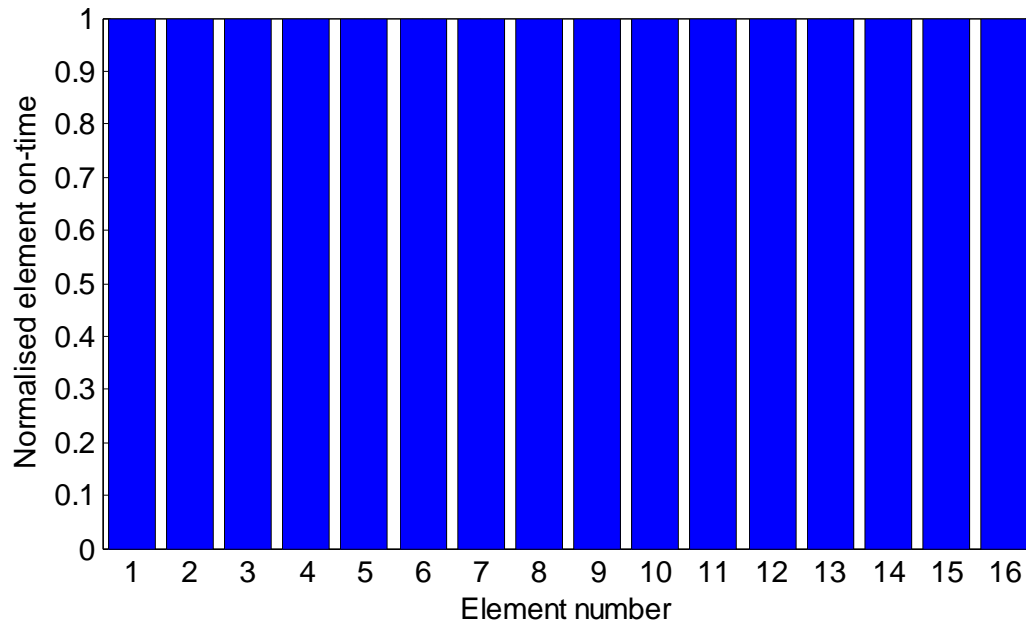
Fig 2.8. Time sequence of 16-element time moduled linear array switched on for a entire
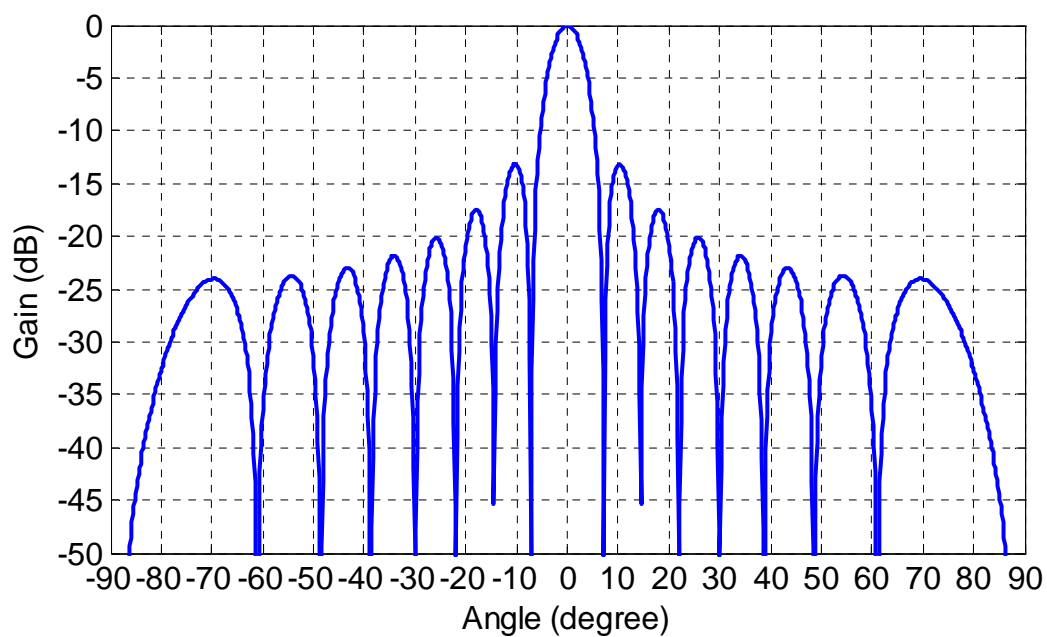
switching period T_0.

Fig 2.9. Corresponding array factor of Fig 2.8.

If all elements are energised for an entire modulating period, the radiation pattern simplifies to the case of uniform amplitude linear array (w_n=1 for all 16 elements). At the fundamental frequency when m = 0, $a_{0n} = \tau_{noff} - \tau_{non} = 1$, but the Fourier coefficients at harmonics or sidelobes (m ≠ 0) equal zero, because sin(mπ)=0 for any given number of harmonics m.

We will now extend this analysis to implement -30dB Taylor distribution to the time modulated linear array. From the previous discussion, we know that amplitude weighting functions are determined by the effective on times of array elements, which in turn control the radiation pattern at the operating frequency. The time sequence of a 16-element Taylor array and its radiation patterns at fundamental frequency and first positive three harmonics are plotted in Fig 2.10 and Fig 2.11 respectively.
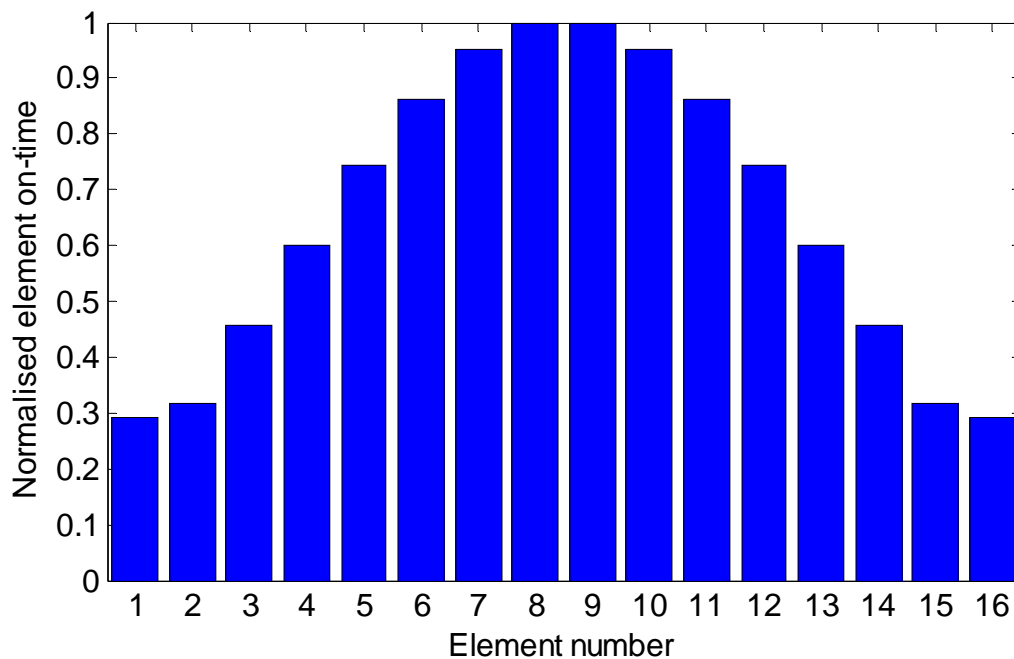
Fig 2.10. Time sequence of 16-element time moduled linear array designed to prodce a beampattern with -30dB Taylor sidelobe level at the fundamental frequency.
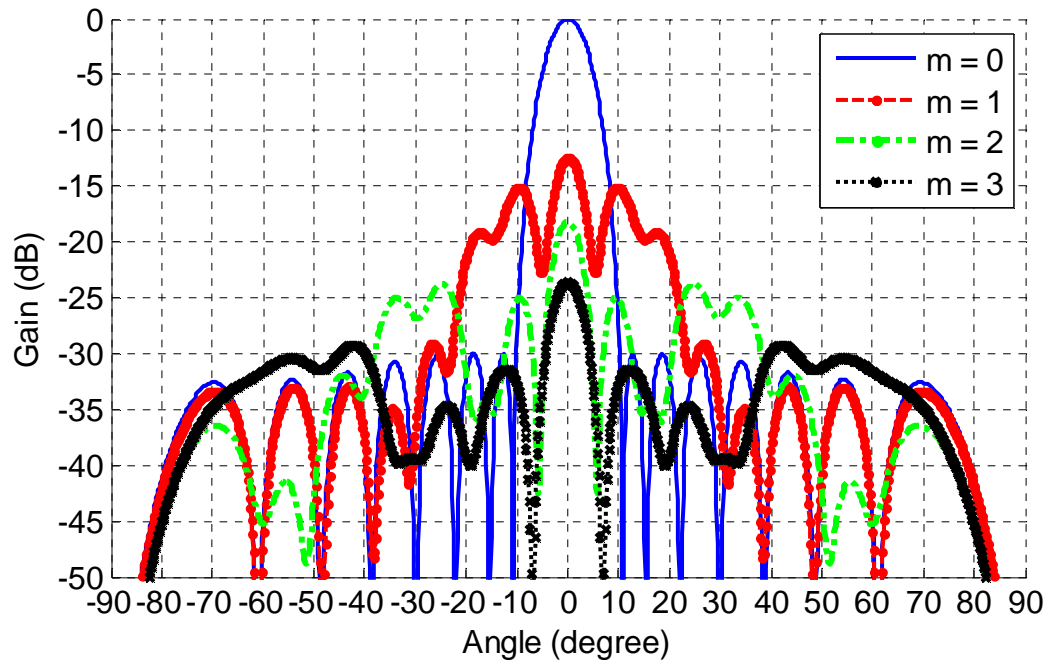
Fig 2.11. Corresponding array factors of Fig 2.10 (m=0 refers to fundamental frequency, m=1

refers to the 1st harmonic, m=2 refers to the 2nd harmonic and m=3 refers to the 3rd

harmonic).

It can be noticed from Fig 2.11 that the beampattern produces a maximum sidelobe level of -

30dB at fundamental frequency, along with infinite number of harmonics at multiples of the

modulation frequency. Since sidebands consume parts of the total input power, it tends to

degrade the system performance and is undesirable. Recent works have been focused on

investigating appropriate techniques for suppressing harmonic radiations by various adaptive

optimisation algorithms [20-21, 25-26, 28-34]. We will deal with this issue and discuss it in a

more detail in the following chapter.

2.3.2 Harmonic beam scanning

One of the most significant features of a phased array system is the capability of performing

real-time electronic beam steering. By properly adjusting the relative phase delay of each

element, the pattern is able to form a high directive main beam in the desired direction. A

variety of techniques, including true-time delay [51], ferroelectric phased array [52] and frequency scanning array [53], have been studied and investigated for decades, but these technologies are not yet well-developed to provide a low-cost system. In 1959, Shanks and Bickmore [14] proposed an idea of time modulation and demonstrated the mathematical potential of implementing electronic scanning in the time domain. This approach is simple and reliable, and most importantly it eliminates the use of costly phase shifters.

Referring back to equation (2.15), each Fourier coefficients a_{mn} corresponds to a different harmonic frequency. Therefore, there is a possibility in which each harmonic pattern can be controlled to point to various spatial directions.

Fourier Transform theory dictates that a shift in the time domain is equivalent to a change in phase in the frequency domain [54]. Thus in order to achieve the identical effect of a progressive phase delay between each array element as in the conventional phased array system, each array element in the time modulated antenna array has to be energised in a similar way. The most straightforward form is the binary switching (on or off) scheme. In this case, a rectangular pulse shape is used for simple illustration as is shown in Fig 2.12 and defined by the equation (2.13):
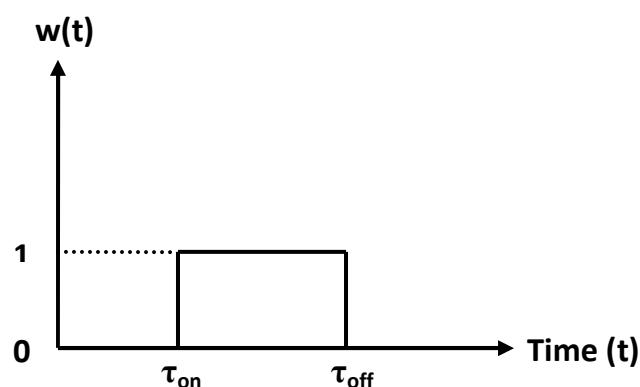

Fig 2.12. A rectangular pulse of N-element time modulated linear array.

$$w_n(t) = \begin{cases} 1 & 0 \leq \tau_{non} < t < \tau_{noff} \leq T_0 \\ 0 & \text{elsewhere} \end{cases}$$

where τ_{on} and τ_{off} represent the element switching on and off time respectively. In the next step, we will examine the physical excitation arrangement for a N-element linear array. The first antenna of the array is turned on for a small portion of a modulation period T_0 (denoted as N/ T_0) and then switched off immediately. Repeating the same procedure across the entire array, thus the corresponding excitation time of the nth element is denoted as:

$$\frac{nT_0}{N} \leq t \leq \frac{(n+1)T_0}{N} \tag{2.21}$$

Using (2.21), we calculate the Fourier coefficients as:

$$a_{mn} = \frac{1}{T_0} \int_{\tau_{non}}^{\tau_{noff}} e^{-jm\omega_o t} dt$$

$$= \frac{1}{T_0} \frac{1}{-jm\omega_o} [e^{-jm\omega_o t}]_{\frac{nT_o}{N}}^{\frac{(n+1)T_o}{N}}$$

$$= \frac{1}{T_0} \frac{1}{-jm\omega_o} (e^{-jm\frac{2\pi}{T_o}\frac{(n+1)T}{N}} - e^{-jm\frac{2\pi}{T_o}\frac{nT_o}{N}})$$

$$= \frac{1}{2\pi / \omega_o} \frac{j}{m\omega_o} (e^{-\frac{j2\pi m(n+1)}{N}} - e^{-\frac{j2\pi mn}{N}})$$

$$= \frac{j}{2\pi m} (e^{-\frac{j2\pi m(n+1)}{N}} - e^{-\frac{j2\pi mn}{N}})$$

$$= \frac{j}{2\pi m} e^{-\frac{j2\pi mn}{N}} (e^{-\frac{j2\pi m}{N}} - 1)$$

$$= \frac{j}{2\pi m} e^{-\frac{j2\pi mn}{N}} e^{-\frac{j\pi m}{N}} (e^{-\frac{j\pi m}{N}} - e^{\frac{j\pi m}{N}})$$

$$= \frac{j}{2\pi m} e^{-\frac{j2\pi mn}{N}} e^{-\frac{j\pi m}{N}} (-2j\sin(\frac{\pi m}{N})) \tag{2.22}$$

$$= \frac{1}{\pi m} \sin(\frac{\pi m}{N}) e^{-\frac{j2\pi mn}{N}} e^{-\frac{j\pi m}{N}}$$

Substituting (2.22) into equation (2.14) we can obtain:

$$AF(\theta,t) = \sum_{m=-\infty}^{\infty} e^{j(\omega+m\omega_o)t} \sum_{n=0}^{N-1} a_{mn} e^{jknd\sin\theta}$$

$$= \sum_{m=-\infty}^{\infty} e^{j(\omega+m\omega_o)t} \sum_{n=0}^{N-1} \frac{1}{\pi m}\sin(\frac{\pi m}{N})e^{jknd\sin\theta}e^{-\frac{j2\pi mn}{N}}e^{-\frac{j\pi m}{N}} \tag{2.23}$$

$$= e^{-\frac{j\pi m}{N}} \sum_{m=-\infty}^{\infty} e^{j(\omega+m\omega_o)t} \sum_{n=0}^{N-1} \frac{1}{\pi m}\sin(\frac{\pi m}{N})e^{j\pi n(\sin\theta-\frac{2m}{N})}$$

The radiation pattern has a maximum response at $\sin\theta = \frac{2m}{N}$, where $\theta = \sin^{-1}(\frac{2m}{N})$. Thus for a given number of elements, the phase angle is purely dependant on the given number of harmonics m. For example, the beampatterns at first negative harmonic (m=-1), fundamental frequency (m=0) and first negative harmonic (m=1) are expressed as:

$$AF(\theta,t)_{m=-1} = e^{j(\omega-\omega_o)t} \sum_{n=0}^{N-1} \frac{1}{-\pi}\sin(\frac{-\pi}{N})e^{j\pi n(\sin\theta+\frac{2}{N})}$$

$$AF(\theta,t)_{m=0} = e^{j\omega t} \sum_{n=0}^{N-1} \frac{1}{N}e^{j\pi n\sin\theta} \tag{2.24}$$

$$AF(\theta,t)_{m=1} = e^{j(\omega+\omega_o)t} \sum_{n=0}^{N-1} \frac{1}{\pi}\sin(\frac{\pi}{N})e^{j\pi n(\sin\theta-\frac{2}{N})}$$

From the knowledge gained in the non-uniform linear array section, equation (2.24) implies that each individual Fourier coefficient determines the spatial characteristic of beampattern at a specific harmonic frequency. The above discussion provides a basic understanding of realising electronic beam scanning in the time modulated antenna array without the use of phase shifters. A spatial illustration of beam scanning plotted in Fig 2.13. Considering an example of 16-element linear array with d=0.5λ, the time sequence and corresponding radiation patterns at different harmonic frequencies are shown in Fig 2.14 and Fig 2.15.
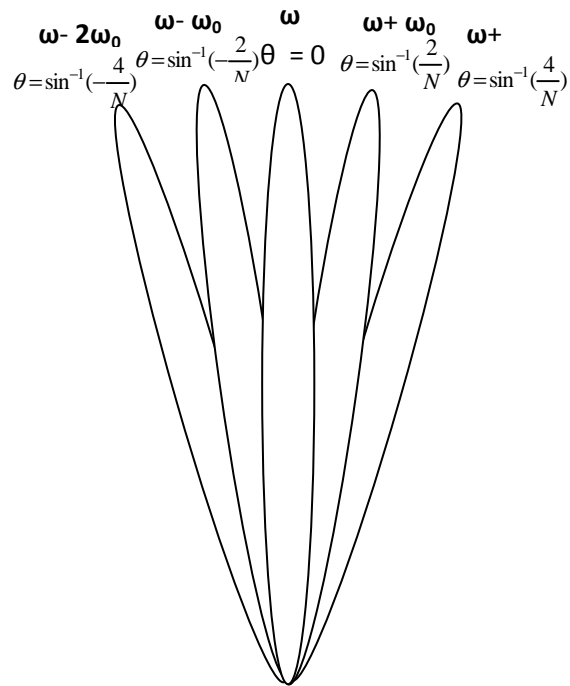
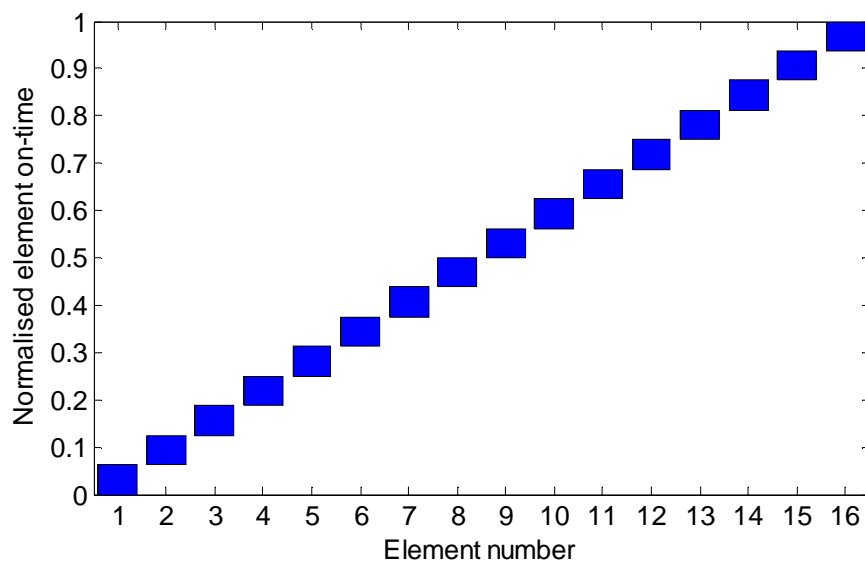Fig 2.13. Spatial illustration of beam scanning.

Fig 2.14. Time sequence of 16 elements linear array to be energised in a progressive way.
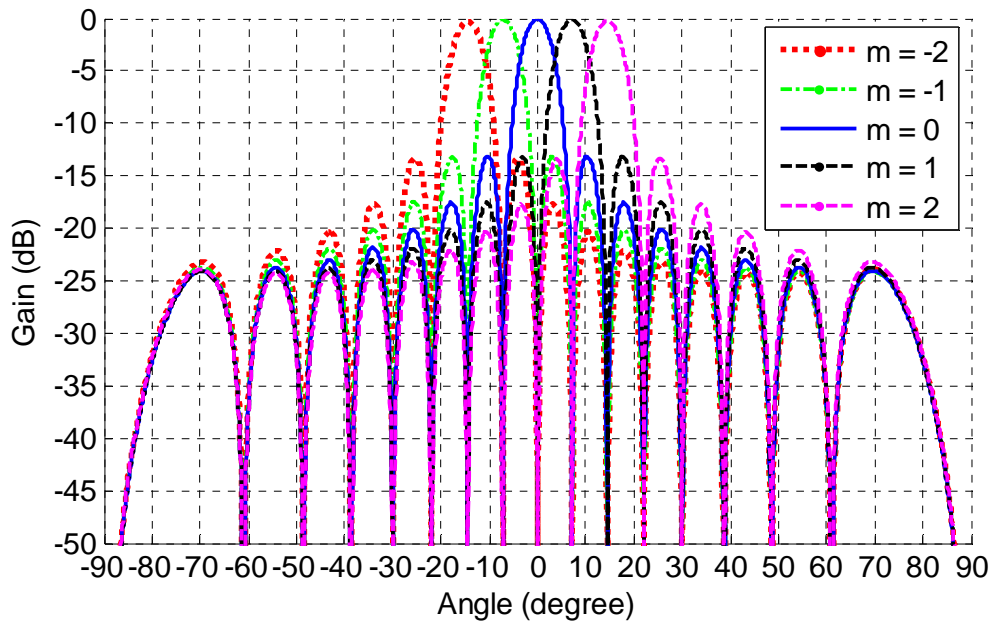
Fig 2.15. Corresponding array factors of time sequence in Fig 2.14.(m=-2 relates to 2nd

negative harmonic, m=-1 relates to 1st negative harmonic, m=0 relates to fundamental

frequency, m=1 relates to 1st positive harmonic, m=2 relates to 2nd positive harmonic)

The beampattern at the fundamental angular frequency ω has a maximum response at the

boresight direction (θ=0), while the beampatterns at 1st and 2nd positive and negative sideband

steer the main beam towards the direction of $\pm\sin^{-1}(\frac{2}{16})$ (or $\pm 7.18°$) and $\pm\sin^{-1}(\frac{4}{16})$ (or

14.47°) respectively. Hence the simulation results agree very well with the theoretical

model, where beampatterns can be controlled to scan in different angles as a function of

harmonic number m.

Up to this point, we have concluded some crucial points: 1) every harmonic or sideband has

same sidelobe level of -13dB as in the conventional uniform linear array; 2) there are a finite

number of beams covering the full hemisphere even though infinite numbers of harmonics

are generated; 3) the sinc function $\dfrac{\sin(\pi m / N)}{\pi m / N}$ in equation (2.23) decreases in amplitude as

harmonic frequency m increases.

2.4 Conclusion

A brief introduction of the general theory behind the conventional uniform amplitude linear array was given at the beginning of this chapter. Three classic types of non-uniform amplitude linear array models are discussed in the later section. In the case of Binomial linear array, the excitation coefficients can be obtained by the expansion of binomial series and array pattern generates no sidelobes. For the Dolph-Chebyshev linear array, the excitation coefficients are determined by the Chebyshev polynomials and it produces constant sidelobe levels. For the Taylor linear array, the excitation coefficients corresponds to Taylor distribution and it yields a beam pattern with decayed sidelobe level.

With these fundamental principles in mind, we extend the analysis to a time modulated linear array in the second part of the chapter. The essence of time modulation is the utilisation of time as an additional parameter to control the characteristic of the radiation pattern at the fundamental frequency. Unlike a conventional array system, there are two distinguished benefits provided by the time modulation technique. Pattern synthesis can be accomplished in a time average sense by periodically switching on and off each array element in a prescribed manner. This provides a more flexible and accurate way of producing desired beampatterns with low or ultralow sidelobe level compared with the conventional methods. However, due to the nature of periodic time modulation, the harmonics are generated and consumed parts of the input power. Another promising feature provided by the time modulated linear array is to realise electronic beam scanning without the use of expensive phase shifters. This is also

achieved through periodically switching on and off array elements progressively across the array.

References

[1] S. A. Schelkunoff, "A Mathematical Theory of Linear Arrays", Bell System Technical Journal, vol. 22, Jan. 1943, pp. 80-87.

[2] D. R. Rhodes, "On a fundamental principle in the theory of planar antennas", Proceeding of the IEEE, vol. 52, no. 9, Sep. 1964, pp. 1013 – 1021.

[3] H. P. Neff and J. D. Tillman, "An omnidirectional circular antenna array excited parasitically by a central driven element", Transactions of the American Institute of Electrical Engineers, Part I: Communication and Electronics, vol. 79, no. 2, May 1960, pp. 190-192.

[4] C. A. Balanis, Antenna Theory: analysis and design, Chapter 6: Arrays: Linear, Planar and Circular, 3rd edition, Wiley Interscience, 2005, pp. 283-371.

[5] J. S. Stone, United States Patents No. 1643323 and No. 1715433.

[6] C. L. Dolph, "A Current Distribution for Broadside Arrays Which Optimizes the Relationship between Beamwidth and Side-Lobe Level", Proceeding of IRE and Waves and Electronics, vol. 34, no. 6, June 1946, pp. 335–348.

[7] H. J. Riblet, Discussion on "A Current Distribution for Broadside Arrays Which Optimizes the Relationship between Beamwidth and Side-Lobe Level", Proceeding of the IRE, vol. 35, May 1947, pp. 489-492.

[8] D. Barbiere, "A method for Calculating the Current Distribution of Tschebyscheff Arrays", Proceeding of the IRE, vol. 40, January 1952, pp. 78-82.

[9] R. J. Stegen, "Excitation Coefficients and Beamwidths of Tschebyscheff Arrays", Proceeding of the IRE, vol. 41, November 1953, pp. 1671-1674.

[10] C. J. Drane, Jr., "Useful Approximation for the Directivity and Beamwidth of Large Scanning Dolph-Chebyshev Arrays", Proceeding of the IEEE, vol. 56, November 1968, pp. 1779-1787.

[11] T. T. Taylor, "Design of Line-Source Antennas for Narrow Beamwidth and Low Sidelobes", IRE Transac. Antennas Propagation, vol. 3, no. 1, January 1955, pp. 16–28.

[12] T. T. Taylor, "One Parameter Family of Line-Sources Producing Modified Sin(πu)/πu Patterns", Hughes Aircraft Co. Technical Memo. 324, Culver City, Calif., Contract AF 19(604)-262-F-14, September 4, 1953.

[13] L. C. Godara, "Application of Antenna Arrays to Mobile Communications, Part II: Beamforming and Direction-of-Arrival Considerations", Proceedings of IEEE, vol. 85, no. 8, July 1997, pp. 1195-1245.

[14] H. E. Shanks and R. W. Bickmore, "Four-dimensional electromagnetic radiators", Canadian Journal of Physics, vol. 37, 1959, pp. 263-275.

[15] H. E. Shanks, "A new technique for electronic scanning," IEEE Transactions on Antennas and Propagation, vol. 9, no. 2, Mar., 1961, pp. 162–166.

[16] W. H. Kummer, A. T. Villeneuve, T. S. Fong, and F. G. Terrio, "Ultra-low sidelobes from time-modulated arrays", IEEE Transactions on Antenna and Propagation, vol. 11, no. 6, Nov., 1963, pp. 633-639.

[17] W. H. Kummer, A. T. Villeneuve and F. G. Terrio, "New antenna idea - Scanning without Phase Shifters," Electronics, vol. 36, March, 1963, pp. 27-32.

[18] B. L. Lewis and J. B. Evins, "A new technique for reducing radar response to signals entering antenna sidelobes", IEEE Transactions on Antennas and Propagation, vol. 31, no. 6, Nov.1983, pp. 993-996.

[19] S. Yang, Y. B. Gan and A. Qing, "Sideband suppression in time-modulated linear arrays by the differential evolution algorithm", IEEE Antennas Wireless Propagation Letters, vol. 1, no. 9, 2002, pp. 173-175.

[20] S. Yang, Y. B. Gan and P. K. Tan, "A new technique for power-pattern synthesis in time-modulated linear arrays", IEEE Antenna Wireless Propagation Letters, vol. 2, no. 20, 2003, pp. 285-287.

[21] J. Fondevila, J. C. Bregains, F. Ares and E. Moreno, "Optimising uniformly excited linear arrays through time modulation", IEEE Antennas Wireless Propagation Letters, vol. 3, pp. 298-300, 2004.

[22] S. Yang, Y. B. Gan, A. Qing, and P. K. Tan, "Design of uniform amplitude time modulated linear array with optimized time sequences", IEEE Transactions on Antenna and Propagation, vol. 53, no. 7, July, 2005, pp. 2337-2339.

[23] A. Tennant and B. Chambers, "Control of the harmonic radiation patterns of time-modulated antenna arrays," IEEE Antenna and Propagation conference, July, 2008, pp. 1-4.

[24] X. Zhu, S. Yang and Z. Nie, "Full-Wave Simulation of Time Modulated Linear Antenna Arrays in Frequency Domain," IEEE Transactions on Antennas and Propagation, vol. 56, no. 5, May, 2008, pp. 1479-1482.

[25] L. Manica, P. Rocca, L. Poli, A. Massa, "Almost time-independent performance in time-modulated linear arrays," IEEE Antennas Wireless Propagation Letter, vol. 8, Aug., 2009, pp. 843-846.

[26] P. Rocca, L. Manica, L. Poli and A. Massa, "Synthesis of compromise sum-difference arrays through time-modulation," IET Radar Sonar Navigation, vol. 3, Nov., 2009, pp. 630-637.

[27] G. Li, S. Yang, Y. Chen, and Z. Nie, "A novel electronic beam steering technique in time modulated antenna array," Progress In Electromagnetics Research, vol. 97, 2009, pp. 391-405.

[28] P. Rocca, L. Poli, L. Manica and A. Massa, "Compromise pattern synthesis by means of optimized time-modulated array solutions," IEEE Antennas and Propagation Society International Symposium, June, 2009, pp. 1 - 4.

[29] X. Huang, S. Yang, G. Li and Z. Nie, "Power-pattern synthesis in time modulated semicircular arrays," IEEE Antennas and Propagation Society International Symposium, June, 2009, pp. 1 - 4.

[30] L. Poli, L. Manica, P. Rocca and A. Massa, "Subarrayed time-modulated arrays with minimum power losses," IEEE Antennas and Propagation Society International Symposium, July, 2010, pp. 1 - 4.

[31] L. Poli, P. Rocca, L. Manica and A. Massa, "Pattern synthesis in time-modulated linear arrays through pulse shifting," IET Microwaves, Antennas & Propagation, vol. 4, no. 9, Sep., 2010, pp. 1157-1164.

[32] A. Basak, S. Pal, S. Das, A. Abraham and V. Snasel, "A modified Invasive Weed Optimization algorithm for time-modulated linear antenna array synthesis," IEEE Congress on Evolutionary Computation, July, 2010, pp. 1- 8.

[33] E. Aksoy and E. Afacan, "Thinned Nonuniform Amplitude Time-Modulated Linear Arrays," IEEE Antennas Wireless Propagation Letter, vol. 9, May, 2010, pp. 514 -517.

[34] G.R., Hardel, N.T., Yallaparagada, D., Mandal and A.K., Bhattacharjee; "Introducing deeper nulls for time modulated linear symmetric antenna array using real coded genetic algorithm", 2011 IEEE Symposium on Computers & Informatics (ISCI), 20-23 March 2011, pp. 249-254.

[35] M. D'Urso, A. Iacono, A. Iodice and G. Franceschetti, "Optimizing uniformly excited time-modulated linear arrays", 2011 Proceedings of the Fifth European Conference on Antennas and Propagation (EuCAP), Rome, Italy, 11 – 15 April, 2011, pp. 2082-2086.

[36] S.K., Mandal , R. Ghatak and G.K., Mahanti, "Minimization of side lobe level and side band radiation of a uniformly excited time modulated linear antenna array by using Artificial Bee Colony algorithm", 2011 IEEE Symposium on Industrial Electronics and Applications (ISIEA), 25-28 Sept. 2011, pp. 247-250.

[37] G. Li, S. Yang and Z. Nie, "Adaptive beamforming in time modulated antenna arrays based on beamspace data," Asia Pacific Microwave Conference, Singapore, Dec., 2009, pp. 743-736.

[38] G. Li, S. Yang, and Z. Nie, "A study on the application of time modulated antenna arrays to airborne pulsed Doppler radar," IEEE Transactions on Antennas and Propagation, vol. 57, no. 5, May, 2009, pp. 1578–1582.

[39] A. Tennant and B. Chambers, "Time-switched array analysis of phase switched screens," IEEE Transactions on Antennas and Propagation, vol. 57, no. 3, Mar., 2009, pp. 808–812.

[40] A. Tennant and B. Chambers, "A two-element time-modulated array with direction-finding properties", IEEE Antennas Wireless Propagation Letter, vol. 6, 2007, pp. 64–65.

[41] G. Li, S. Yang, Y. Chen, and Z. Nie, "Direction of arrival estimation in time modulated linear arrays," IEEE Antennas and Propagation Society International Symposium, June, 2009, pp. 1-4.

[42] A. Tennant, " Experimental two-element time-modulated direction finding array, " IEEE Transactions on Antennas and Propagation, vol. 58, no. 3, Mar., 2010, pp. 986-988.

[43] G. Li, S. Yang and Z. Nie, "Direction of arrival estimation in time modulated linear arrays with unidirectional phase center motion, " IEEE Transactions on Antennas and Propagation, vol. 58, no. 4, April, 2010, pp. 1105-1111.

[44] Y. Tong and A Tennant, "Simultaneous control of sidelobe level and harmonic beam steering in time-modulated linear arrays," IET Electronics Letters, vol. 46, no.3, Feb., 2010, pp. 200-202.

[45] Y. Tong and A. Tennant, "A Wireless Communication System Based on a Time-Modulated Array", IEEE Loughborough Antennas and Propagation Conference, Loughborough, UK, 8 – 9 Nov., 2010, pp. 245 – 248.

[46] L. Poli, P. Rocca, G. Oliveri and A. Massa, "Adaptive nulling in time-modulated linear arrays with minimum power losses," IET Microwaves, Antennas & Propagation , vol. 5, no. 2, Jan., 2011, pp. 157-166.

[47] R. L., Haupt, "Time-modulated receive arrays", 2011 IEEE International Symposium on Antennas and Propagation (APSURSI) , 3-8 July 2011, pp. 968-971.

[48] G., Oliveri, "Smart antennas design exploiting time-modulation", 2011 IEEE International Symposium on Antennas and Propagation (APSURSI), 3-8 July 2011, pp. 2833-2836.

[49] Y. Tong and A. Tennant, "A Two-Channel Time Modulated Linear Array with Adaptive Beamforming", IEEE Transactions on Antenna and Propagation, vol. 60, no. 1, January, 2012, pp. 141-147.

[50] J. Fourier, "The Analytical Theory of Heat", English translation by Freeman, 1878; republication by Dover, New York, 1955.

[51] W. Ng, A. A. Walston, G. L. Tangonan and J. J. Lee, "The first demonstration of an optically steered microwave phased array antenna using true-time-delay", Journal of Lightwave Technology, vol. 9, no. 9, Sep. 1991, pp. 1124-1131.

[52] L. C. Sengupta and S. Sengupta, "Novel ferroelectric materials for phased array antennas", IEEE Transactions on Ultrasonics, Ferroelectrics and Frequency Control, Vol. 44, no. 4, July 1997, pp. 792-797.

[53] A. Ishimaru and H. S. Tuan, "Theory of frequency scanning of antennas", IRE Transactions on Antennas and Propagation, vol. 10, no. 2, March 1962, pp. 144-150.

[54] B. P. Lathi, "Signal Processing and Linear Systems", Berkeley Cambridge, 1998.

Chapter 3 Sideband Suppression in Time Modulated Linear Array

3.1 Introduction

Because of increasing concern regarding the signal quality and channel capacity in communication systems, phased arrays antennas with controlled low sidelobe level have long been studied for commercial and military applications over the past few decades [1]. The challenge of the conventional system is how to generate proper amplitude weighting functions for the array elements and produce a desired array beampattern with controlled low sidelobe level. In this case, the system must be capable of having a very fine tolerance control in the design of feed network.

By introducing time as an additional parameter into the antenna design, the concern of generating a radiation pattern with low or ultralow sidelobe level can be easily achieved by periodically modulating the array elements in a prescribed sequence with RF switches [2]. This novel approach provides an effective way of obtaining the array weights since time is easier and more accurate to control. Despite of the benefits offered by the concept of time modulation, harmonics or sidebands will be generated and consume fractions of the total radiated power, which will degrade the system performance.

In this chapter, two innovative approaches will be introduced to suppress sideband levels and hence minimise sideband radiations. The first technique is based on

reducing the static element weights of the outer elements of a linear array using simple 3dB power dividers, while the other one utilises the fixed bandwidth of the radiating elements of the array to filter out-of-band harmonics.

3.2 Sideband suppression with half-power sub-array techniques

As discussed in Chapter 2, the amplitude weights in a time modulated linear array are synthesised in a time averaged sense, so that the array is controlled by an external programmed circuit with a high degree of precision. Furthermore, a time modulated array is an inherently adaptive system configured to compensate for power variations in the feed networks to individual elements and also to provide real-time pattern control. However, as a consequence of periodic time switching, the array radiates energy at multiples of the modulating frequency.

Much of the recent, and current, research into time-modulated arrays has investigated effective ways for reducing the wasted power radiated into the sidebands, often by employing various adaptive optimisation techniques such as Genetic Algorithms (GA) [3-5], Differential Evolution (DE) Algorithm [6-9] and more recently Particle Swarm Optimisation (PSO) [10-15]. Other approaches to controlling harmonic radiation patterns have included unequal element spacing [16], as well as asymmetrically positioned pulses [17] and pulsing shaping technique [18].

In this particular section, we will examine a new approach based on reducing the

static weights of the outer elements by using simple 3dB power dividers. This approach allows the relative switch-on times of the outer array elements to be increased, which decreases the transients in the time-domain output from the array and results in lower sideband levels [19].

3.2.1 Mathematical model

In a conventional phased array, the static element weights may be chosen to produce a prescribed low-sidelobe radiation pattern using well known distribution functions such as Chebyshev or Taylor weights. However, the static weights in a time-modulated antenna array are set to unity and elements are energised to provide a time-average equivalent weighting coefficients across the array. The energisation times correspond to the effective on-time of each element at the operating frequency, that is $a_{0n} = \tau_{noff} - \tau_{non}$, where a_{0n} represent a prescribed normalised element weighting function. Although this approach produces the desired low sidelobe pattern at the fundamental angular frequency ω, it also generates significant harmonic, or sideband, components at multiples of the modulating angular frequency ω_0. The total power P_T radiated by the antenna array can be evaluated as:

$$P_T = P_0 + P_{SB} \qquad\qquad (3.1)$$

where P_0 is the power at the fundamental frequency and P_{SB} represents the sideband power losses. By definition, the total radiated power is calculated as the square of the magnitude of the array factor, which is given by:

$$P_T = \left| AF(\theta,t) \right|^2 = \left| \sum_{m=-\infty}^{\infty} e^{j(\omega+m\omega_o)t} \sum_{n=0}^{N-1} A_n a_{mn} e^{jknd\sin\theta} \right|^2 \qquad (3.2)$$

Removing the signal modulation (the exponential term) for the purpose of simplicity,

equation (3.2) reduces to $P_T = \left| \sum_{m=-\infty}^{\infty} \sum_{n=0}^{N-1} A_n a_{mn} e^{jknd\sin\theta} \right|^2$. In Bregains et al. [20],

the final closed-form expression of the power losses after a series of derivations is

written as:

$$P_T = \sum_{n=0}^{N-1} \left\{ |A_n|^2 \sum_{m=-\infty}^{\infty} |a_{mn}|^2 \right\} + 2\sum_{\substack{q=1\\q\neq n}}^{N-1} \left\{ \mathrm{Re}\left\langle A_q A_n^* \right\rangle * \mathrm{sinc}[k(d_q - d_n)] \sum_{m=-\infty}^{\infty} a_{mq} a_{mn} \right\}$$

where $\mathrm{sinc}(x) = \sin(x)/x$. The sideband power in the above equation ($m \neq 0$ terms)

results in:

$$P_{SB} = \sum_{n=0}^{N-1} \left\{ |A_n|^2 \sum_{\substack{m=-\infty\\m\neq 0}}^{\infty} |a_{mn}|^2 \right\} + 2\sum_{\substack{q=1\\q\neq n}}^{N-1} \left\{ \mathrm{Re}\left\langle A_q A_n^* \right\rangle * \mathrm{sinc}[k(d_q - d_n)] \sum_{\substack{m=-\infty\\m\neq 0}}^{\infty} a_{mq} a_{mn} \right\}$$

Substituting $d = 0.5\lambda$ into the above equation leads to:

$$P_{SB} = \sum_{n=0}^{N-1} \left\{ |A_n|^2 \sum_{\substack{m=-\infty\\m\neq 0}}^{\infty} |a_{mn}|^2 \right\} + 2\sum_{\substack{q=1\\q\neq n}}^{N-1} \left\{ \mathrm{Re}\left\langle A_q A_n^* \right\rangle * \mathrm{sinc}[\pi(q - n)] \sum_{\substack{m=-\infty\\m\neq 0}}^{\infty} a_{mq} a_{mn} \right\}$$

The second term in the brackets is removed as the sinc function equals zero. The final

term can be obtained:

$$P_{SB} = \sum_{n=0}^{N-1} \left\{ |A_n|^2 \sum_{\substack{m=-\infty\\m\neq 0}}^{\infty} |a_{mn}|^2 \right\} \qquad (3.3)$$

It can be seen that the sideband power losses are only a function of two variables, the static element weights A_n and the harmonic Fourier coefficients a_{mn}.

By definition, the directivity associated with an array factor of a linear array is given by [21]:

$$D_0 = \frac{U_{max}}{P_{rad} / 4\pi}$$

$$= \frac{\max \left| \sum_{n=0}^{N-1} A_n e^{jknd \sin\theta} \right|^2}{\frac{1}{4\pi} \int_0^{2\pi} \int_0^{\pi} \left| \sum_{n=0}^{N-1} A_n e^{jknd \sin\theta} \right|^2 \sin\theta \, d\theta \, d\phi} \tag{3.4}$$

where U_{max} is the maximum radiation intensity and P_{rad} is total radiated power. The directivity of time modulated linear array is evaluated by [22]:

$$D_0 = \frac{U_{max}}{P_{rad} / 4\pi}$$

$$= \frac{\max \left| \sum_{m=-\infty}^{\infty} \sum_{n=0}^{N-1} A_n a_{mn} e^{jknd \sin\theta} \right|^2}{\frac{1}{4\pi} \int_0^{2\pi} \int_0^{\pi} \left| \sum_{m=-\infty}^{\infty} \sum_{n=0}^{N-1} A_n a_{mn} e^{jknd \sin\theta} \right|^2 \sin\theta \, d\theta \, d\phi} \tag{3.5}$$

The final closed form can be written as:

$$D_0 = \frac{\max \left| \sum_{n=0}^{N-1} A_n a_{0n} e^{jknd \sin\theta} \right|^2}{a_0 \sum_{n=0}^{N-1} (A_n a_{0n})^2 [1 + 2\sum_{m=1}^{\infty} \mathrm{sinc}^2(\pi m a_{0n})] + \sum_{n=0}^{N-1} \sum_{\substack{t=0 \\ t\neq n}}^{N-1} (A_n a_{0n})(A_t a_{0t})[a_1 \frac{\sin kd(n-t)}{kd(n-t)}}$$

$$+ a_2 \frac{\cos kd(n-t)}{kd(n-t)}] \left\{ 1 + 2\sum_{m=1}^{\infty} \mathrm{sinc}^2(\pi m a_{0n}) \mathrm{sinc}^2(\pi m a_{0t}) \cos[\pi m(a_{0n} - a_{0t})] \right\} \tag{3.6}$$

where $a_0=1$, $a_1=1$, $a_2=0$ for isotropic element, and t is the element number that is not equal to n. Assuming the element spacing d = 0.5λ, equation (3.6) simplifies to:

$$D_0 = \frac{\max\left|\sum_{n=0}^{N-1} A_n a_{0n} e^{jknd\sin\theta}\right|^2}{a_0 \sum_{n=0}^{N-1} (A_n a_{0n})^2 [1 + 2\sum_{m=1}^{\infty} \mathrm{sinc}^2(\pi m a_{0n})]} \qquad (3.7)$$

The second term in the denominator goes to zero as sine term equals zero (because $\sin kd(n\text{-}t) = \sin[\frac{2\pi}{\lambda}*0.5\lambda(n\text{-}t)] = \sin[\pi(n\text{-}t)] = 0$, where (n-t) is a positive integer).

3.2.2 Design procedures for the feed network

A variety of approaches for reducing the sideband levels in time-modulated antenna arrays have been investigated, including the use of off-set element switching [23] and the use of combined time-switching with variable static weights [24]. The latter approach introduces an extra degree of flexibility into the design and has been used in conjunction with adaptive optimisation techniques to design time-modulated arrays with reduced sideband levels. The philosophy behind this approach is to combine a set of static weights with element energisation times, which satisfy the following relationship at the fundamental frequency: $a_{0n} = A_n (\tau_{noff} - \tau_{non})$.

However, although the dynamic range of static weights may be constrained, the actual magnitudes of the weights may take any value within the range. Consequently, in a practical implementation of this design, the amplitudes of static weights would need

to be derived from a specific power dividing networks or by using a set of attenuators - an approach which undermines the original simplicity of the time modulated linear array concept.

Hence we propose a new technique [19] in which the elements of a time modulated array are designed to have fixed amplitude coefficients B_n given by $2^{-x/2}$ where x is a positive integer indicating the level of the feed network. Such a scheme can easily be implemented using simple combinations of 3dB power dividing networks. Under this modified scheme, the new relationship for the element energisation times at fundamental frequency becomes $a_{0n} = B_n (\tau_{noff} - \tau_{non})$.

We also note the constraint that the product $B_n (\tau_{noff} - \tau_{non})$ must be less than or equal to unity, which implies that 3dB power dividing networks can only be applied to the outer few elements of the array. The exact number of elements that can be driven with power dividing networks will depend on the weighting function, but in general the lower the prescribed sidelobe level, the greater will be the number of elements to which the power dividing network can be applied. An example topology employing half-power sub-arraying is shown in Fig.3.1.
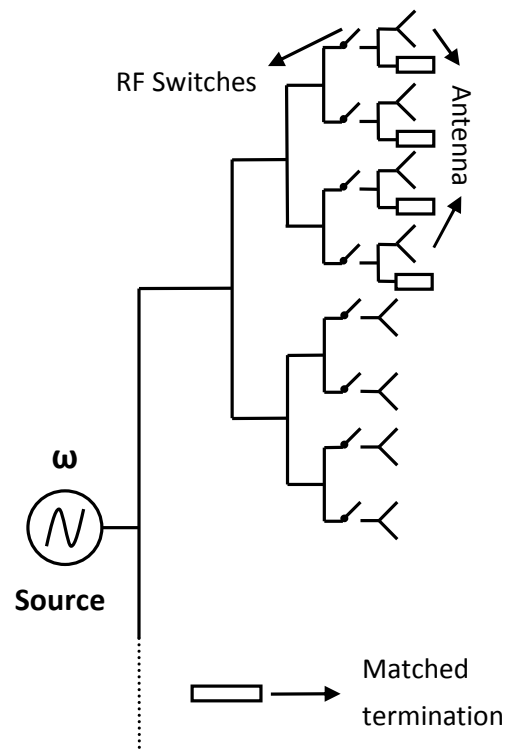
Fig.3.1. Example topology of a time-modulated array with half-power sub-arraying

(Case B).

To better illustrate the half-power sub-array technique we consider three cases based

on a 16-element time modulated linear array with half-wavelength element spacing,

each example is designed to produce -40dB Taylor sidelobe levels at the fundamental

frequency of operation and all the examples are implemented by using MATLAB

software.

Case A: A conventional time modulated array with uniform amplitude static

element weights (x=0).

Case B: A time modulated array in which elements 5-12 have uniform amplitude and elements 1-4 and 13-16 are energised with a relative amplitude of $\dfrac{1}{\sqrt{2}}$ (x=1).

Case C: A time modulated array in which elements 5-12 have uniform amplitude, elements 3-4 and 12-13 are energised with a relative amplitude of 0.5 (x=2) and elements 1-2 and 15-16 with a relative amplitude of 0.25 (x=4).

3.2.3 Numerical examples
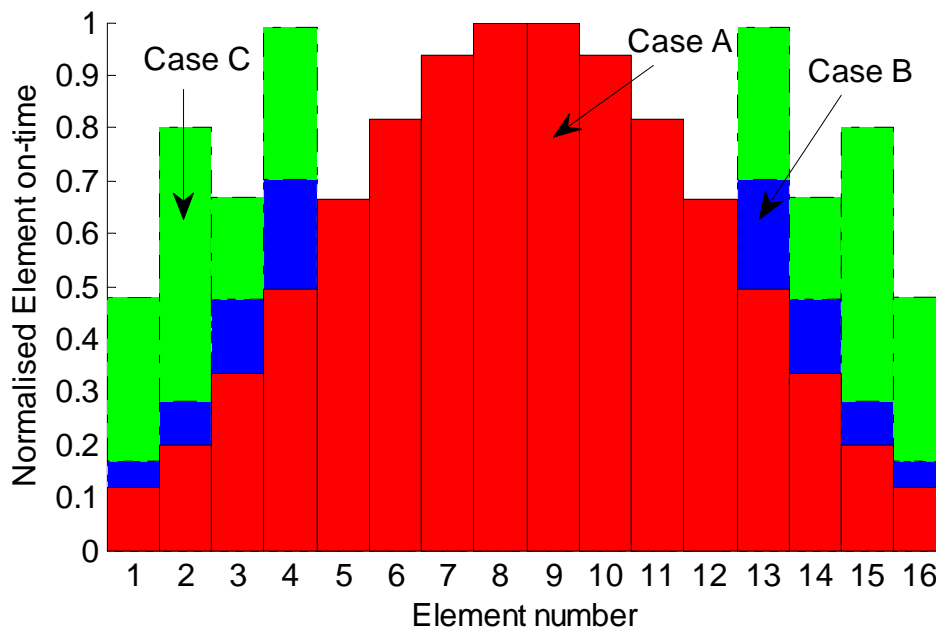
Fig.3.2. Time sequence corresponds to -40 dB Taylor weights. (Red – Case A, Blue –

Case B and Green – Case C)
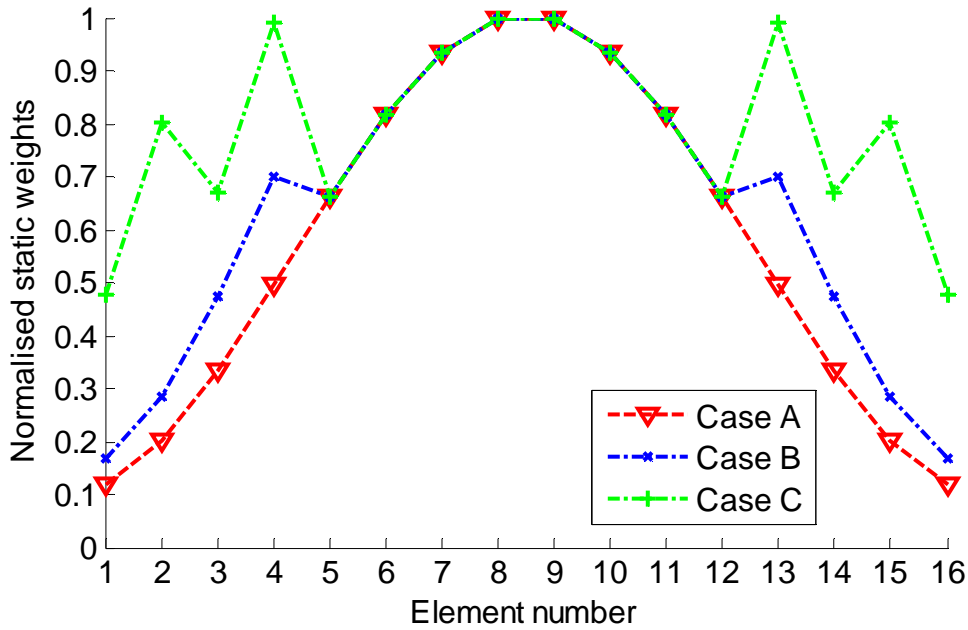
Fig.3.3. Normalised amplitude weighting corresponds to -40 dB Taylor weights. (Red

– Case A, Blue – Case B and Green – Case C)

The corresponding normalised element energisation time sequence and related

amplitude weighting function for each of the above cases are shown in Fig.3.2 and

Fig.3.3. For case A (uniform amplitude static weights) the normalised element

on-times relates to the Taylor distribution. For case B, the on-times of the outermost 4

elements of the array are increased by $\sqrt{2}$ to account for the 3dB reduction in power.

Similarly, for case C, the on-time of the elements driven with relative power levels of

-6dB and -12dB has been increased by factors of 2 and 4 respectively.

To understand how this approach can reduce sideband radiation, we know that the

effective on-times ($\tau_{noff} - \tau_{non}$) control the magnitude of the Fourier coefficients. In

particular, as ($\tau_{noff} - \tau_{non}$) approaches 1 the amplitude of the Fourier coefficients (for

$|m| > 0$) tends to zero, as described in [20]. Hence by increasing the on-time of the

array elements using 3dB power dividing networks, we can decrease the magnitude of

the Fourier coefficients and thus reduce the sideband radiation. An alternative and

perhaps more intuitive insight can be gained by examining the time domain output

from the array defined by:

$$S_{out}(t) = \max \left| \sum_{n=0}^{N-1} B_n e^{jknd \sin \theta} \right| \qquad (3.8)$$
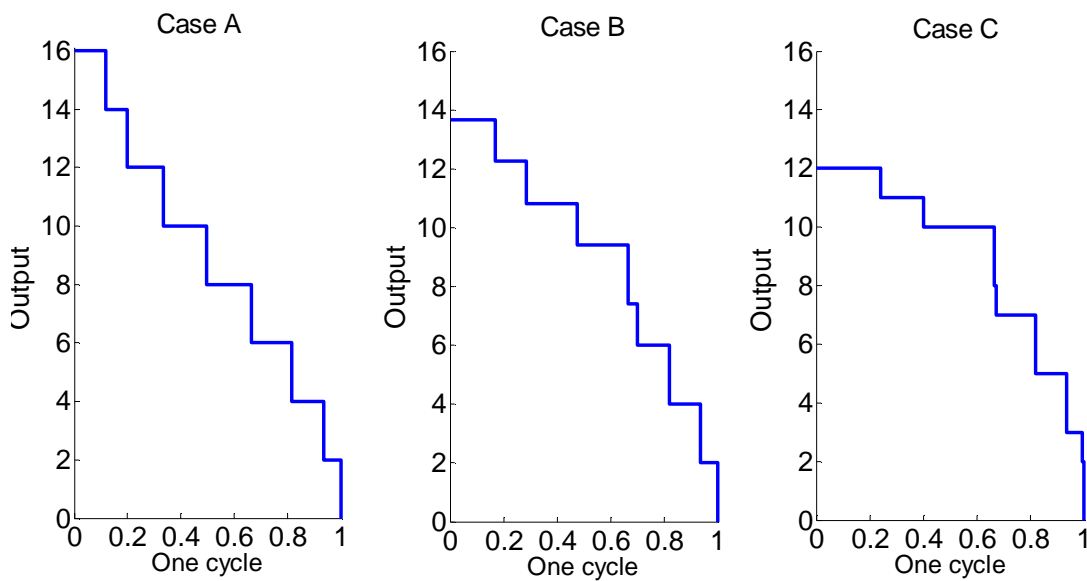
Fig.3.4. Time-domain array output signal at boresight over one switching cycle.

An example is given in Fig.3.4 which shows the output signal from the array at the

boresight direction ($\theta=0$) over one switching cycle for each of the above 3 cases (note

that $\theta=0$ is the direction of maximum radiation intensity). Basic Fourier analysis

informs us that transients in the time domain give rise to harmonics in the frequency

domain, so reducing time domain transients will consequently decrease the harmonic

content of the signal.

For case A, the output signal resembles a staircase waveform with a peak value of 16

which corresponds to all the elements of the array being simultaneously energised. As

in this example of static weights is unity, the output from the array then reduces in

magnitude by units of 2 as pairs of elements are switched off. For case B, where the

outer elements of the array are energised with $\sqrt{2}$ amplitude weighting, both the peak

output level and the transients in the output signal have been reduced compared to

case A. A further reduction of the transients in the time domain output signal is seen

for case C, where the amplitude weights have been applied to the outer elements of

the array increased by a magnitude of 2 and 4 respectively.
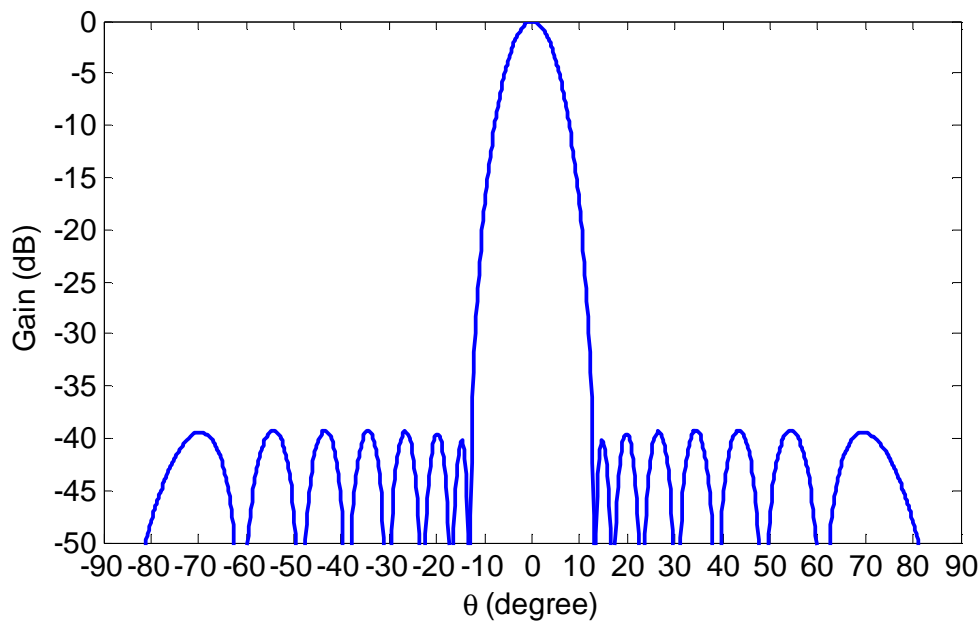
Fig.3.5. Array pattern at the fundamental frequency, for case A, B and C with -40dB

Taylor weighting function.

Fig.3.5 shows the array pattern at the fundamental angular frequency ω, obtained from Cases A, B and C. In each case the desired -40dB sidelobe level has been achieved. To quantify the effectiveness of the proposed scheme in reducing the energy radiated in the harmonic frequencies, Fig.3.6 and Fig.3.7 show the maximum sideband level and the average power level of the harmonic patterns for each of the three example cases. The value of the average power level has been derived numerically from pattern integration and the maximum sideband level is obtained by a simple numerical search algorithm. The sampling frequency used to plot the radiation pattern is chosen to be 20 samples per degree.
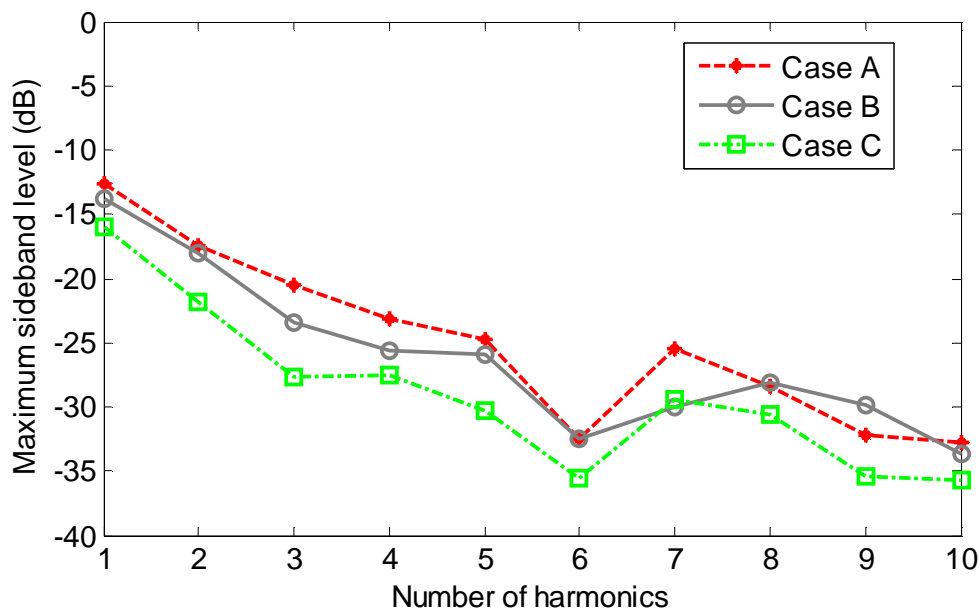
Fig.3.6. Maximum sideband level at the first 10 harmonic frequencies. (Red – Case A,

Gray – Case B and Green – Case C)
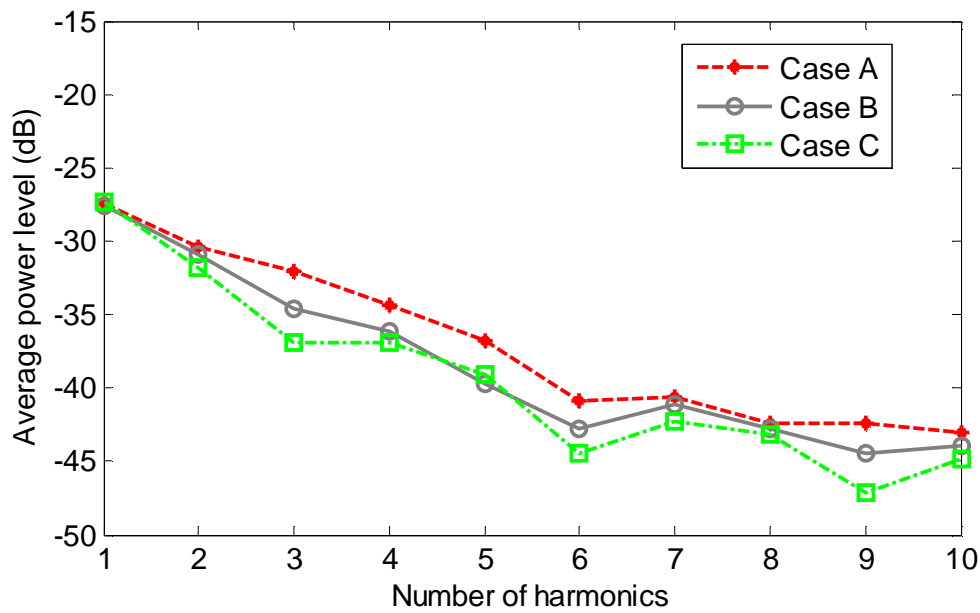
Fig.3.7. Average power level at the first 10 harmonic frequencies.

The radiation pattern of first harmonic for all cases is shown in Fig.3.8. The power in

all the sidebands in percentage terms is defined as $\eta_{SB} = \dfrac{\text{power in all sidebands}}{\text{Total radiated power}}$. For

each of the above three examples cases, η_{SB} is 25.51%, 19.6% and 13.08%

respectively. It is worth mentioning that although some ports of the feed network are

terminated by loads, the total power radiated by the array remains constant in Case A,

Case B and Case C, since the areas under each curve in Fig.3.4 are equal. On the other

hand, the improved efficiency can be better explained by calculating the directivity

using equation (3.7). The results are 9.1378, 9.9412 and 10.2808 respectively.
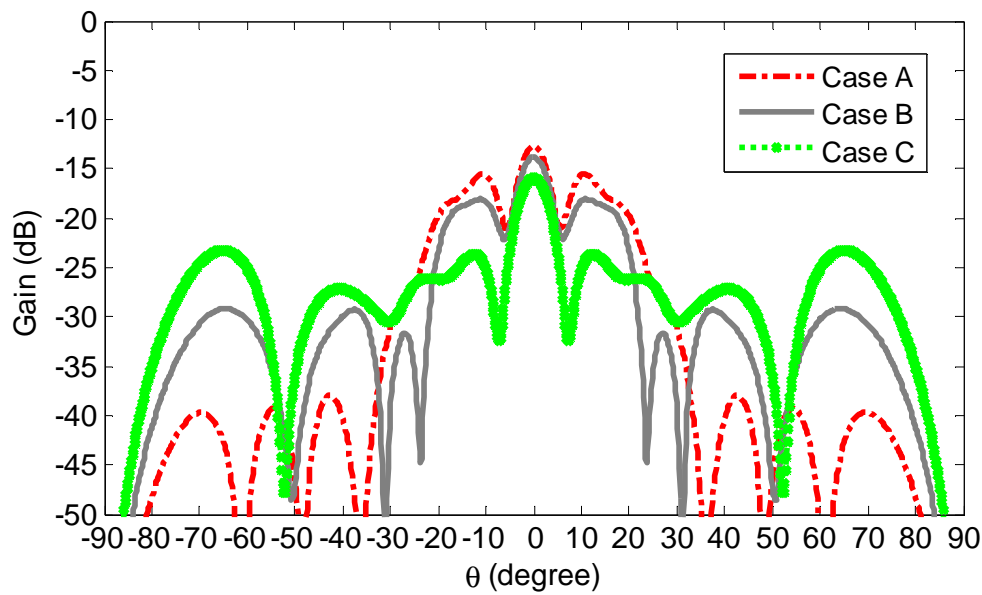
Fig.3.8. First harmonic radiation pattern for Case A, B and C. (Red – Case A, Gray –

Case B and Green – Case C)

3.2.4 Summary

A new approach to reducing the sideband radiation of low-sidelobe time-modulated

arrays has been described. The technique combines conventional time-switching with

$2^{-x/2}$ static weights of selective array elements. Such an amplitude weighting scheme

is simple to implement using 3dB power dividing networks in the array feed network.

When compared to a conventional time-switching scheme, the new approach has

demonstrated a reduction in both the maximum sideband levels and average power

levels at the harmonic patterns, and provides a significant improvement for

minimising the sideband radiation power from 25.51% to 13.08%, as well as

increasing directivity from 9.1378 to 10.2808.

3.3 Sideband suppression with fixed bandwidth elements techniques

The utilisation of a TMLA with a simple 3dB power dividing networks combined with a conventional time sequence has a great advantage of reducing the sideband levels and improving radiation efficiency. In this section, another approach for suppressing the sideband levels in time-modulated linear arrays (TMLA) with uniform static weights is presented [25-26].

The technique utilises the fixed bandwidth of the radiating elements of the array to act as band-pass filters to suppress the out of band harmonics generated by the time-modulation process. It is combined with a new switching sequence which divides the original switching sequence into sub-sequences that can be designed to redistribute the dominant harmonic components of the TMLA to predetermined frequencies, which are outside the bandwidth of the array elements. This method does not require the use of any optimisation algorithm to generate the TMLA switching sequences and is applicable to a TMLA configured to synthesise arbitrary low-sidelobe patterns. Numerical results are presented to illustrate the proposed approach by considering a 16-element array of patch antenna elements designed to provide a radiation pattern with a -30dB sidelobe levels. A significant reduction of sideband levels from -13.5dB to -28.7dB has been achieved.

3.3.1 Theoretical background

Fourier coefficients in the Time modulated Antenna Array is given by:

$$a_{mn} = (\tau_{noff} - \tau_{non}) \frac{\sin[m\pi(\tau_{noff} - \tau_{non})]}{m\pi(\tau_{noff} - \tau_{non})} e^{-j\pi m(\tau_{noff} + \tau_{non})} \qquad (3.9)$$

where τ_{non} and τ_{noff} are the switched on and off time of the nth elements respectively.

Different Fourier coefficients correspond to different harmonic radiation patterns.

In (3.9), we can see that the magnitude of Fourier coefficients are determined by the

effective on times of array elements and the sinc function $\frac{\sin[m\pi(\tau_{noff} - \tau_{non})]}{m\pi(\tau_{noff} - \tau_{non})}$,

where sinc(x) = sin(x)/x. Bregains et al. [20] suggested a way of reducing the

sideband radiation by decreasing the magnitude of Fourier coefficients and increasing

the angular frequency separation from the carrier frequency.

With a good antenna design in hand, the next step is to design a proper time scheme

that is able shift harmonics outside the bandwidth of the receiving antenna. Dividing a

continuous time sequence into multiple equal smaller time steps provide the benefits

of controlling the radiation characteristics of harmonics. A representation of this

switching scheme is drawn below:
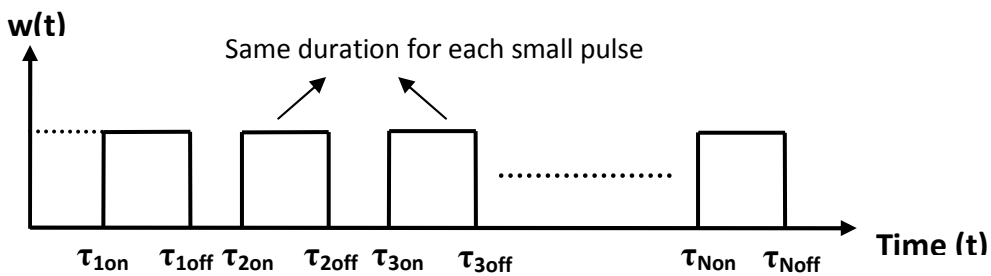
Fig.3.9. A representation of the new switching scheme.

Considering a generalised case of dividing a normal time sequence into N equal steps, the Fourier coefficients can be rearranged as:

$$a_{mn} = \frac{\sin[m\pi(\tau_{1\text{off}} - \tau_{1\text{on}})]}{m\pi} \, e^{-j\pi m(\tau_{1\text{off}} + \tau_{1\text{on}})} + \frac{\sin[m\pi(\tau_{2\text{off}} - \tau_{2\text{on}})]}{m\pi} \, e^{-j\pi m(\tau_{2\text{off}} + \tau_{2\text{on}})}$$

$$+ \text{........} + \frac{\sin[m\pi(\tau_{N\text{off}} - \tau_{N\text{on}})]}{m\pi} \, e^{-j\pi m(\tau_{N\text{off}} + \tau_{N\text{on}})} \tag{3.10}$$

Such design technique is analogous to decreasing the modulation period by a factor of x, so the harmonics are re-distributed over the space depending on the number of x (as f = 1/T).

3.3.2 Design Procedures of new time sequence and patch antenna

The starting point for our investigation is a conventional 16 elements time modulated linear array which is assumed to consist of isotropic elements spaced by half wavelength. Firstly a 16-element TMLA is designed to produce a Chebyshev array with -30dB sidelobe level at the fundamental frequency. Such a sequence is shown in Fig.3.10 and it demonstrates that all the array elements have a common switch on time and a switch off time corresponding to the Chebyshev amplitude weighting function. The maximum sideband levels produced by the time sequence at the first 30 positive harmonic frequencies are drawn in Fig.3.11, where it is observed that the sideband levels of the first harmonic is relatively high at levels of around -12dB.
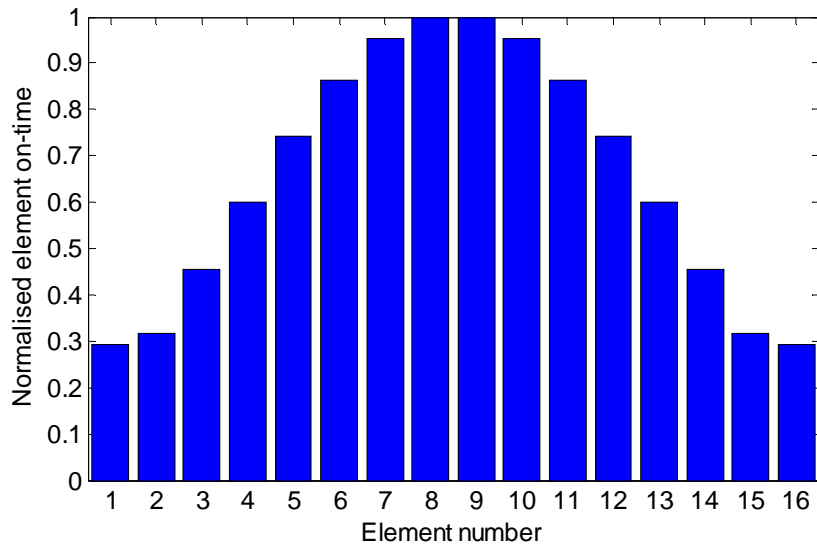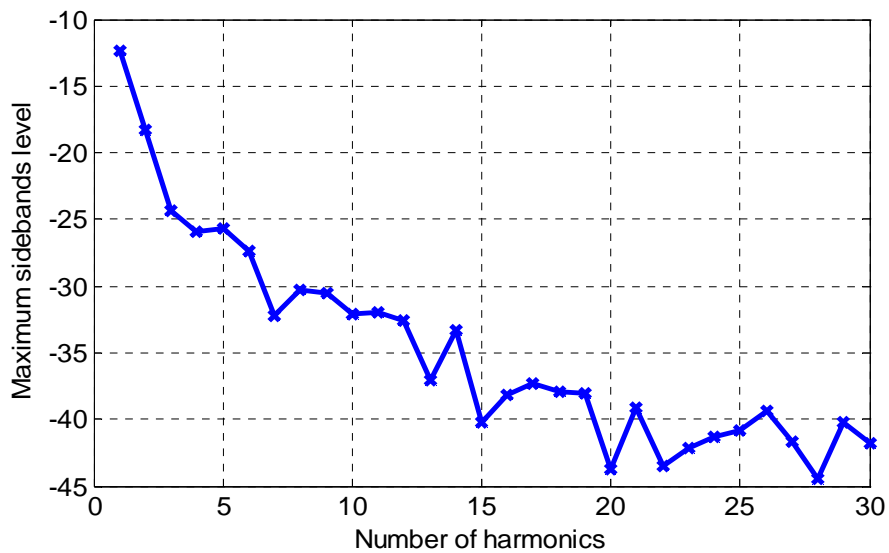
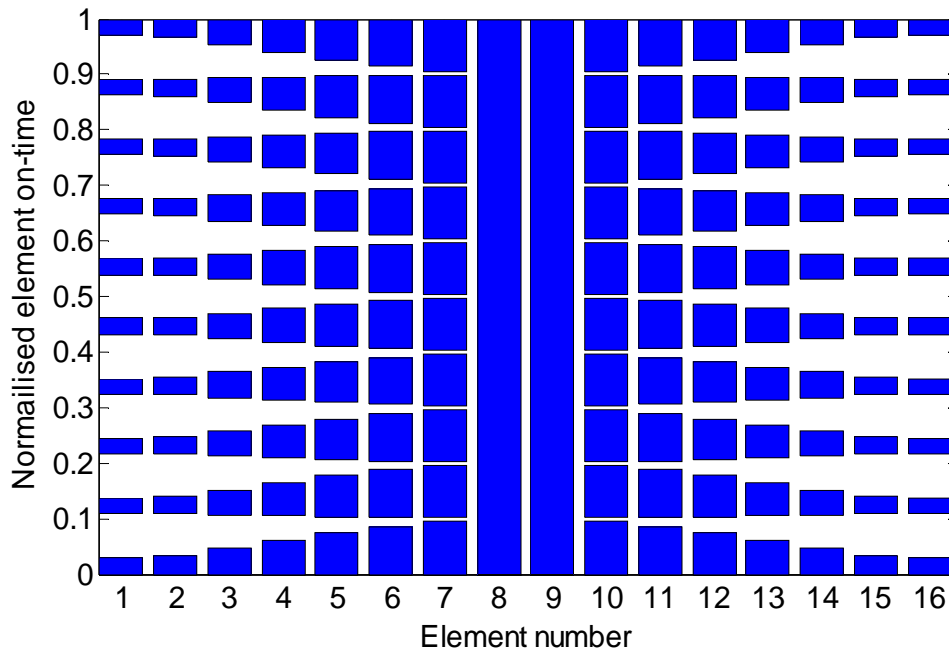Fig.3.10. Conventional time switching sequence.
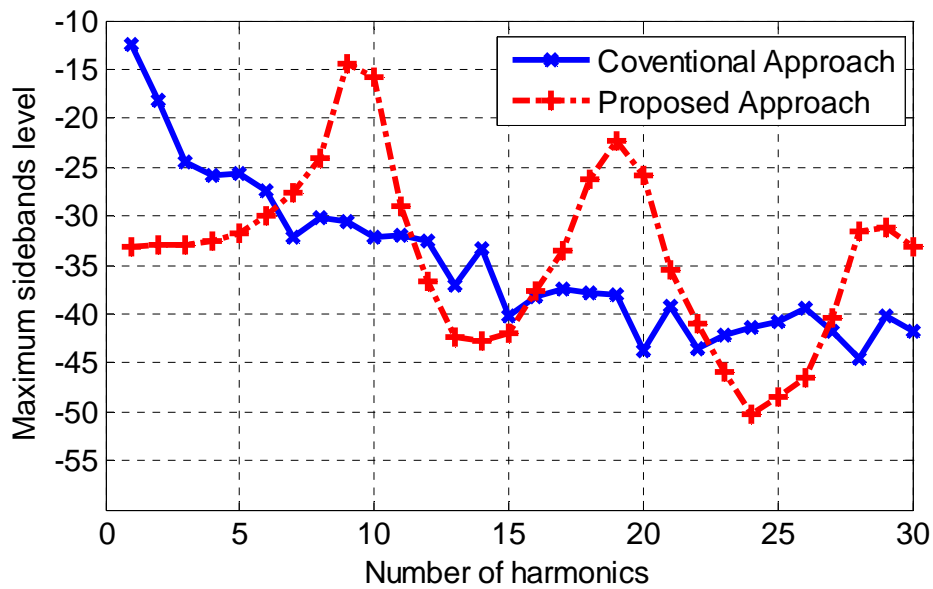

Fig.3.11. The maximum sideband levels of the first 30 positive harmonics produced

by the conventional and the proposed switching sequence。

Now consider a modification of the conventional switching sequence in which 'on'

time of the array elements (excluding the 2 central elements) has been subdivided into

10 smaller energisation periods as shown in Fig.3.12.This switching sequence still

maintains the beampattern with desired sidelobe level at the fundamental frequency,

but the distribution of energy within the harmonic frequencies has been changed

significantly.

Fig.3.12. Modified time switching sequence.

Fig.3.13. The maximum sideband levels of the first 30 positive harmonics produced

by the conventional and the proposed switching sequence.

In Fig.3.13, it can be noticed that the maximum sideband levels at the 30 positive harmonics have been redistributed at an approximate factor of 10 compared to the conventional approach.

To explore this concept, the next step is to deal with the design of the proper antenna element. The simulation software used is CST Microwave Studio®, which is a computing package based on Finite Integration Technique (FIT). It provides a good solution for electromagnetic modelling like static filed calculation, as well as the radio frequency (RF) circuit design.

In this example, a simple patch antenna was simulated in the Transient Solver in CST and it is designed to operate at 2.45GHz with a fixed bandwidth of 30MHz. Slotted lines are used to match the patch to the 50 Ohm microstrip line with a width of 3mm. The substrate material used in this design is normal FR-4 with a thickness of 1.6mm and a relativity permittivity of 4.5. Detailed geometry of the patch antenna and its bottom view are described in Fig.3.14 and Fig.3.15 respectively.
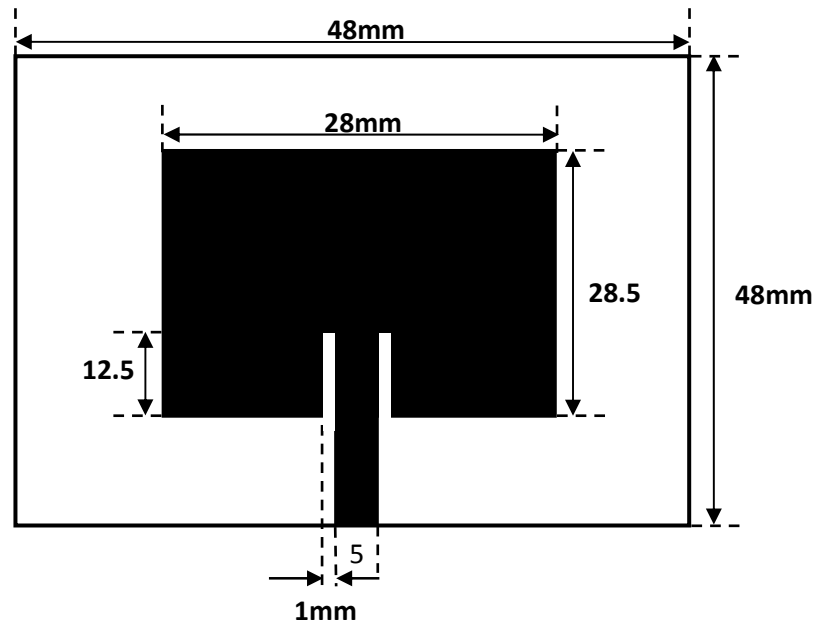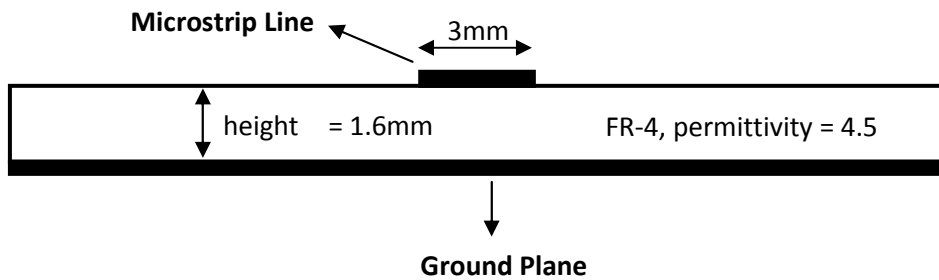
Fig.3.14. Detailed geometry of the patch antenna (mm).

Fig.3.15. Bottom view of the patch antenna.

3.3.3 Simulation results of the patch antenna

The scattering parameters are often used to describe the antenna performance. The reflection coefficient Γ of an antenna is defined by the ratio of the power reflected back to the total input power [27]. The reflection coefficient in dB is expressed as $20\log|\Gamma|$. In this particular example, the transmission line impedance is 50 ohms and the reflection coefficient of the patch antenna element is plotted in Fig.3.16.
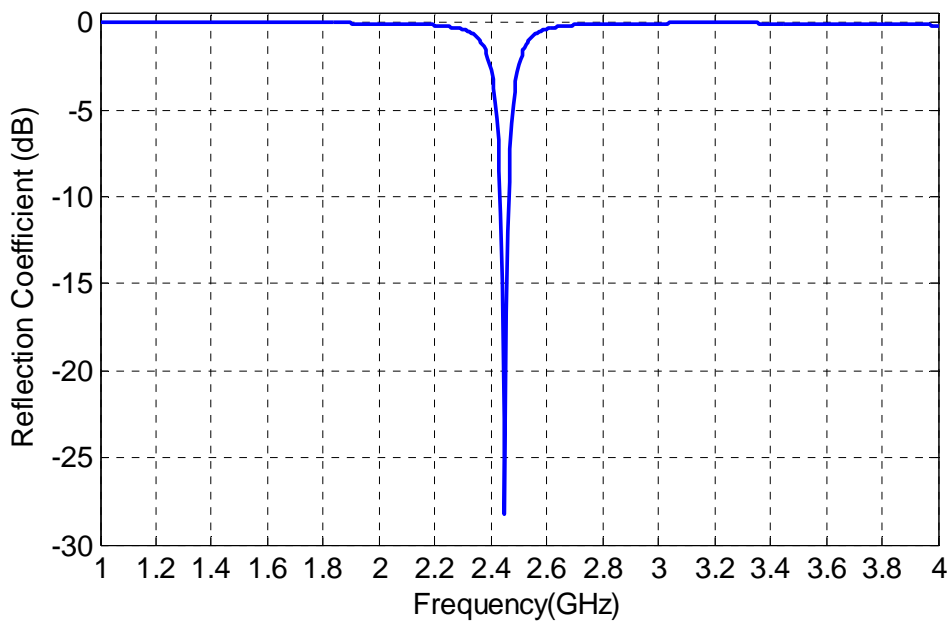
Fig.3.16. Reflection coefficient in dB of patch antenna.

From the graph, we can see that the designed patch antenna operates at 2.45GHz with

a -10dB bandwidth from 2.435GHz to 2.465GHz. Another important S-parameter is

transmission coefficient τ which measures the efficiency of transmitted power defined

by [27] $\upsilon = 1 - |\Gamma|^2$. The normalised transmission coefficient of interest in the linear

form is drawn in Fig.3.17. The results presented so far have only considered an array

consisting of isotropic radiators, mainly the array factor. However, an array with a

more directive element pattern – such as a patch antenna is considered for this design,

then the principle of pattern multiplication has to be utilised. Assuming there is no

mutual coupling between the patch antenna, and the theory of pattern multiplication

describes that the total field of the array is the product of radiation pattern of a single

element multiplied by the array factor [22]. The element pattern of designed patch
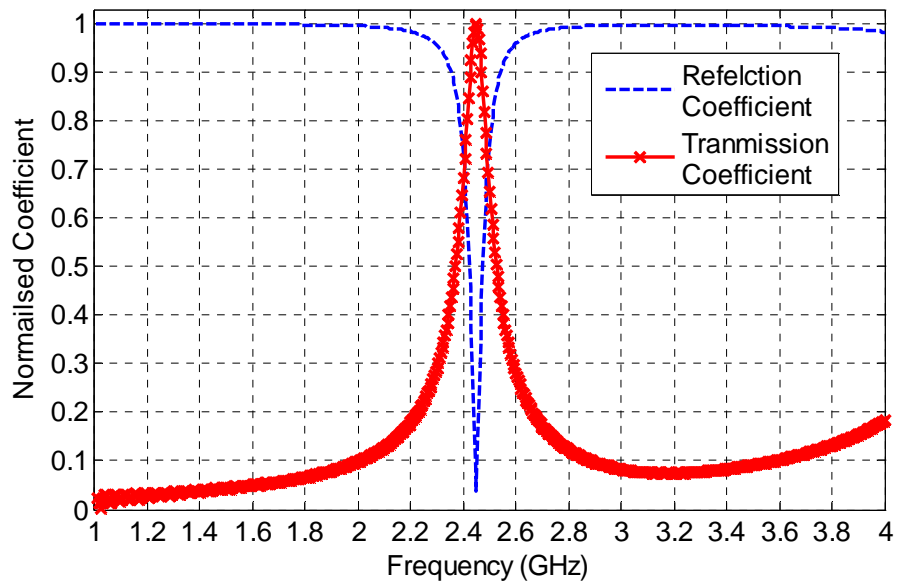
antenna is presented in Fig.3.18.

Fig.3.17. The reflection and transmission coefficient of a printed patch antenna

designed to operate at 2.45GHz.

With these principles in mind, let us examine a situation where the new switching

time sequence is combined with the patch antenna designed to work at 2.45GHz of

30MHz fixed bandwidth. The resultant radiation pattern at the fundamental frequency

is calculated as the product of the conventional array factor multiplied by the element

pattern of the patch antenna. The corresponding pattern is shown in Fig.3.19.
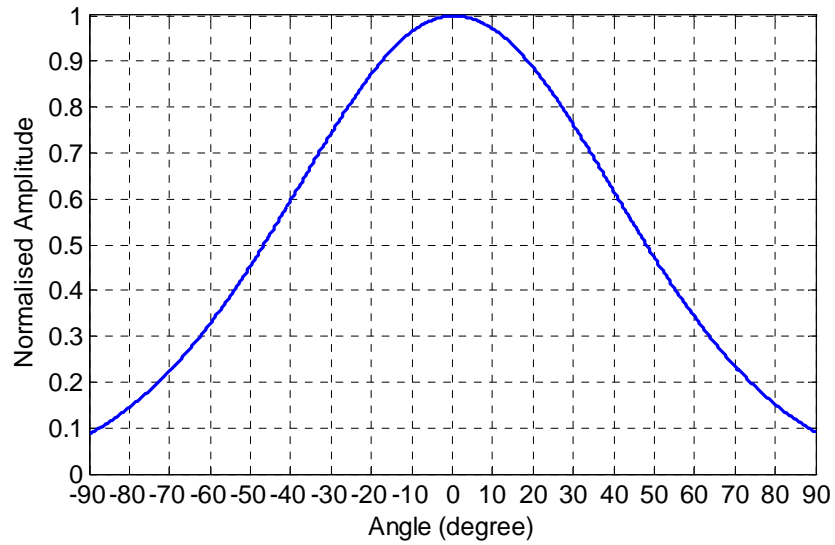
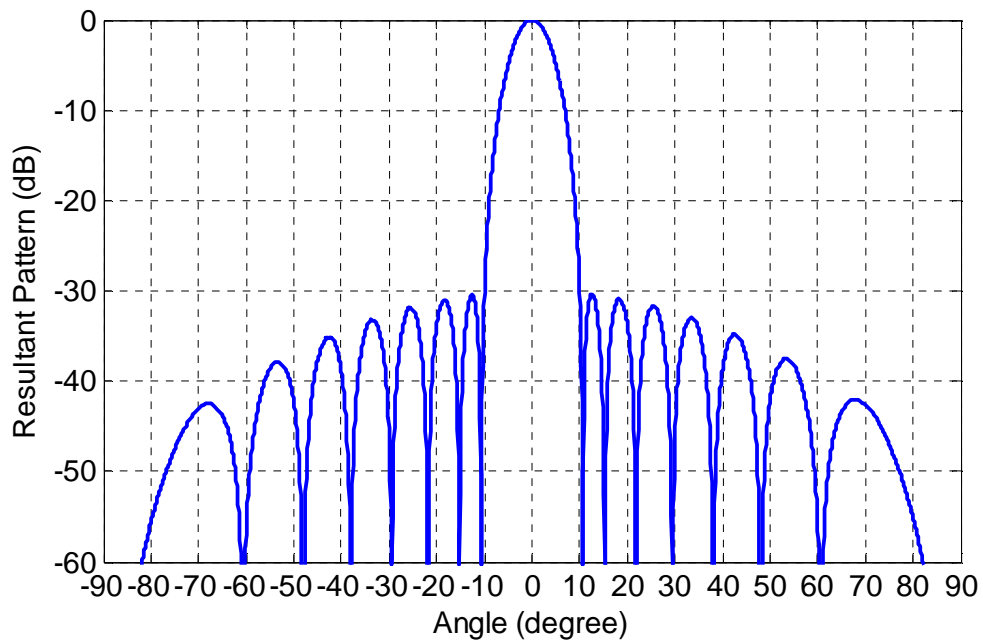Fig.3.18. Element pattern of a single patch antenna designed to work at 2.45GHz.

Fig.3.19. The resultant radiation pattern of combining the new switching sequence

(Fig.3.12) with the designed patch antenna (Fig.3.14).

In Fig.3.19 the resultant beam pattern still produces the desired sidelobe levels of -30dB at the fundamental frequency, but at a decayed rate defined by the element pattern of patch antenna. If the modulation period is chosen to be 25MHz, the first positive harmonic is at 2.475GHz (2.45+0.025) which is outside the bandwidth of the patch antenna, as well as all the remaining harmonic patterns. The comparison of sidebands levels at the first positive 30 harmonics between the conventional approach and the proposed scheme is demonstrated in Fig.3.20.
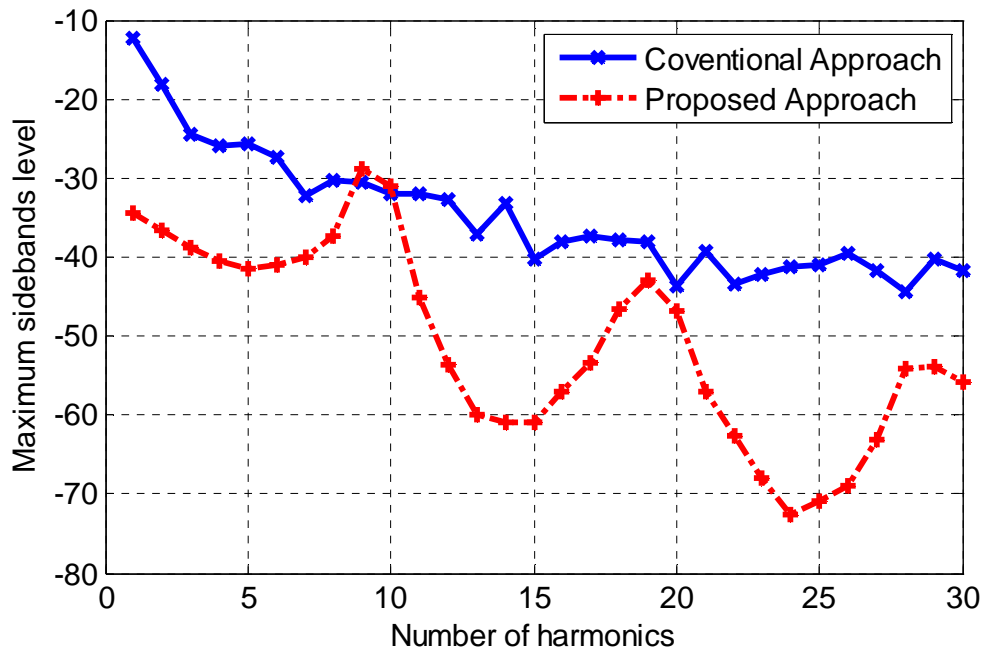

Fig.3.20. The maximum sideband levels at the first 30 positive harmonics produced by the conventional and the proposed switching sequence when combined with the patch antenna of finite bandwidth (modulation frequency = 25MHz).

Combining the designed patch antenna of finite bandwidth with the modified
sequence in Fig.3.12, the sideband levels of all the harmonics are suppressed to
approximately below -28.7dB and this is shown in Fig.3.20. Therefore, the proposed
approach demonstrates a much better performance of an additional 12.4dB reduction
of the sideband level compared to the conventional technique.

Another example is to double the modulation frequency from 25MHz to 50MHz, the
corresponding maximum sideband levels of first positive 30 harmonics between the
conventional approach and the proposed scheme are illustrated in Fig.3.21.
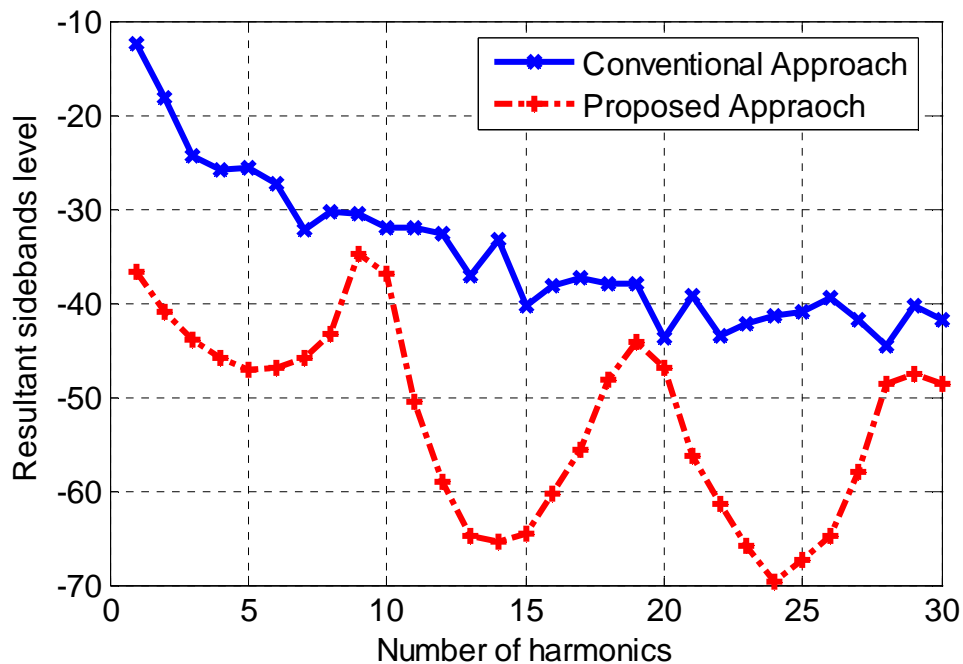

Fig.3.21. The maximum sideband levels at the first 30 positive harmonics produced

by the conventional, proposed switching sequence when combined with the designed

patch antenna of finite bandwidth (modulation frequency = 50MHz).

It can be easily seen that increasing the modulation frequency exhibits superior performance, because harmonics can be shifted out of the antenna bandwidth. The maximum sideband levels are all reduced to below -35dB, the results have shown a significant improvement compared with the conventional method. Apart from these, this proposed technique is also compatible with the half power sub-array approach. Assuming a modified time scheme of 16-element linear array to synthesise a radiation pattern with a -30dB Chebyshev sidelobe level at the fundamental frequency, elements 4-13 have uniform amplitude and elements 1-3 and 14-16 are energised with relative amplitude of 2. Now the switched on-times of arrays elements (excluding the 2 central elements) has been partitioned into 10 smaller equal periods as shown in Fig.3.22.
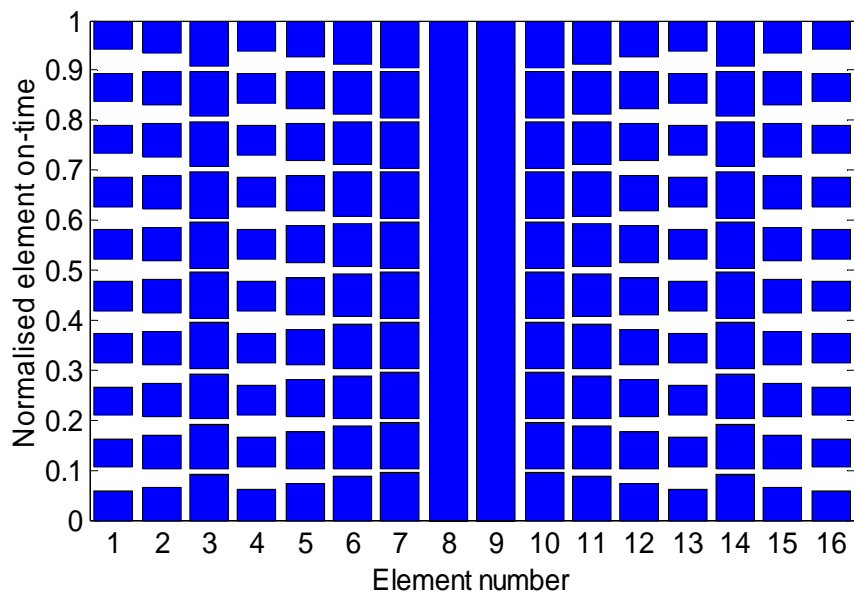

Fig.3.22. Modified time sequence combined with half-power subarray technique.

The modulation frequency is assumed to be 25MHz and the results for maximum sideband levels at first 30 positive harmonics between the conventional method, proposed approach and the proposed approach combined with half power subarray technique are shown below:
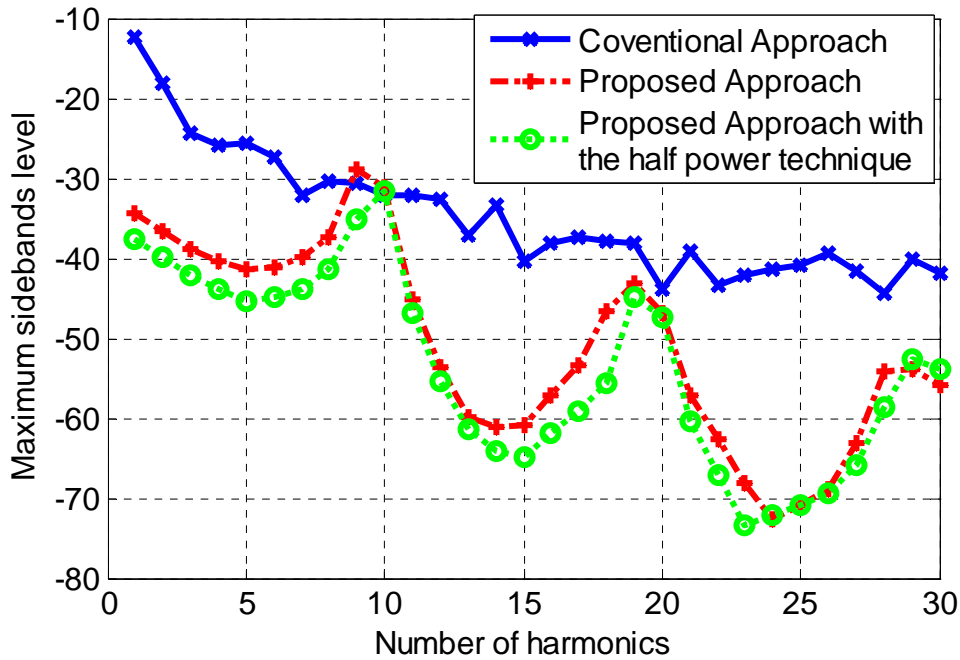

Fig.3.23. The maximum sideband levels at the first 30 positive harmonics produced by the conventional, the proposed switching sequence and the proposed approach when combined with half power subarray technique (modulation frequency = 25MHz).

Fig.3.23 states that the maximum sideband level is reduced by 3dB from -28.7 dB to -31.7dB and all the harmonic patterns are successfully suppressed below -30dB. More

importantly, the sideband radiation power has been reduced significantly from 24.2%

to 15.6% in the case of using half power technique.

However, the drawback of this proposed approach is that there might be a possibility

when multiple resonant frequencies of the designed patch antenna are coincident with

the harmonic frequencies. In this case, harmonics outside the bandwidth of the pstvh

antenna can not be suppressed successfully.

3.3.4 Summary

A new approach to the problem of sideband level suppression in time-modulated

linear arrays has been introduced. The technique uses subdivision of the array element

energisation periods to redistribute the sideband energy to higher order harmonic

modes. Combining this method with an array element designed to have a finite

pass-band, the proposed technique has a significant reduction in sideband levels. A

number of numerical examples have shown that all sideband levels can be

successfully decreased to below -28.7dB in a comparison with a conventional

time-switching scheme. Furthermore, the half power subarray technique can be

applied directly to the proposed technique in order to improve the radiation efficiency

by approximately 10%.

3.4 Conclusion

Two novel approaches of reducing the sideband levels and sideband radiation power have been introduced in this chapter. Conventional techniques address the problem by using various optimisation algorithms. The half-power subarray technique is based on adjusting the amplitude of the static element weights by simply using 3dB power dividers and the on-times of selected elements are increased by a magnitude of $2^{x/2}$, where x is a positive integer. The transient time domain variation of the signal for each array element is well reduced from the time domain prospective. Finally, simulation results are given to demonstrate a significant improvement for the sideband level reduction and radiation efficiency can be achieved compared to the conventional method.

In the practical system, the array elements are not ideal isotropic radiators, so another methodology is proposed to use a directional element pattern with a fixed bandwidth. This provides an additional degree of freedom when controlling the time sequence to produce desired radiation patterns with controlled sidelobe level. By dividing the conventional time scheme into multiple equal steps, we are able to shift the harmonics outside the bandwidth of the antenna array. In this case, maximum sideband levels can be reduced to approximately below -28.7dB. Finally, it is worth mentioning that half power subarray technique can also be applied to further suppress the sideband level and improve the radiation efficiency.

References

[1] B. Allen and M. Ghavami, Adaptive Array Systems: Fundamentals and Applications. John Wiley & Sons, Inc., Chichester, UK, 2005.

[2] H. E. Shanks and R. W. Bickmore, "Four-dimensional electromagnetic radiators", Canadian Journal of Physics, vol. 37, 1959, pp. 263-275.

[3] S. Yang, Y. B. Gan, A. Qing, and P. K. Tan, "Design of uniform amplitude time modulated linear array with optimized time sequences", IEEE Transactions on Antenna and Propagation, vol. 53, no. 7, July 2005, pp. 2337-2339.

[4] G. R. Hardel, N. T. Yallaparagada, D., Mandal and A. K. Bhattacharjee; "Introducing deeper nulls for time modulated linear symmetric antenna array using real coded genetic algorithm", 2011 IEEE Symposium on Computers & Informatics (ISCI) , 20-23 March 2011, pp. 249-254.

[5] S. K. Mandal, R. Ghatak and G. K. Mahanti, "Influence on side band radiation of uniformly excited TMAA during reduction of SLL of the main beam", Indian Antenna Week, Dec. 2011, pp. 1-4.

[6] S. Yang, Y. B. Gan and A. Qing, "Sideband suppression in time-modulated linear arrays by the differential evolution algorithm", IEEE Antennas Wireless Propagation Letters, vol. 1, no. 1, 2002, pp. 173-175.

[7] S. Yang, Y. B. Gan and P. K. Tan, "A new technique for power-pattern synthesis in time-modulated linear arrays", IEEE Antenna Wireless Propagation Letters, vol. 2, no. 1, 2003, pp. 285-287.

[8] S. Yang, Z. Nie and F. Yang, "Synthesis of low sidelobe planar antenna arrays with time modulation", Asia-Pacific Conference Proceedings, vol. 3, Dec. 2005, pp. 1-3.

[9] E. Aksoy and E. Afacan, "Thinned Nonuniform Amplitude Time-Modulated Linear Arrays," IEEE Antennas Wireless Propagation Letter, vol. 9, May 2010, pp. 514 -517.

[10] L. Manica, P. Rocca, L. Poli, A. Massa, "Almost time-independent performance in time-modulated linear arrays," IEEE Antennas Wireless Propagation Letter, vol. 8, Aug. 2009, pp. 843-846.

[11] P. Rocca and A. Massa, "Innovative approaches for optimized performance in time-modulated linear arrays", IEEE Antennas and Propagation Society International Symposium, June 2009, pp. 1-4.

[12] P. Rocca, L. Poli, L. Manica and A. Massa, "Compromise pattern synthesis by means of optimized time-modulated array solutions", IEEE Antennas and Propagation Society International Symposium, June 2009, pp. 1-4.

[13] L. Poli, P. Rocca, L. Manica, and A. Massa, "Handling sideband radiations in time-modulated arrays through particle swarm optimization," IEEE Transactions on Antennas and Propagation, vol. 58, no. 4, April, 2010, pp. 1408-1411.

[14] L. Poli, P. Rocca, L. Manica, and A. Massa, "Pattern synthesis in time-modulated linear arrays through pulse shifting," IET Microwaves, Antennas & Propagation, vol. 4, no. 9, Sept. 2010, pp. 1157-1164.

[15] S. K., Mandal , R. Ghatak and G.K., Mahanti, "Optimizing time delay of time modulated linear array elements to reduce the side band radiation level", IEEE International Conference on Signal Processing, Communication and Computing (ICSPCC), Aug. 2011, pp. 556-559.

[16] G. Li, S. Yang, M. Huang and Z. Nie, "Sidelobe Suppression in Time Modulated Linear Arrays with Unequal Element Spacing", Journal of Electromagnetic Waves and Applications, vol. 24, no. 5-6, 2010, pp. 775 – 783.

[17] E. Aksoy and E. Afacan, "Calculation of Sideband Power Radiation in Time Modulated Arrays with Asymmetrically Positioned Pulses", IEEE Antennas and Wireless Propagation Letters, vol. 11, 2012, pp 133-136.

[18] E. T. Bekele, P. Rocca and A. Massa, "Pulse shaping in time-modulated antenna array", IEEE International Conference on Wireless Information Technology and Systems (ICWITS), Nov. 2012, pp. 1-4.

[19] Y. Tong and A. Tennant, "Reduced sideband levels in time-modulated arrays using half-power sub-arraying techniques", IEEE Transactions on Antenna and Propagation, vol. 59, no. 1, January, 2011, pp. 301-303.

[20] J. C. Bregains, J. Fondevila, G. Franceschetti, and F. Ares, "Signal radiation and power losses of time-modulated arrays", IEEE Transactions on Antenna and Propagation, vol. 56, no.6, June 2008, pp. 1799-1804.

[21] S. Yang, Y. B. Gan and P. K. Tan, "Evaluation of directivity and gain for time modulated linear antenna arrays", Microwave and Optical Technology Letters, vol. 42, no. 2, July 2004, pp. 167-171.

[22] C. A. Balanis, Antenna Theory: analysis and design, Chapter 6: Arrays: Linear, Planar and Circular, 3rd edition, Wiley Interscience, 2005, pp. 283-371.

[23] A. Tennant and B. Chambers, "Control of the harmonic radiation patterns of time-modulated antenna arrays", IEEE Antenna and Propagation conference, July 2008, pp 1-4.

[24] S. Yang, Y. B. Gan and P. K. Tan, "A new technique for power-pattern synthesis in time-modulated linear arrays", IEEE Antenna Wireless Propagation Letters, vol. 2, 2003, pp 285-287.

[25] Y. Tong and A. Tennant, "Sideband Suppression in Time-Modulated Arrays Using Fixed Bandwidth Elements", 2012 Proceedings of the Sixth European

Conference on Antennas and Propagation (EuCAP), Prague, Czech Republic, 26 – 30 March, 2012, pp. 1 – 5.

[26] Y. Tong and A. Tennant, "Sideband level suppression in Time-modulated linear arrays using modified switching sequences and fixed bandwidth elements," IET Electronics Letters, vol. 48, no. 1, January 2012, pp. 10-11.

[27] D. M. Pozar, Microwave Engineering, 2nd Edition, Chapter 4, John Wiley & Sons, Inc, 1998, pp. 182-234.

Chapter 4 Beam Steering in Time Modulated Linear Arrays

4.1 Introduction

In the previous chapter we have shown that time modulated linear array can be used to produce a beam pattern with controlled low sidelobe levels (below -30dB), but at the expense of having undesired radiations into sidebands or harmonics. Therefore, two novel approaches were proposed to suppress sideband radiation while maintaining desired radiation characteristics with low sidelobe level and hence improve radiation efficiency at the fundamental frequency.

Another attractive feature of a phased array antenna is the ability to perform real time electronic beam scanning. The maximum radiation of any array antenna can be directed to the direction of interest by controlling the relative phase difference between each element of the array.

In practice, beam steering in phased array antenna can be achieved by either true-time delay techniques [1] or by using phase shifters [2]. For 'real-time' operation, the antenna system must be capable of rapidly adjusting the phase difference continuously. The benefits offered by the phased array technology are typically found in the expensive state-of-art military applications. Hence there is much interest in developing an alternative system but with much lower cost. The breakthrough

occurred in 1961 when Shanks proposed a new concept of realising electronic beam scanning in the time domain [3]. The general principle is to modulate each array element in a periodic manner so that multiple harmonic patterns are generated to scan in various directions.

In this chapter, we will examine how to realise the electronic beam scanning as well as the controlled low sidelobe levels in the time modulated linear array without the use of any phase shifters [4-5]. Following that, we will apply null steering techniques in a time modulated linear array in an effort to filter out the interference under various scenarios.

4.2 Harmonic beam steering with a controlled low sidelobe radiation pattern

The topology of a time-modulated antenna array is described in Fig.4.1, where it is shown that a group of high speed RF switches are connected to modulate array elements. To synthesize an effective, time-average weighting function, each array element may be switched on for a period that corresponds to a conventional amplitude coefficient of the array elements. For example, if a particular array element has a relative amplitude weight of 0.3, then in the time-modulated array implementation the element can be switched on for a time of $0.3T_0$, where T_0 is the overall modulation period. Hence, this technique allows any conventional array weights to be synthesised in a time average sense. More importantly, as the switches can be controlled

electronically, the modulating sequence can be easily reprogrammed to obtain any

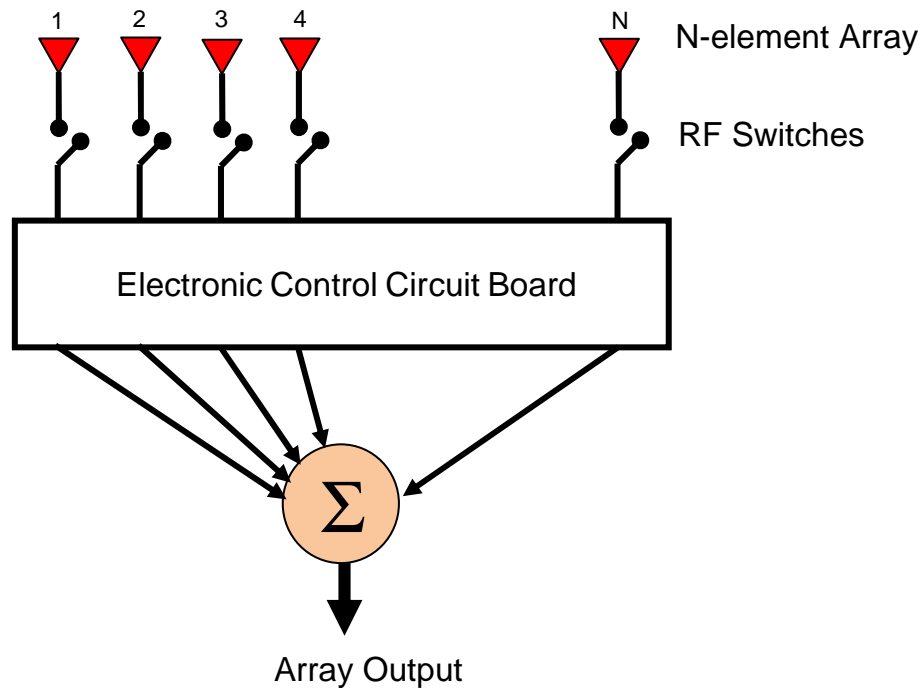arbitrary amplitude weights in real time and thus provides an adaptive array solution.

Fig.4.1. A time modulated linear array structure.

However, as a consequence of periodic time modulation, the array also radiates

energy at harmonics of the switching frequency. Much of the recent research into

time-modulated arrays has investigated techniques for reducing the wasted power

radiated into sidebands, often by employing a variety of adaptive optimisation

techniques [6-16]. Other approaches have included applying sub-array switching

techniques [17], or combinations of both [18].

Although in many applications the harmonics generated by time modulation process are unwanted, in certain situations they can be exploited. For example, a sequential switching sequence applied to the elements across the length of a linear array can be used to generate harmonic radiation patterns which are scanned in angle [4], and in [20] a technique for generating scanned nulls at the first harmonic frequencies of a two-element array for direction finding applications is described.

The harmonic beam steering property of time-modulated arrays is a potentially powerful attribute, but ideally an array designer would like to combine this function with low sidelobe performance. Although this requirement can be achieved by applying conventional static weights across the face of the array, it is desirable to simultaneously realise both functions in the time-modulation method alone. An attempt to address this problem was recently investigated in [21], where adaptive optimization was used to simultaneously control beam steering and the sidelobe level at the first harmonic beam pattern. In this section we will develop an analytical approach to show how it is possible to accomplish beam steering and low sidelobe levels at multiple harmonic patterns simultaneously.

4.2.1 Mathematical model

Basic Fourier Transform theory describes that a change of phase in the frequency domain corresponds to a time change in the time domain [22]. For a time modulated linear array, the equivalent phase shift can be achieved by applying a progressive time

delay to the successive array elements. Assuming each element is an isotropic source, spaced by half wavelength. The array factor of a time modulated linear array is expressed as:

$$AF(\theta,t) = e^{j\omega t}\sum_{n=0}^{N-1}A_n w_n(t)\,e^{jknd\sin\theta} = \sum_{m=-\infty}^{\infty}e^{j(\omega+m\omega_o)t}\sum_{n=0}^{N-1}A_n a_{mn}e^{jknd\sin\theta} \quad (4.1)$$

where k = $2\pi/\lambda$ is the propagation constant, λ is the wavelength, ω_0 is the modulating angular frequency given by $\omega_0 = 2\pi/T_0$, m is the number of the harmonic, A_n is the complex static weight of the element, and a_{mn} represent the Fourier series coefficients of the periodic signal $w_n(t)$ defined by:

$$a_{mn} = \frac{1}{T_0}\int_0^{T_o}w_n(t)e^{-jm\omega_o t}dt \quad (4.2)$$

Now let's move to the physical excitation arrangement of an N-element linear array, where the first antenna of the array is switched on for a small portion of the modulation period T_0, defined by N/T_0 and then switched off immediately. Repeating the same procedure across the entire array, the corresponding excitation time of the nth array element is:

$$\frac{nT_0}{N} \le t \le \frac{(n+1)T_0}{N} \quad (4.3)$$

Using equation (4.3) to evaluate the Fourier coefficients a_{mn} in the case of the static weights A_n equals unity results in:

$$a_{mn} = \frac{\sin[m\pi(\tau_{noff}-\tau_{non})]}{m\pi}\,e^{-j\pi m(\tau_{noff}+\tau_{non})} \quad (4.4)$$

The Fourier coefficients may be interpreted as complex weights in which the term

$\dfrac{\sin[m\pi(\tau_{noff} - \tau_{non})]}{m\pi}$ controls the amplitude weightings of the array elements, and the

term $e^{-j\pi m(\tau_{noff} + \tau_{non})}$ introduces a progressive linear phase shift at the harmonic

frequency defined by m.

4.2.2 Design model of time sequence

Now if we apply time-average amplitude weights to the array defined by a set of real

valued array weights w_n and a progressive linear phase delay β, the weighting

coefficients can be written in the form of $w_n = |w_n| e^{j\beta}$. If the radiation pattern at

the first positive harmonic is of interest, so substituting m =1 into (4.4) to obtain the

magnitude of the array weights at the first positive harmonic frequency:

$$|w_n| = \frac{\sin[\pi(\tau_{noff} - \tau_{non})]}{\pi} \qquad (4.5)$$

and hence the effective on-time of the elements can be reformulated as:

$$\tau_{noff} - \tau_{non} = \frac{1}{\pi} \sin^{-1}(\pi |w_n|) \qquad (4.6)$$

Since a progressive phase difference between each element is the essential condition

to realise electronic beam scanning, so the expression may be written as:

$$\tau_{noff} + \tau_{non} = n\beta \qquad (4.7)$$

where β is the progressive linear phase delay between each array element. Solving

equations (4.6) and (4.7) together, we could easily arrive at the following critical

relationships for the switching on and off times of the nth array element:

$$\tau_{noff} = \frac{1}{2}[n\beta + \frac{1}{\pi}\sin^{-1}(\pi|w_n|)] \qquad (4.8)$$

$$\tau_{non} = \frac{1}{2}[n\beta - \frac{1}{\pi}\sin^{-1}(\pi|w_n|)] \qquad (4.9)$$

We will use this conclusion to design a proper time sequence that is able to produce

multiple harmonic patterns scanning to various directions.

4.2.3 Numerical examples of sequential time sequence

The following examples all relate to a 16 element linear array with half wavelength

element spacing and uniform static weights. Let us first look at a simple situation

where each element of the array is sequentially energised for a period of $T_0/16$ within

the modulating cycle. For a normalised modulation period ($T_0=1$), the sequential time

switching sequence is shown in Fig.4.2. The switch-on time of the nth element in the

array is $\tau_{non} = \frac{n}{16}$ and corresponding switch-off time is $\tau_{noff} = \tau_{non} + \frac{1}{16}$.
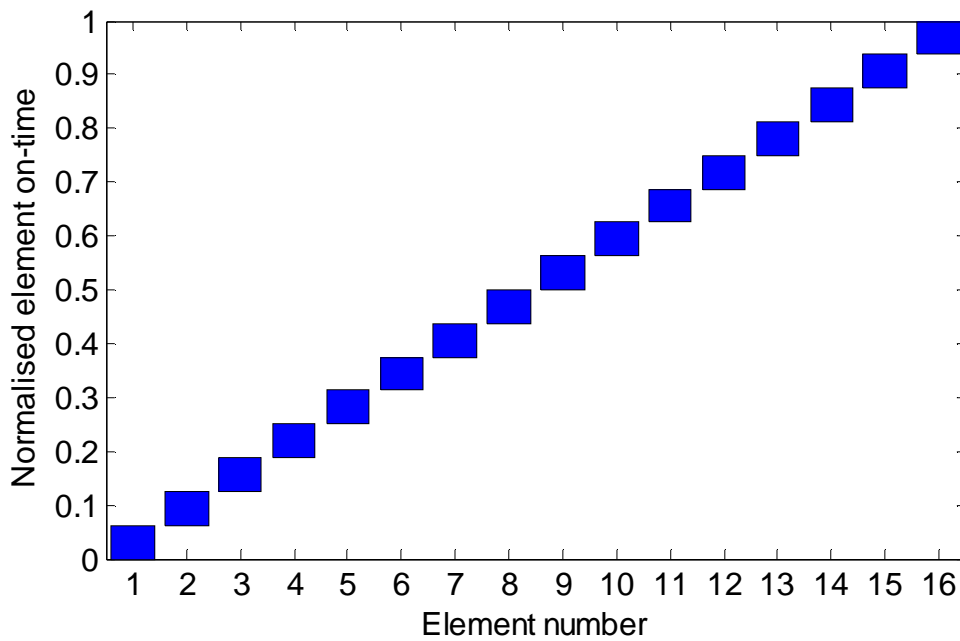
Fig.4.2. The sequential time switching sequence designed to produce multiple

harmonic main beams scanning at different directions.

The sequential switching scheme generate many harmonic patterns at multiples of the

modulation frequency f_o. This is illustrated in Fig.4.3 which has shown the radiation

patterns at the fundamental frequency f and first, third and fifth positive as well as the

negative harmonic frequencies $f - 5f_o$, $f - 3f_o$, $f - f_o$, $f + f_o$, $f + 3f_o$ and $f + 5f_o$.

Each Fourier coefficient is associated with a different spatial beampattern at a

specified harmonic frequency. In Fig.4.3 the maximum radiation at the fundamental

frequency f is at the boresight direction but the beampatterns at the harmonic

components are scanned in an angle related to the harmonic number. In this example,

the positive harmonic patterns steer the main beam in the direction of 7.2°, 14.5° and

38.7$^{°}$. The negative harmonics generated by the switching sequence in Fig.4.2 scan

the main beam in the opposite angular direction. Hence by periodically modulating

the array elements on and off in a sequential way, multiple harmonic patterns can be
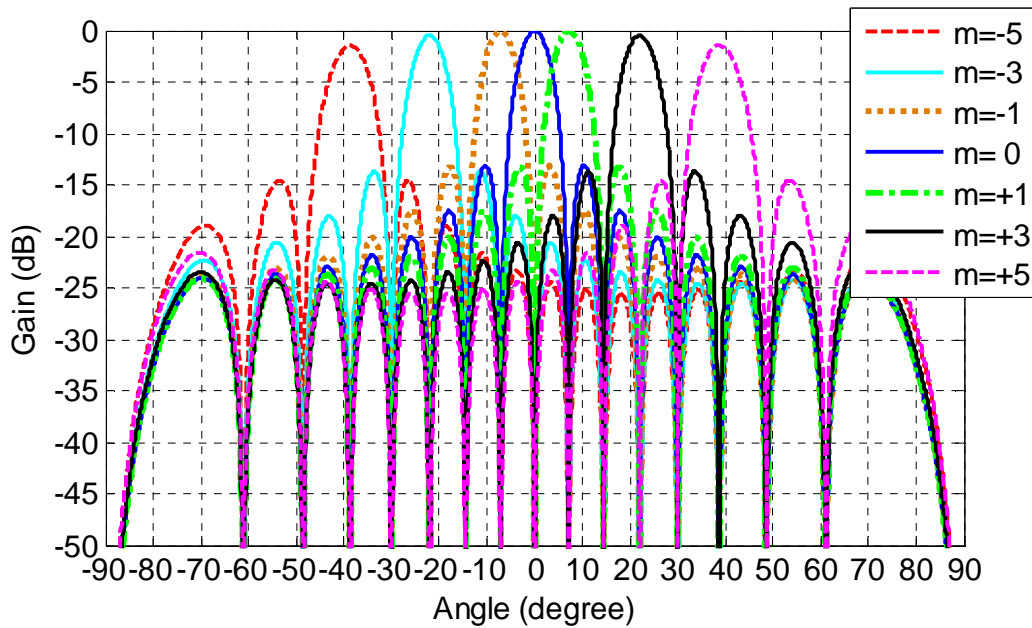
generated to scan over a full hemisphere.

Fig.4.3. The radiation patterns at fundamental frequency, first, third and fifth positive

and negative harmonic frequencies. The harmonics scan the main beam at $\pm 7.2^{°}$,

$\pm 14.5^{°}$ and $\pm 38.7^{°}$ respectively (m=0 refers to fundamental frequency, m=-1 refers

to the 1st negative harmonic and m=+2 refers to the 2nd positive harmonic)

The above investigations serve as the basic foundation of understanding how to

realise electronic beam steering in a time modulated array. Now the following step is

to combine the controlled low or ultralow sidelobe level performance with the

proposed technique. Considering a 16-element linear array with half wavelength

element spacing designed to generate a beampattern with -30dB Chebyshev sidelobe

levels at the fundamental frequency and steer the first positive harmonic pattern in the

direction of 7.2°. In this example, the linear phase difference β between the each array

elements is chose to be 7.2° and the element switching sequence can be derived from

equations (4.8) and (4.9). The time sequence and the corresponding beampatterns at

the fundamental and first 5 positive harmonic frequencies are shown in Fig.4.4 and

Fig.4.5 respectively.
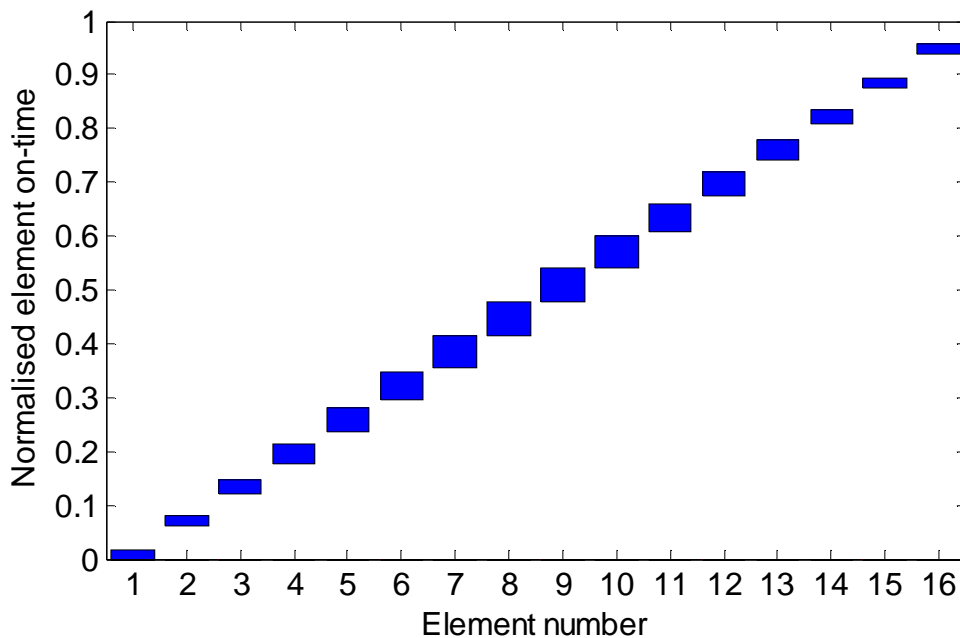
Fig.4.4. Switching sequence designed to produce -30dB Chebyshev sidelobe levels

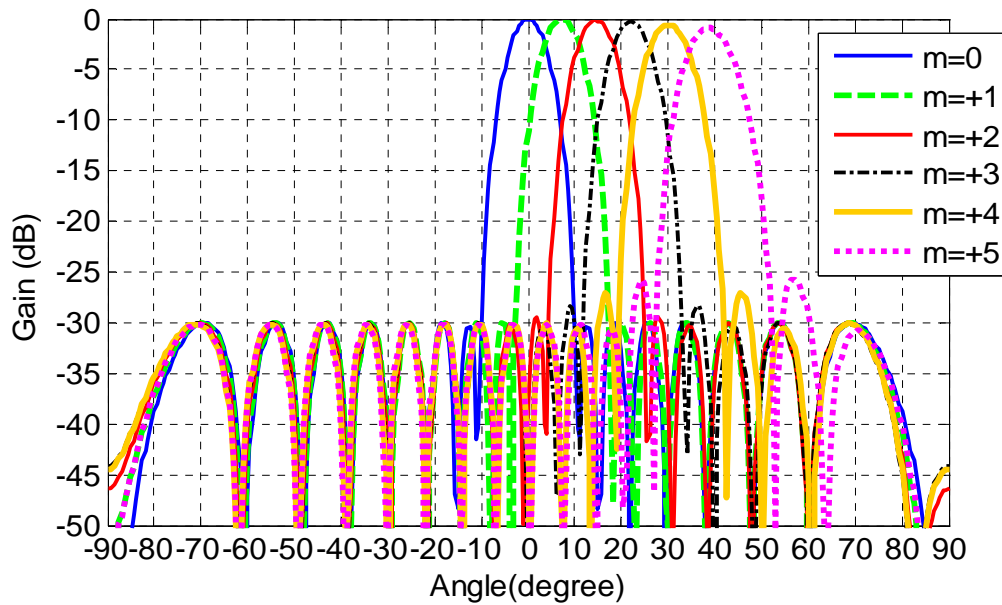and a first positive harmonic beam scans in angle of 7.2°.

Fig.4.5. The corresponding beampatterns at the fundamental and the first 5 harmonic

frequencies produced by the switching sequence in Fig.4.4. (m=0 refers to

fundamental frequency, m=+1 refers to the 1st positive harmonic and m=+5 refers to

the 5th positive harmonic)

It can be observed that beampattern with desired -30dB sidelobe level has been

produced at both fundamental and first positive harmonic. In contrast to the

conventional sequential time scheme where each element is switched on for a period

of time 1/N, the effective on-time of the array elements in this example corresponds to

the Chebyshev weighting functions designed to generate a beampattern with a -30dB

sidelobe level. According to the Fourier Transform theory, a shift in the time domain

is equivalent to a change of phase in the frequency domain. Therefore the relative

time delays between each array element determine the progressive phase difference as

in the conventional array system and is used to scan the harmonic pattern in the desired direction.

From Fig.4.5 it can seen that sidelobe levels tend to increase as the number of harmonic goes up (from the forth to the higher harmonics), but the maximum radiation remains unchanged in the desired direction as required. This phenomenon can be better explained by examining equation (4.5) and re-arranging it gives:

$$a_{mn} = (\tau_{noff} - \tau_{non}) \frac{\sin[m\pi(\tau_{noff} - \tau_{non})]}{m\pi(\tau_{noff} - \tau_{non})} \; e^{-jm\pi(\tau_{noff} + \tau_{non})} \qquad (4.10)$$

The sinc function $\dfrac{\sin[m\pi(\tau_{noff} - \tau_{non})]}{m\pi(\tau_{noff} - \tau_{non})}$ has no significant impact on the effective on-time $(\tau_{noff} - \tau_{non})$ or the equivalent amplitude weights at lower number of harmonics. However, this term starts to take effect and tapers the amplitude weights at a rate of sin(x)/x as the number of the harmonic increases. The sideband levels at higher harmonic frequency can be still maintained below -25.0dB and maximum radiation of harmonic patterns in the desired direction remained unchanged.

Another example will be presented to implement -40dB Taylor amplitude weights to a time modulated linear array with a scanning angle of 15° at the first positive harmonic. The time switching sequence is shown in Fig.4.6 and the corresponding beampatterns at first 5 positive and negative harmonic frequencies are plotted in Fig.4.7.
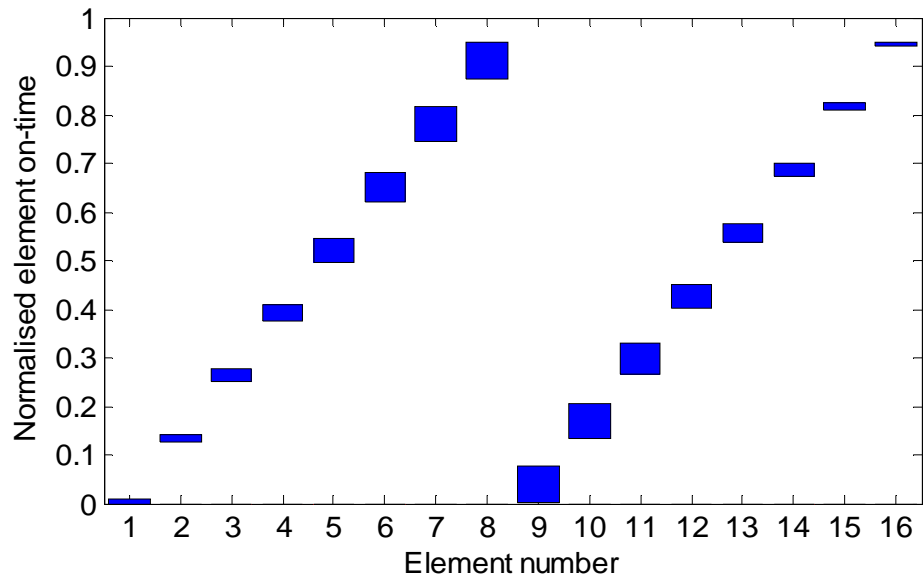
Fig.4.6. Switching sequence designed to produce a radiation pattern with -40dB

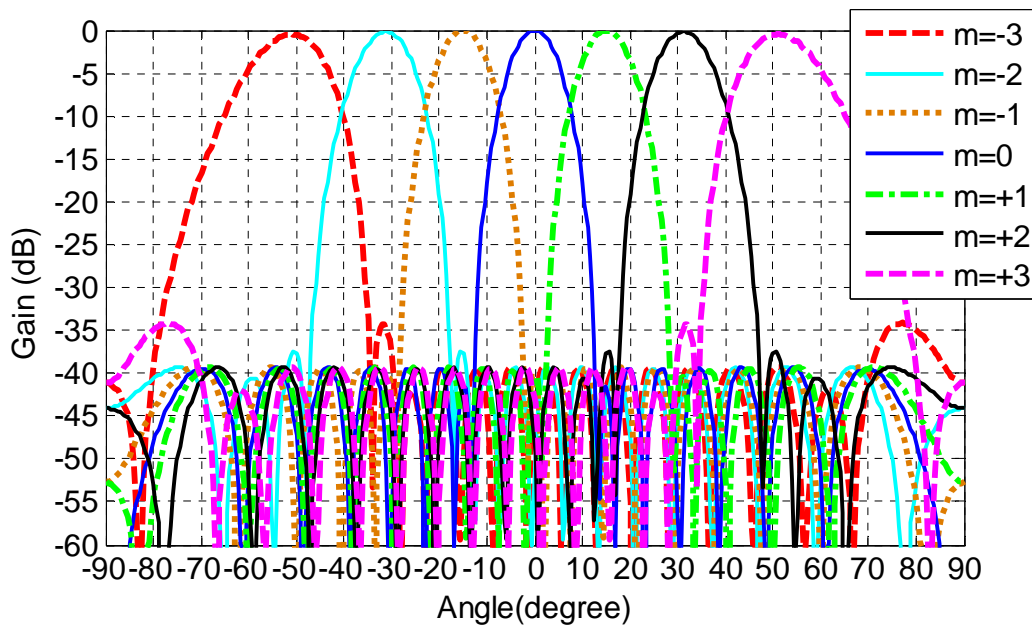Taylor sidelobe levels and a first positive harmonic beam scans in an angle of 15.0°.

Fig.4.7. The corresponding array factors at the fundamental and the first 5 positive

and negative harmonic frequencies produced by the switching sequence in Fig.4.6.

(m=0 refers to fundamental frequency, m=+1 refers to the 1st positive harmonic and

m=-3 refers to the 3rd negative harmonic)

From Fig.4.7 a radiation pattern with -40dB Taylor sidelobe level has been produced at both fundamental and other harmonic frequencies and the first positive harmonic pattern steers the main beam towards the desired angle of 15.0° as expected. In addition, other harmonic beampatterns scan at various directions with a crossover at a level of -9.5dB between the adjacent beams.

4.2.4 Summary

A new approach to achieving simultaneous beam steering and low sidelobe levels in time-modulated linear arrays has been presented. The technique does not require the use of phase shifters or amplitude tapering of the array element weights. Various numerical results have been discussed for a 16 element linear array designed to produce harmonic beam steering at different angles with prescribed low sidelobe levels.

4.3 Null steering with controlled low sidelobe levels

In the past few decades, the expansion of wireless technology continues to place great importance on the development of a low cost system. Beamforming, as a spatial filtering technique, can be combined with digital signal processing algorithms to provide a practical solution of improving signal quality and channel capacity over a conventional system. This technique can not only perform real-time electronic beam

scanning, but are also capable of suppressing unwanted interference from other directions.

From the previous section, harmonic beam steering with controlled low sidelobe levels in a time modulated linear array was introduced. However, in a scenario where strong interference signal are present, a beampattern with low sidelobe level may not sufficient to attenuate the inferring signal. In this section, we will extend the analysis of harmonic beam steering and propose a way of dealing with the scenario of strong interference presented. This novel approach will combine the digital signal processing algorithm with the model developed so far.

4.3.1 Theoretical background of null steering in TMLA

As described in Beamforming Basics (section 2.3.2), the output of a linear array is the summation of signal received from each antenna multiplied by a complex weight coefficient, which is expressed as [23]:

$$y(t) \; = \; \sum_{n\,=\,0}^{N-1} w_n x_n(t) \tag{4.11}$$

Denoting array weights in the vector notation as:

$$w \; = \; [w_0^* \,,\, w_1^* \,,\, w_2^* \,,\, ... \,,\, w_{N-1}^*]^T \tag{4.12}$$

where $(\cdot)^*$ represents the complex conjugate, signal received from all elements as:

$$x(t) \; = \; [x_0(t) \,,\, x_1(t) \,,\, x_2(t) \,,\, ... \,,\, x_{N-1}(t)]^T \tag{4.13}$$

where superscript $[\cdot]^{T}$ implies the transpose. The output of the array becomes:

$$y(t) = \mathbf{w}^{H}\mathbf{x}(t) \tag{4.14}$$

where $(\cdot)^{H}$ denotes the complex conjugate transpose of a vector. The output power of

the array is calculated as the square of the magnitude of the output:

$$P(t)=\left|y(t)\right|^{2}$$
$$= y(t)y^{*}(t) \tag{4.15}$$

Substituting equation (4.14) into (4.15), the output power is written as:

$$P(t) = \mathbf{w}^{H}\mathbf{x}(t)\mathbf{x}^{H}(t)\mathbf{w} \tag{4.16}$$

Assuming the received signal x(t) can be modelled as zero mean process, then the

mean power of the array output is given by [23]:

$$P(t) = E[\mathbf{w}^{H}\mathbf{x}(t)\mathbf{x}^{H}(t)\mathbf{w}]$$
$$= \mathbf{w}^{H}E[\mathbf{x}(t)\mathbf{x}^{H}(t)]\mathbf{w} \tag{4.17}$$
$$= \mathbf{w}^{H}\mathbf{R}_{x}\mathbf{w}$$

where $E(\cdot)$ indicates the expectation operation and $\mathbf{R_x}$ is the covariance matrix of x(t)

defined as:

$$\mathbf{R}_{x}=E[\mathbf{x}(t)\mathbf{x}^{H}(t)] \tag{4.18}$$

Frost [24] advanced the prior theory developed by Griffiths [25] and proposed a

simpler and a more robust algorithm, called Linearly Constrained Minimum Variance

(LCMV), for controlling the array response. As its name implies, the fundamental

principle is to impose multiple linear constraints to preserve the main beam response

at the desired directions while minimising the total output power of the array. The

problem becomes how to find an optimum set of weights to satisfy the following

relationship [25]:

$$\min_{\mathbf{w}} \mathbf{w}^H \mathbf{R}_{xx} \mathbf{w} \quad \text{subject to} \quad \mathbf{w}^H \mathbf{C} = \mathbf{f}^T \tag{4.19}$$

where $\mathbf{C}$ is termed as the constrained matrix and f is a vector consisting of all zeros

except for the first element which equals one, written as $\mathbf{f} = [1, 0, 0, \ldots, 0]$.

Therefore, equation (4.19) can be interpreted as finding an optimum set of weights to

minimise the output power of the array while ensuring the beampattern has a unity

response to signals arriving from specific directions and zero response towards the

direction of the interfering signals. The equations are written as [25]:

$$\mathbf{w}^H \mathbf{a}(\theta_d) = 1 \tag{4.20}$$

$$\mathbf{w}^H \mathbf{a}(\theta_{ij}) = 0, \ j = 1, 2, \ldots, h \tag{4.21}$$

where $a(\theta)$ is called array response or steering vector defined by:

$$\mathbf{a}(\theta) = [1, e^{-jkd\sin\theta}, e^{-2jkd\sin\theta}, \ldots, e^{-j(N-1)kd\sin\theta}]^T \tag{4.22}$$

By means of Lagrange multipliers described in [26], an optimum solution to equation

(4.21) is given by [25]:

$$\mathbf{w}_{opt} = \mathbf{R}_{xx}^{-1} \mathbf{C} (\mathbf{C}^H \mathbf{R}_{xx}^{-1} \mathbf{C})^{-1} \mathbf{f} \tag{4.23}$$

The constrained matrix $\mathbf{C}$ associated with steering vectors from all directions is:

$$\mathbf{C} = [a(\theta_d), a(\theta_{i1}), a(\theta_{i2}), ... , a(\theta_{ij})] \tag{4.24}$$

where j is number of the interference signal.

4.3.2 Design Procedures to implement null steering in TMLA

In order to implement LCMV technique in the time modulated linear array, the same principle is applied as in the case of harmonic beam steering with controlled low sidelobe levels. A set of complex weights must be first determined to maintain beampattern response at the desired direction while suppressing the interfering signal from other directions. Following that the corresponding switching time sequence of each array element at the given harmonic can be obtained through the following relationship:

$$\tau_{noff} = \frac{1}{2}[n\beta + \frac{1}{\pi m}\sin^{-1}(\pi m|w_n|)] \tag{4.25}$$

$$\tau_{non} = \frac{1}{2}[n\beta - \frac{1}{\pi m}\sin^{-1}(\pi m|w_n|)] \tag{4.26}$$

where n is the number of elements, β is the progressive phase delay between each array element, w_n is the array weights and m represents the given number of harmonics.

4.3.3 Numerical examples

Now let us first consider a TMLA of 16 isotropic elements spaced by half wavelength distance and with uniform amplitude weights. To illustrate the concept, an example of

a simple situation where only one desired signal and one interfering signal will be considered. A signal of interest (SOI) is transmitted from a far field source at $\theta_d = 15^{\circ}$ and another signal not of interest (SNOI) impinges the array from the direction $\theta_I = -20^{\circ}$. The fist positive harmonic is designed to extract signal from the direction of SOI and attenuate interference at -20°, the switching on and off time of array elements in this case can be acquired from solving equation (4.25) and (4.26). The time sequence and corresponding beampatterns at the fundamental and first positive harmonic are shown in Fig.4.8 and Fig.4.9 respectively.
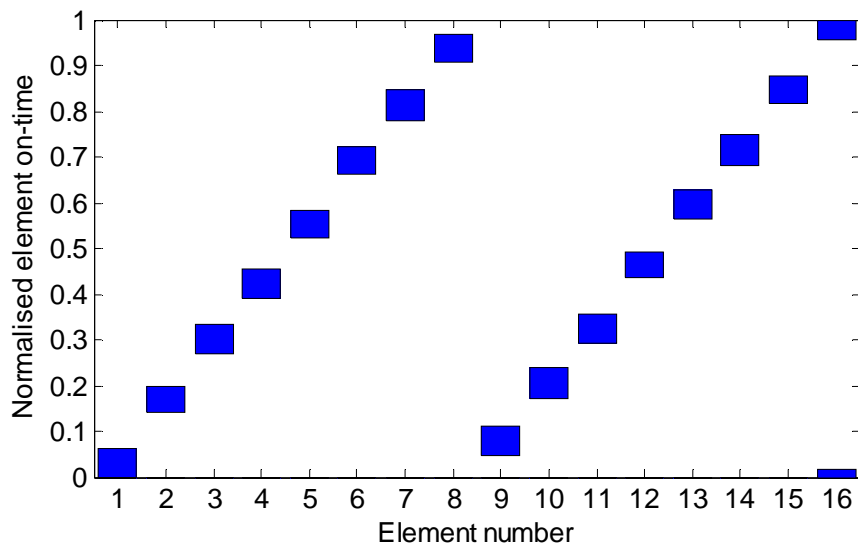
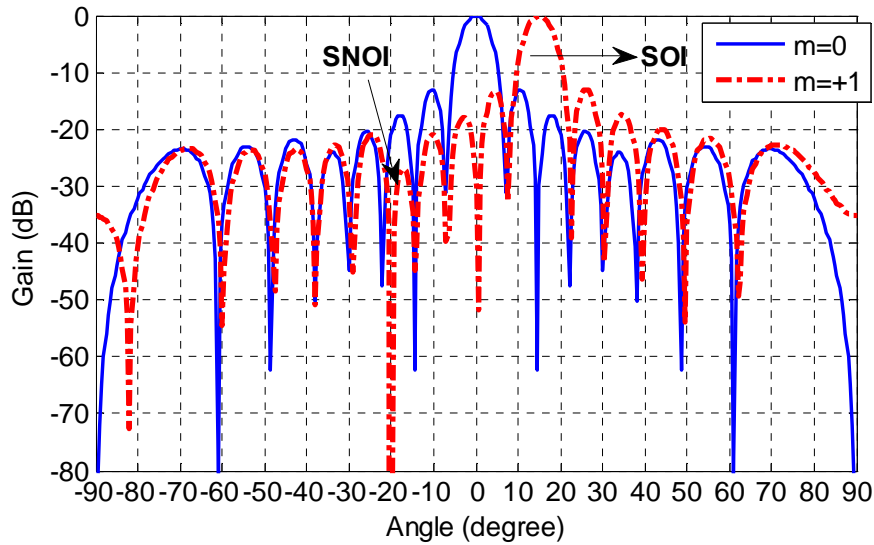Fig.4.8. Time sequence designed to have SOI at $\theta_d = 15^{\circ}$ and SNOI at $\theta_I = -20^{\circ}$.

Fig.4.9. First positive harmonic has SOI at $\theta_d = 15^\circ$ and SNOI at $\theta_I = -20^\circ$.

From Fig.4.9 the requirements of a beampattern with uniform amplitude weighting have been successfully satisfied at the first positive harmonic frequency. It can be noted that maximum radiation is directed towards the desired angle of 15.0° and deep null has formed in the direction of the interfering signal at $\theta_I = -20.0^\circ$.

Another example of 16-element antenna array is given to consider a situation with one desired signal at $\theta_d = -25^\circ$ and three unwanted signals impinge from $\theta_{I1} = -10^\circ$, $\theta_{I2} = 10^\circ$ and $\theta_{I3} = 20^\circ$ respectively. Same principles will be applied at the first positive harmonic. The switching time sequence and beampatterns at the fundamental and first positive harmonic components are drawn in Fig.4.10 and Fig.4.11 respectively.
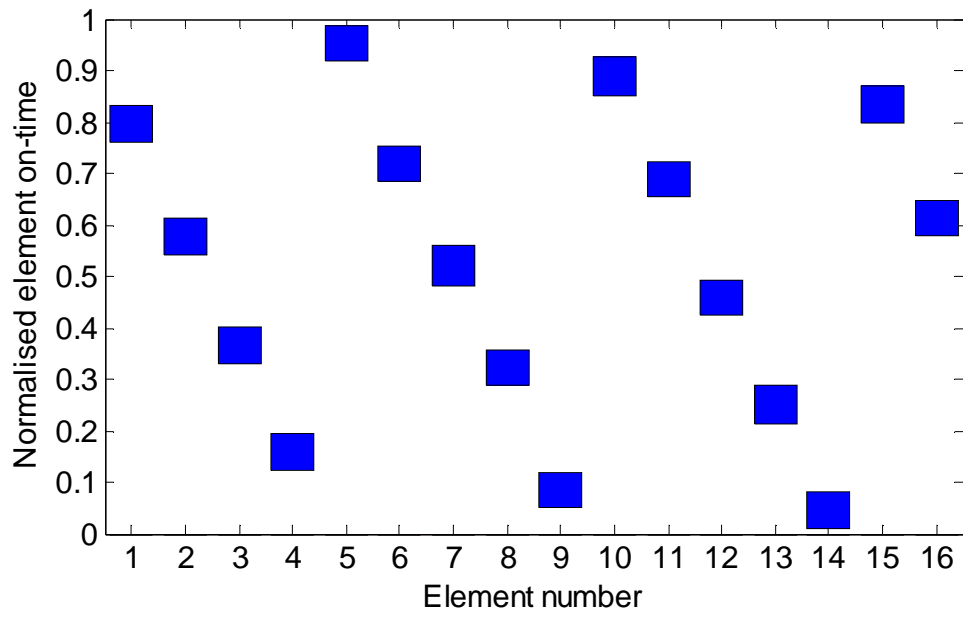
Fig.4.10. Time sequence designed to have SOI at $\theta_d = -25°$ and SNOI at $\theta_{I1} = -10°$ at θ_{I2}
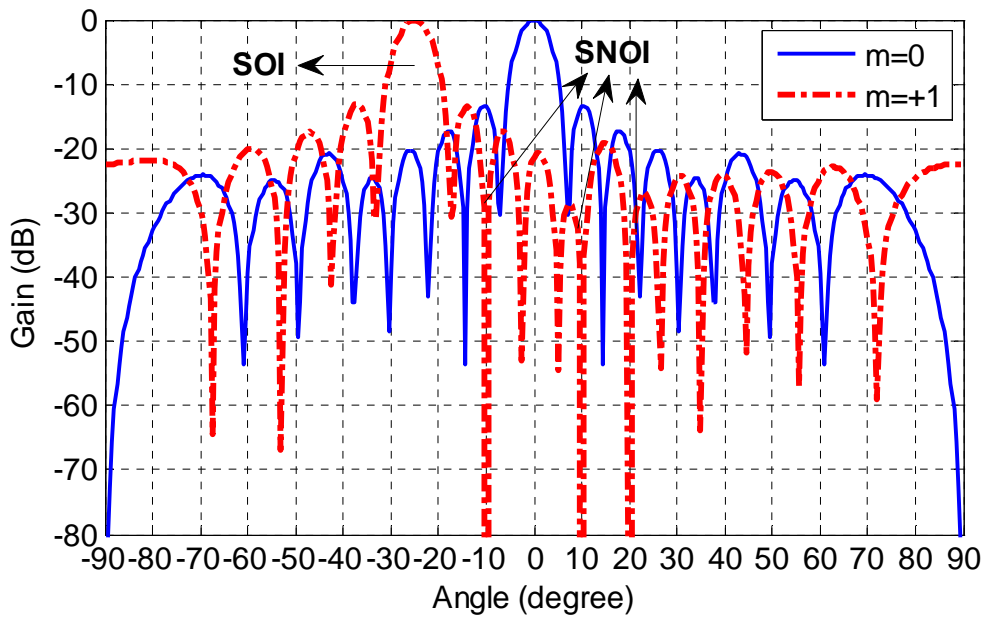
$= 10°$ and $\theta_{I3} = 20°$.

Fig.4.11. First positive harmonic has SOI at $\theta_d = -25°$ and SNOI at $\theta_{I1} = -10°$ at $\theta_{I2} =$

$10°$ and $\theta_{I3} = 20°$.

It is obvious to see that the maximum array response maintains at the direction of signal of interest ($\theta_d = -25°$), and three deep nulls are placed to suppress the interference from the angles of $\theta_{I1} = -10°$, $\theta_{I2} = 10°$ and $\theta_{I3} = 20°$ as required at the first positive harmonic pattern.

The proceeding two examples only illustrate the situation where uniform amplitude weights are considered. However, the proposed technique of harmonic beam steering with controlled low sidelobe levels can also be employed in this section to attenuate unwanted signals. We still consider an example of 16-elment uniform linear array with half wavelength element spacing.

Another scenario where a signal of interest comes from the direction of $\theta_d = 30°$ and the unwanted signal arrives from $\theta_I = -5°$ will be studied. This example is designed to have radiation patterns with -30dB Chebyshev amplitude weight both at the fundamental frequency and second positive harmonic frequency. Equation (4.26) and (4.27) when m = 2 are used to compute the switched on and off time of the array elements. The time sequence and associated beampatterns are shown in Fig.4.12 and Fig.4.13 respectively.
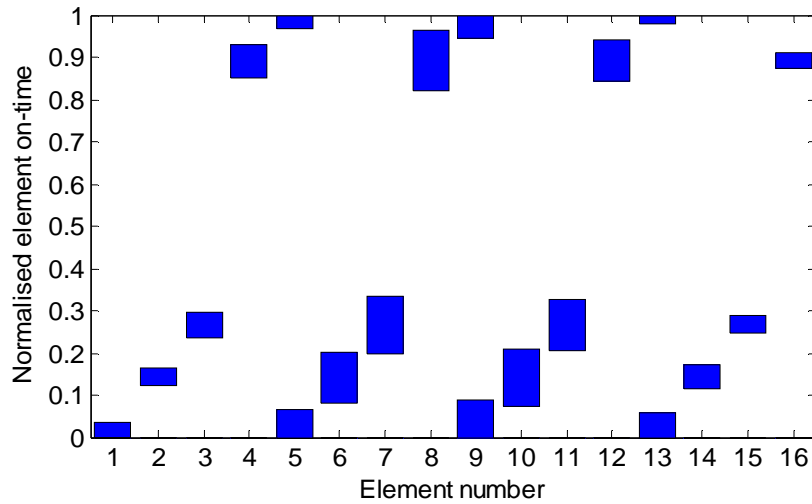
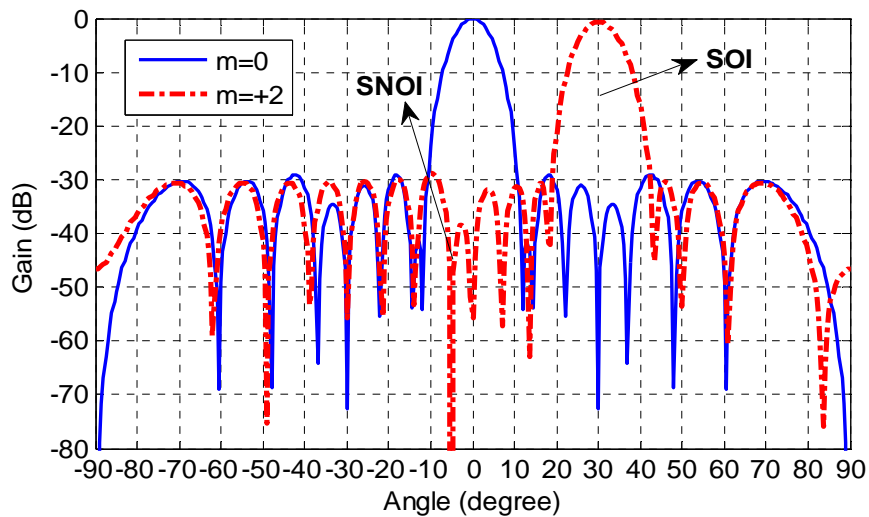Fig.4.12. Time sequence designed to have SOI at $\theta_d = 30^\circ$ and SNOI at $\theta_I = -5^\circ$.

Fig.4.13. Second positive harmonic has SOI at $\theta_d = 30^\circ$ and SNOI at $\theta_I = -5^\circ$.

The desired radiation characteristics of -30dB sidelobe level pattern at the fundamental frequency, as well as at the given number of harmonic are completely achieved. The first positive harmonic has a maximum array response at $\theta_d = 30^\circ$ and a deep null steers to the direction of the interference at $\theta_I = -5^\circ$ as expected.

In the last example we will examine the capability of applying the proposed technique

to deal with the case of multiple interfering signals presented. Assuming a 16-element

time modulated linear array is designed to produce a radiation pattern with -30dB

Chebyshev amplitude weights. Second positive harmonic is chosen to perform null

steering to suppress three interferences from the angles of $\theta_{I1} = 5°$, $\theta_{I2} = 15°$ and $\theta_{I3} =$

$30°$. The time sequence and simulation results of related radiation patterns are

presented in Fig.4.14 and Fig.4.15.

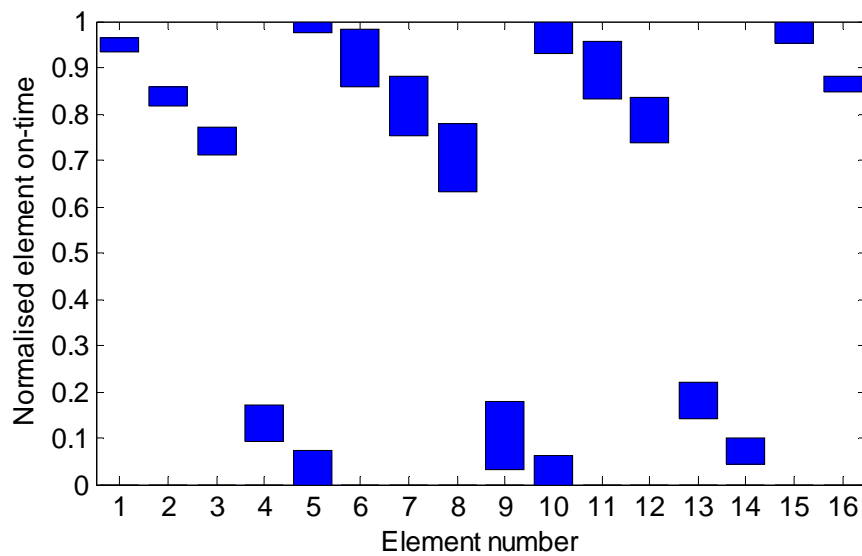Fig.4.14. Time sequence designed to have -30dB Chebyshev pattern with SOI at $\theta_d =$

-25° and SNOI at $\theta_{I1} = 5°$ at $\theta_{I2} = 15°$ and $\theta_{I3} = 30°$.
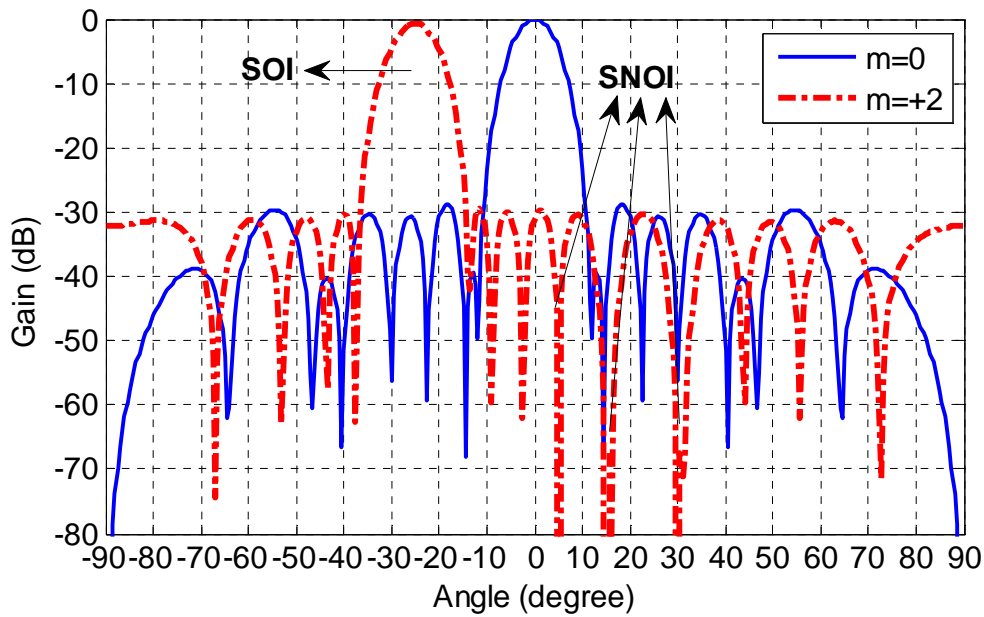
Fig.4.15. Second positive harmonic designed to have -30dB Chebyshev sidelobe with

SOI at $\theta_d = -25°$ and SNOI at $\theta_{I1} = 5°$ at $\theta_{I2} = 15°$ and $\theta_{I3} = 30°$.

4.3.4 Summary

An innovative approach for null steering technique to be implemented in a time modulated linear array has been presented with digital signal processing algorithms. LCMV algorithm is used to receive desired signals arriving from prescribed directions while suppressing interfering signals from other direction. A number of simulation results are given to demonstrate the effectiveness of this proposed technique under different scenarios. This novel approach does not require the use of phase shifters.

4.4 Conclusion

A way of realising multiple beam steering and interference suppression in a TMLA has been presented in this chapter. Conventional phased array technology requires phase shifters in order to perform real-time electronic beam scanning. The first part of the chapter introduces a novel approach to achieve harmonic beam scanning with controlled low sidelobe levels in time-modulated linear arrays by merely manipulating relative time delay between each array element. Multiple beams associated with different harmonic frequencies are generated to scan in various directions in a full hemisphere. With this principle in mind, the analysis of harmonic beam steering can be extended and combined with digital signal processing algorithm to suppressing interference under a strong interference environment. The proposed approach uses LCMV algorithm to preserve the main beam response to extract desired signal while minimising the contribution from the interferences. Several numerical examples were given to verify the robustness of the proposed technique under different circumstances.

References

[1] W. Ng, A. A. Walston, G. L. Tangonan and J. J. Lee, "The first demonstration of an optically steered microwave phased array antenna using true-time-delay", Journal of Lightwave Technology, vol. 9, no. 9, Sep. 1991, pp. 1124-1131.

[2]   J. White, "Diode Phase Shifters for Array Antenna", IEEE Transactions on Microwave Theory and Techniques, vol. 22, no. 6, June 1974, pp. 658-674.

[3]   H. E. Shanks, "A new technique for electronic scanning," IEEE Transactions on Antennas and Propagation, vol. 9, no. 2, Mar., 1961, pp. 162–166.

[4]   Y. Tong and A. Tennant, "Beam Steering Techniques for Time-Switched Arrays", IEEE Loughborough Antennas and Propagation Conference, Loughborough, UK, pp. 233 – 236, 12 – 13 November, 2009.

[5]   Y. Tong and A. Tennant, "Simultaneous control of sidelobe level and harmonic beam steering in time-modulated linear arrays," IET Electronics Letters, vol. 46, no. 3, pp. 200-202, February, 2010.

[6]   S. Yang, Y. B. Gan and A. Qing, "Sideband suppression in time-modulated linear arrays by the differential evolution algorithm", IEEE Antennas Wireless Propagation Letters, vol. 1, no. 9, 2002, pp. 173-175.

[7]   J. Fondevila, J. C. Bregains, F. Ares and E. Moreno, "Optimising uniformly excited linear arrays through time modulation", IEEE Antennas Wireless Propagation Letters, vol. 3, pp.   298-300, 2004.

[8]   S. Yang, Y. B. Gan, A. Qing, and P. K. Tan, "Design of uniform amplitude time modulated linear array with optimized time sequences", IEEE Transactions on Antenna and Propagation, vol. 53, no. 7, July, 2005, pp. 2337-2339.

[9] A. Tennant and B. Chambers, "Control of the harmonic radiation patterns of time-modulated antenna arrays," IEEE Antenna and Propagation conference, July, 2008, pp. 1-4.

[10] L. Manica, P. Rocca, L. Poli, A. Massa, "Almost time-independent performance in time-modulated linear arrays," IEEE Antennas Wireless Propagation Letter, vol. 8, Aug., 2009, pp. 843-846.

[11] P. Rocca, L. Poli, L. Manica and A. Massa, "Compromise pattern synthesis by means of optimized time-modulated array solutions," IEEE Antennas and Propagation Society International Symposium, June, 2009, pp. 1 - 4.

[12] X. Huang, S. Yang, G. Li and Z. Nie, "Power-pattern synthesis in time modulated semicircular arrays," IEEE Antennas and Propagation Society International Symposium, June, 2009, pp. 1 - 4.

[13] E. Aksoy and E. Afacan, "Thinned Nonuniform Amplitude Time-Modulated Linear Arrays," IEEE Antennas Wireless Propagation Letter, vol. 9, May, 2010, pp. 514 -517.

[14] G. R., Hardel, N.T., Yallaparagada, D., Mandal and A.K., Bhattacharjee; "Introducing deeper nulls for time modulated linear symmetric antenna array using real coded genetic algorithm", 2011 IEEE Symposium on Computers & Informatics (ISCI), 20-23 March 2011, pp. 249-254.

[15] M. D'Urso, A. Iacono, A. Iodice and G. Franceschetti, "Optimizing uniformly excited time-modulated linear arrays", 2011 Proceedings of the Fifth European Conference on Antennas and Propagation (EuCAP), Rome, Italy, 11 – 15 April, 2011, pp. 2082-2086.

[16] E. Aksoy and E. Afacan, "Calculation of Sideband Power Radiation in Time Modulated Arrays with Asymmetrically Positioned Pulses", IEEE Antennas and Wireless Propagation Letters, vol. 11, 2012, pp 133-136.

[17] Y. Tong and A. Tennant, "Sideband level suppression in Time-modulated linear arrays using modified switching sequences and fixed bandwidth elements," IET Electronics Letters, vol. 48, no. 1, pp. 10-11, January, 2012.

[18] Y. Tong and A. Tennant, "Reduced sideband levels in time-modulated arrays using half-power sub-arraying techniques", IEEE Transactions on Antenna and Propagation, vol. 59, no. 1, pp. 301-303, January, 2011.

[19] G. Li, S. Yang and Z. Nie, "A novel beam scanning technique in time modulated linear arrays", IEEE APS Conference, June 2009, pp. 1-5.

[20] A. Tennant and B. Chambers, "A two-element time-modulated array with direction-finding properties" IEEE Antennas Wireless Propagation Letter, vol. 6, 2007, pp. 64–65.

[21] G. Li, S. Yang, Y. Chen, and Z. Nie, "A novel electronic beam steering technique in time modulated antenna array," Progress In Electromagnetics Research, vol. 97, 2009, pp. 391-405.

[22] B. P. Lathi, "Signal Processing and Linear Systems", Berkeley Cambridge, 1998.

[23] L. C. Godara, "Application of Antenna Arrays to Mobile Communications, Part II: Beamforming and Direction-of-Arrival Considerations", Proceedings of IEEE, vol. 85, no. 8, July 1997, pp. 1195-1245.

[24] O. L. Frost III, "An algorithm for Linearly Constrained Adaptive Array Processing", Proceeding of the IEEE, vol. 60, no. 8, August 1972, pp. 926-935.

[25] L. J. Griffiths, "A simple adaptive algorithm for real-time processing in antenna arrays", Proceeding of the IEEE, vol. 57, no. 10, Oct. 1969, pp. 1696-1704.

[26] A .E. Bryson, Jr. and Y. C. Ho, Applied Optimal Control, Waltham, Mass., Blaisdell, 1969.

Chapter 5 Introduction of time redundancy in a Time Modulated Linear Array

5.1 Introduction

In the last Chapter we have shown the mathematical model of realising harmonic beam scanning in the time modulated antenna array without the use of phase shifters. The basic philosophy behind the concept is to control the relative time delay of each array element by high speed RF switches connected an external programmed circuit. However, the reported research studies are all based on a common hardware architecture in which the signals from the switched array elements are combined to provide a single output channel at any given harmonic frequency. Although the use of bandpass filters are used to provide multiple array outputs at the fundamental and harmonic frequencies [1], these systems do not exploit the potential time redundancy in the switching sequence of the time modulated linear array.

In the case of multiple harmonic beam steering using an N-element antenna array, the conventional array architecture is inefficient as the elements of the array are only utilised for 1/N of the modulating period. In this chapter we will propose a multiple output channels time modulated linear array which exploits the time redundancy of the conventional systems. The concept is first introduced by considering a

conventional single output beam steering system and then extends the analysis to a

two channels scenario [2].

5.2 Theoretical Analysis of time redundancy in the time modulated linear array

For an N-element time modulated linear array with half wavelength inter-element

spacing, assuming each element is energised sequentially with a period of times given

by 1/N. From Chapter 4 the array factor of the time modulated linear array is given

by:

$$AF(\theta,t) \ = \ \sum_{m=-\infty}^{\infty} e^{j(\omega + m\omega_o)t} \sum_{n=0}^{N-1} \frac{1}{N} \frac{\sin(m\pi/N)}{(m\pi/N)} e^{j\pi n (\sin\theta - \frac{2m}{N})} \qquad (5.1)$$

It indicates that in the case of sequential element switching sequence, the phase shift

introduced is $\theta = \sin^{-1}(2m/N)$. Thus harmonic beam patterns of the array are scanned

in angle as a function of a given number of harmonic m. This explains how electronic

beam scanning property can be realised in the time domain without the use of phase

shifters.

Now we will examine the specific case of a 16-element linear array in which the array

elements are sequentially energised for a period of 1/16 of the normalised modulating

period. The first positive harmonic is designed to steer the main beam towards the

direction of 7.2°. The switching time scheme is shown in Fig.5.1 and associated

beampatterns at the fundamental frequency and the first 5 positive harmonics are
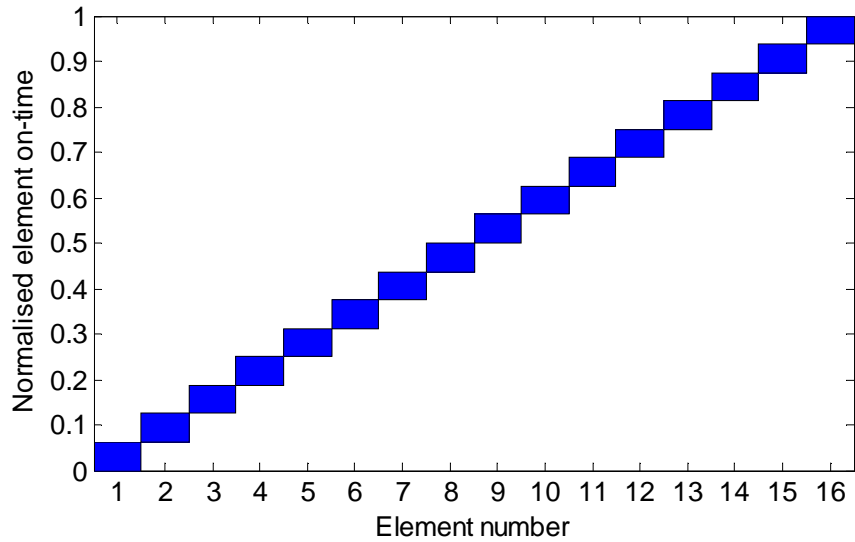
presented in Fig.5.2.

Fig.5.1. Conventional sequential time sequence for a 16 element time modulated array

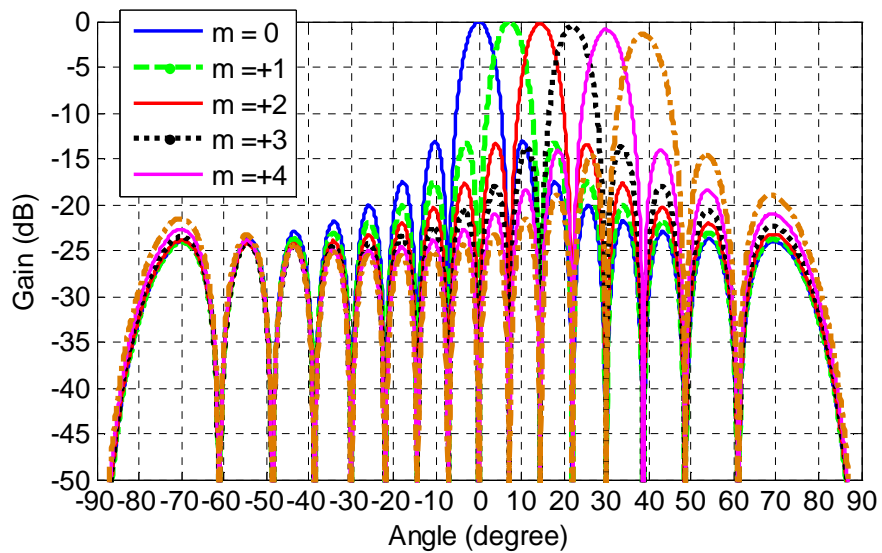designed to generate a first positive harmonic beam pointing at the direction of $7.2°$.

Fig.5.2. Beampatterns at the fundamental and first 5 positive harmonic frequencies

produced by the switching time sequence in Fig.5.1.

In Fig.5.1 this particular switching sequence of the array is only utilised 1/16 of the modulating period and is effectively redundant for the remaining 15/16 of the period. To more fully utilise the capabilities of a time modulated linear array, a technique of modifying the feeding structure and switching mechanism is proposed to control the array elements from a simple single channel system with SPST switches, to a multi-channel system with multi-throw switches [2]. The use of SPMT switches does not incur any significant drawbacks in terms of cost or complexity particularly for low values of M.

A conventional receiving structure of a single channel time modulated linear array is shown in Fig.5.3. Theoretically, an N element linear array could be configured to provide up to N independent channels (depending on the switching sequence used) but a simple case of a two-channel system will be introduced in this chapter. Fig.5.4 draws a generalised diagram representing an N-element time modulated linear array configured to provide two independent outputs. This could be achieved by replacing the simple binary switches of a single channel array with multi-throw switches. In this particular example SP3T switches are used with the third switch state corresponding to the "off" state. Fig.5.4 indicates that a suitably configured time modulated linear array is able to provide multiple output channels which utilise same array elements.
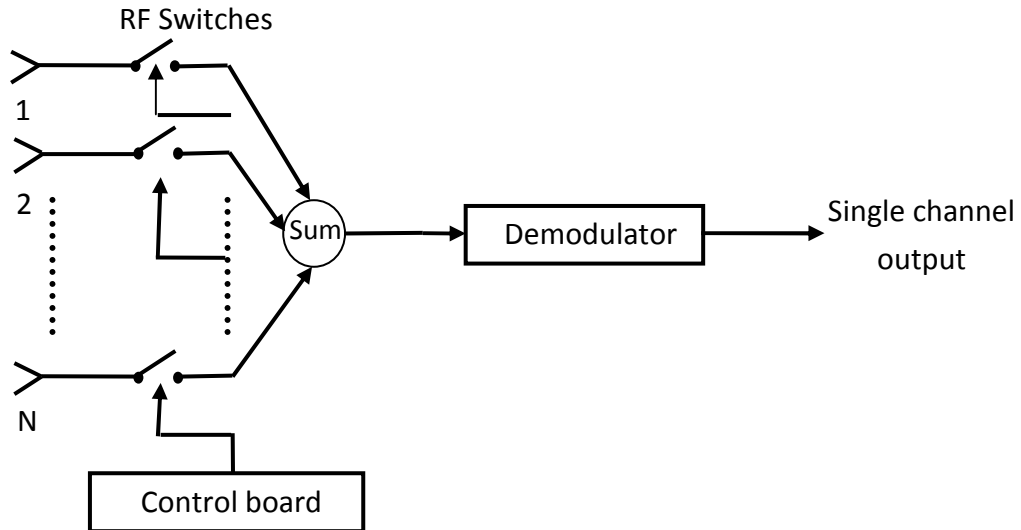
Fig.5.3. Conventional single channel time modulated linear array receiving structure.
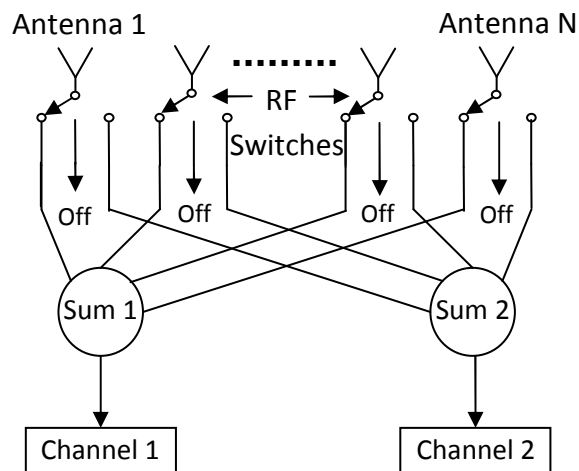

Fig.5.4. Example of a two-channel time modulated linear array receiving structure.

To demonstrate this concept we will return to our example of a 16 element time modulated linear array which has been configured for two channels TMLA application. Fig.5.5 presents the possible arrangement for controlling the array to

provide two independent outputs. For the switching sequences in both two channels, they have produced identical beam patterns that are shown in Fig.5.2. It can be seen that in the case of two channel beamforming application, one of the switching time schemes have been moved up by a half of the normalised modulating period ($0.5T_0$).
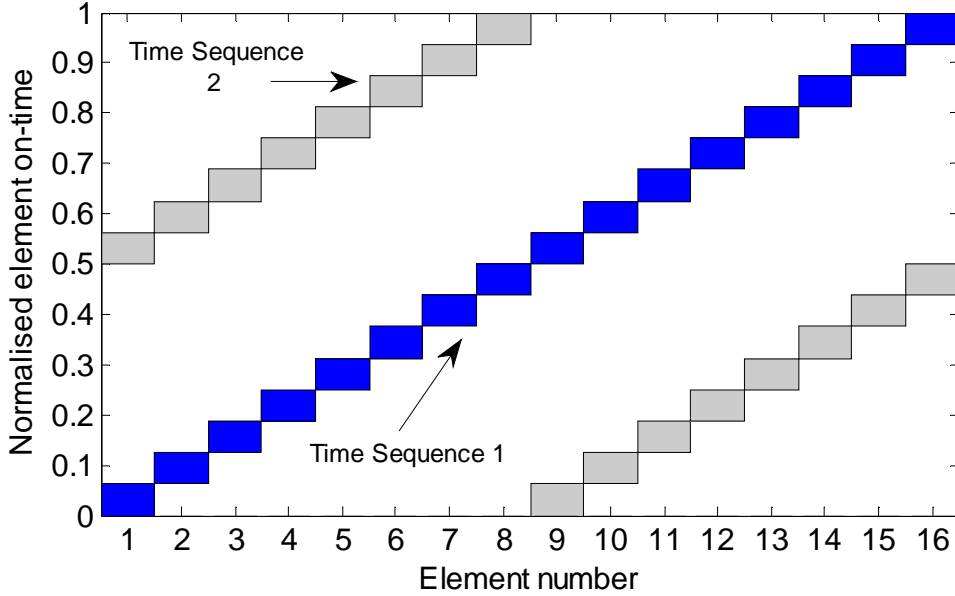

Fig.5.5. Time sequences designed to provide two identical output signals (Blue – Time sequence 1 and Grey – Time Sequence 2).

The above example introduces a great flexibility in exploiting the redundancy of the time sequence, but Fourier coefficients at different harmonics will be modified accordingly. This can be explained by examining the Fourier coefficients of the time modulated linear array given by:

$$a_{mn} = \frac{\sin(\pi m(\tau_{noff} - \tau_{non}))}{\pi m} e^{-j\pi m(\tau_{noff} + \tau_{non})}$$

If an arbitrary number C (less than unity) is imposed to the switching on and off times of each array element, a_{mn} will be modified accordingly as:

$$a_{mn} = \frac{\sin(\pi m(\tau_{noff} - \tau_{non}))}{\pi m} e^{-j\pi m(\tau_{noff} \pm C + \tau_{non} \pm C)}$$

$$= \frac{\sin(\pi m(\tau_{noff} - \tau_{non}))}{\pi m} e^{\pm j2\pi mC} e^{-j\pi m(\tau_{noff} + \tau_{non})} \tag{5.2}$$

The sine term and relative phase delay between each element will remain unchanged so that same harmonic patterns are generated by this approach compared with the conventional time scheme. Although this proposed technique provides a good solution to make the best use of the redundancy of the time sequence and hence improve the system performance, the additional exponential term $\exp(-jm2\pi C)$ introduced by shifting the time sequence has a impact on the phase of original Fourier coefficients. This is of a great importance within the demodulation process and it will be discussed in a more details in the next chapter.

5.3 Conclusions

Time modulated linear array (TMLA) can be configured to perform real time electronic scanning but at much lower cost as they do not require phase shifters. However, the conventional time modulated linear array based on a single output channel topology will only be energised for a certain period of time, so such a topology is inefficient in terms of time utilization of the array elements. In this chapter we have proposed a multiple output channels time modulated linear array which exploits the time redundancy of conventional method. This attractive feature combined with smart antenna technology will find a good potential application in the communication system.

5.3 References

[1] G. Li, S. Yang, Y. Chen, and Z. Nie, "A novel electronic beam steering technique in time modulated antenna array," Progress In Electromagnetics Research, vol. 97, 2009, pp. 391-405.

[2] Y. Tong and A. Tennant, "A Two-Channel Time Modulated Linear Array With Adaptive Beamforming", IEEE Transactions on Antenna and Propagation, vol. 60, no. 1, pp.141-147, January, 2012.

Chapter 6 Application of Time Modulated Linear Arrays in Communication Systems

6.1 Introduction

Phased antenna array systems have been studied extensively in the past decades and are considered a key technology in communication systems. As discussed in the previous chapters, one of the significant characteristics of the time modulated antenna array is to perform real electronic beam scanning without the use of expensive phase shifters. This can be achieved by sequentially energising the elements along the length of the array, so it effectively introduces a linear time delay in the switching sequence across the face of the array and generates harmonic radiation patterns which have a directional response at prescribed steering angles. Therefore a properly controlled time modulated array can be configured to replicate the properties of a phased antenna array. Crucially however, the time modulated antenna array achieves this function without the use of expensive phase shifters.

However, there is little published work based on the application of the time modulated antenna arrays to communication systems. In chapter 4, we have described the principles of realising multiple harmonic beams scanning and null steering technique based on the time modulated linear array. In reality we demand a smart system that automatically steers the main beam to the signal of interest and reject the unwanted

signals. At the beginning of this chapter, we will examine the scenario of applying adaptive beaming in the conventional time modulated antenna array system [7].

One of the main drawbacks of the conventional time modulated antenna arrays architecture is that the sequential switching time scheme only uses 1/N of the modulating period, so it is very inefficient in terms of time utilisation. In Chapter 5, we have introduced a novel way to solve this issue. Moreover, all the predescribed time modulated antenna array are based on a common hardware architecture in which the signals from the switched array elements are combined to provide a single output channel at any given harmonic frequency. In the latter part of this chapter we will propose a multiple output channels based on a time modulated linear array which exploits the time redundancy of the conventional method and hence improve the communication system performance. The concept is first introduced by considering the conventional beam steering system with a single output and then extending the analysis to two-channel adaptive beamforming scenario [7].

6.2 Theoretical Analysis

6.2.1 Beamforming in Time Modulated Linear Array

Assuming an N element linear array of half wavelength element spacing is connected to N simple high speed RF switches and each array element is periodically energised by a rectangular pulse of a period T_0. From Chapter 2 the array factor of a time-modulated linear is given by:

$$AF(\theta,t) \ = \ e^{j\omega t}\sum_{n=0}^{N-1}I_n(t)\,e^{jknd\sin\theta} \ = \ \sum_{m=-\infty}^{\infty}e^{j(\omega+m\omega_o)t}\sum_{n=0}^{N-1}w_{mn}e^{jknd\sin\theta} \qquad (6.1)$$

where $I_n(t)$ are the periodic time modulating signals.

If a narrow band plane wave *s(t)* transmitted from a far field source arrives the array at an angle of θ with respect to the horizontal line, the signal received is denoted as [8]:

$$x(t) = s(t)\sum_{m=-\infty}^{\infty}\sum_{n=0}^{N-1}w_{mn}e^{jknd\sin\theta_d}\,e^{jm\omega_o t} = \mathbf{w}^H\mathbf{a}(\theta)s(t)\sum_{m=-\infty}^{\infty}e^{jm\omega_o t} \qquad (6.2)$$

where $\mathbf{a}(\theta)$ represents the array response or steering vector expressed in a complex vector form as:

$$\mathbf{a}(\theta) = [1\ ,\ e^{-jkd\sin\theta}\ ,\ e^{-2jkd\sin\theta}\ ,\ ....\ ,\ e^{-j(N-1)kd\sin\theta}\ ]^T \qquad (6.3)$$

In the presence of interference and random noise, equation (6.2) becomes:

$$x(t) = s(t)\sum_{m=-\infty}^{\infty}\sum_{n=0}^{N-1}w_{mn}e^{jknd\sin\theta_d}\,e^{jm\omega_o t} + I(t)\sum_{m=-\infty}^{\infty}\sum_{n=0}^{N-1}w_{mn}e^{jknd\sin\theta_I}\,e^{jm\omega_o t} + n(t)$$
$$= \mathbf{w}^H\mathbf{a}(\theta_d)s(t)\sum_{m=-\infty}^{\infty}e^{jm\omega_o t} + \mathbf{w}^H\mathbf{a}(\theta_I)I(t)\sum_{m=-\infty}^{\infty}e^{jm\omega_o t} + n(t) \qquad (6.4)$$

where I(t) and n(t) are interference and noise at any instant time. After down converting the received signal into the baseband, the output of the array can be written in the vector form as:

$$y(t) = \sum_{n=0}^{N-1}w_n x_n(t)$$
$$= \mathbf{w}^H\mathbf{x}(t) \qquad (6.5)$$
$$= \mathbf{w}^H[\mathbf{a}(\theta_d)s(t) + \mathbf{a}(\theta_I)I(t) + n(t)]$$

where the complex weights, signal of interest and interference are:

$$w = [w_0^*, w_1^*, w_2^*, ..., w_{N-1}^*]^T \qquad (6.6)$$

$$s(t) = [s_0(t), s_1(t), s_2(t), ..., s_{N-1}(t)]^T \qquad (6.7)$$

$$I(t) = [I_0(t), I_1(t), I_2(t), ..., I_{N-1}(t)]^T \qquad (6.8)$$

As a result of the growing demand for the increasing number of users in the wireless system, smart antennas technology was proposed to provide solution for improving channel capacity. The fundamental principle is to control the amplitude weights of each array element adaptively by innovative digital signal processing algorithms so that the system produces beam patterns that have maximum radiation in the direction of desired signal and nulls to reject interfering signals. There are a variety of algorithms available in the literature, but one of the simplest and commonly used techniques is the Least Mean Square (LMS) algorithm [9]. The LMS algorithm minimises the squared error between the desired signal *d(t)* and actual output signal *y(t)*. Based upon this criteria, the errors *e(t)* are written as [9]:

$$e(t) = d(t) - y(t) = d(t) - \mathbf{w}^H \mathbf{x}(t) \qquad (6.9)$$

The squared the magnitude of the error is given by:

$$\left| e(t) \right|^2 = \left| d(t) - \mathbf{w}^H \mathbf{x}(t) \right|^2 \qquad (6.10)$$

Thus the error signal is used to adjust the array weights adaptively and the iterative weights are computed as [9]:

$$w(t+1) = w(t) + 2\mu x(t) e^*(t) \qquad (6.11)$$

with the step size μ constrained by:

$$0 < \mu < \frac{1}{\delta_{max}} \qquad (6.12)$$

where δ_{max} indicates the largest eigenvalue of covariance matrix of *x(t)* defined by

$R_x = E[x(t)x^H(t)]$.

6.2.2 BPSK in the Communication Channel

Having introduced the mathematical model of beamforming in the time modulated linear array, we will begin to look at data transmission model in the communication channel. The probability of bit error or bit error rate (BER) is often regarded as an effective measure to examine the accuracy of the date received in the digital transmission. Binary Phase Shift Keying (BPSK) is one of the simplest digital modulations in the system and we will use this model in the following analysis of the chapter. Supposing the linear array is to receive a BPSK signal in the presence of Additive White Gaussian Noise (AWGN) that is symmetrically distributed across the positive and negative frequency, the noise will follow the Gaussian probability distribution function and is given by [10]:

$$p(x) = \frac{1}{\sqrt{2\pi\sigma^2}} e^{\frac{-(x-b)^2}{2\sigma^2}} \qquad (6.13)$$

where the parameter mean b = 0 and variance $\sigma^2 = N_0/2$ with N_0 indicates noise power.

Using equation (6.13) as the basis to compute the probability of error or Bit Error Rate [10]:

$$P_{BPSK} = \frac{1}{2}\text{erfc}(\sqrt{\frac{S}{N_0}}) \qquad (6.14)$$

where S represents signal power and erfc(x) is the complementary error function expressed as [10]:

$$\text{erfc(x)} = \frac{2}{\sqrt{\pi}}\int\limits_{x}^{\infty}e^{-x^2}dx \qquad (6.15)$$

6.3 Smart antenna application in Time Modulated Linear Array

Having gain a basic understanding of beamforming structure based on time modulated linear array, we will start to investigate its potential application in the communication system. Nowadays, antenna arrays are widely used in the wireless communication field, especially in the mobile communication services, because it provides higher gain compared to a single element, as well as greater range coverage and improved channel capacity. Smart antenna technology has been studied extensively in recent years and it offers a better control of the array radiation pattern and improves the system performance. Smart antenna array system can be classified into two main categories: Switched Beam [11] or Adaptive Array [12].

6.3.1 Switched beam system in Time modulated Linear Array

As its name implies, a switched beam system composes of several predefined beam patterns that are able to cover some fixed regions. Let us first look at an example of realising switched beam technique in the time modulated linear array. Considering 16 isotropic elements linear array of half wavelength inter-element spacing with uniform amplitude weights, the system is designed to generate harmonic beams scanning at an interval of $10^{°}$ covering the full hemisphere. In this chapter, all the numerical examples are simulated by using MATLAB. The switching time sequence and resulting beampatterns are drawn in Fig.6.1 and Fig.6.2.
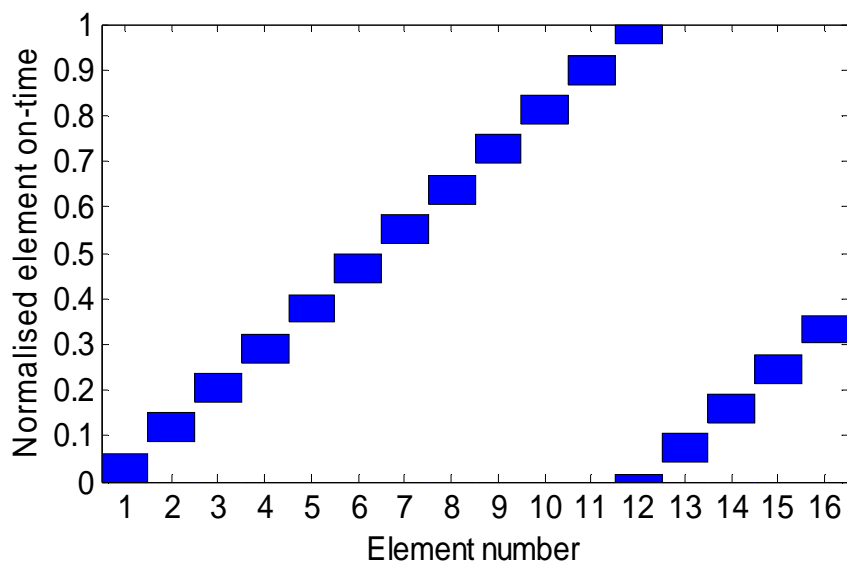
Fig.6.1. Time sequence designed to produce harmonic beams scanning at an interval of $10^{°}$ covering the full hemisphere.
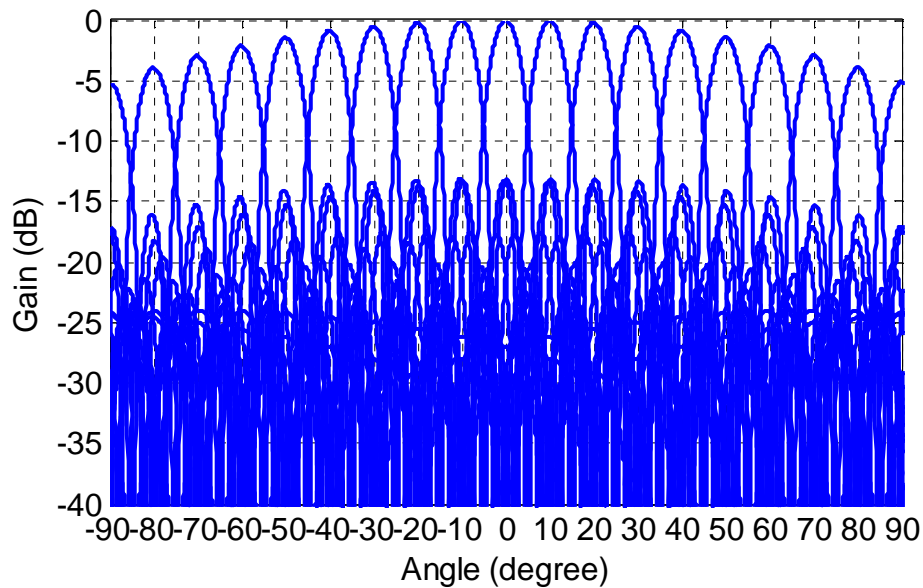
Fig.6.2. Resulting beam patterns of time sequence in Fig.6.1.

The 16-elements linear array is assumed to receive BPSK signals under Additive White Gaussian Noise environment and only one desired signal is considered. In the simulation, the bit error rate (BER) for a range of different signal to noise ratios (SNR) can be calculated by equation (6.14) and the graph is drawn in Fig.6.3.

The switched beam system based upon the requirement chooses the maximum signal strength among the predefined beams at any instant time. In our example, the beam points at direction of $10^{°}$ and the first positive harmonic beam pattern is used to detect the signal. The perfect situation is where desired signal has just aligned with the maximum response of the selected beam (Case A). In most of the cases, desired signal or user may not necessary impinges on the right centre of any beampattern. For instance the direction of arrival angle of the desired signal is now changed to $7^{°}$(Case B), the bit error rate has been computed by equation (6.14) and the simulation result is shown in Fig.6.3.

For a more practical situation, we need to take account of the effect of interfering

signals. In Case C, one desired user and one interfering signal with signal to

interference ratio (SIR) of 0dB coming from $\theta_d = 7^\circ$ and $\theta_i = -6^\circ$ has been considered. A

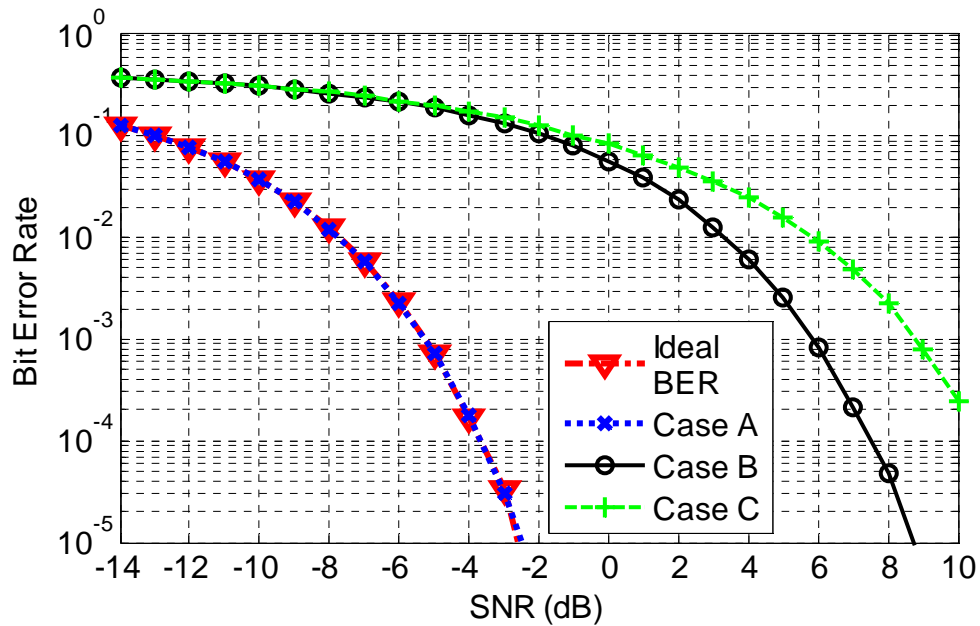comparison of bit error rate graph under three different scenarios is drawn in Fig.6.3.

Fig.6.3. Bit Error Rate graph of the switched beam system under different scenarios.

In fact, the switched beam system suffers from the problem that the bit error rate will be

getting worse and worse as the desired signal moves out the centre of selected main

beam, this situation becomes more apparent in the presence of interferences.

6.3.2 Adaptive Array System in Time Modulated Linear Array

Despite the benefits offered by the switched beam system in terms of simplicity and

cost, the adaptive array exhibits a much better system performance. In this section we

will examine the specific implementation of this technique in the time modulated linear

array. To introduce the concept we will initially consider to apply adaptive beamforming at the first positive harmonic pattern for a conventional time modulated linear array with only a single output. A block diagram of a simple adaptive beamforming structure of time modulated linear array is shown in Fig.6.4.

The following analysis relates to a 16 elements linear array of half wavelength spacing and it is designed to operate in the higher GHz bands, due to the size limitation in the practical design. Same assumptions are made that the array is to receive a Binary Phase Shift Keying (BPSK) signal in an environment that is subject to Additive White Gaussian Noise (AWGN). As discussed in the previous section, the generalised expression of an array output can be written as:

$$y(t) = \mathbf{w}^H \mathbf{x}(t)$$
$$= \mathbf{w}^H [\mathbf{a}(\theta_d) s(t) + \mathbf{a}(\theta_I) I(t) + n(t)]$$

where x(t) is the received signal in the vector form, $x(t) = [x_0(t), x_2(t),\ldots, x_{N-1}(t)]$, $s(t)$, $I(t)$ and $n(t)$ are transmitted signal, interfering signal and Additive White Gaussian Noise respectively. In addition, $a(\theta_d)$ and $a(\theta_I)$ are denoted as the array response of desired signal and interference respectively and W^H implies the complex conjugate transpose of a set of complex array weights W.

The desired array weights W are usually calculated from one of the many techniques described in the literature but in our implementation we have used the adaptive Least Mean Square (LMS) algorithm [9]. Once the required set of weights has been computed, substituting the results into equations (4.26) and (4.27) for the case of m =1 to obtain the corresponding switching sequence.
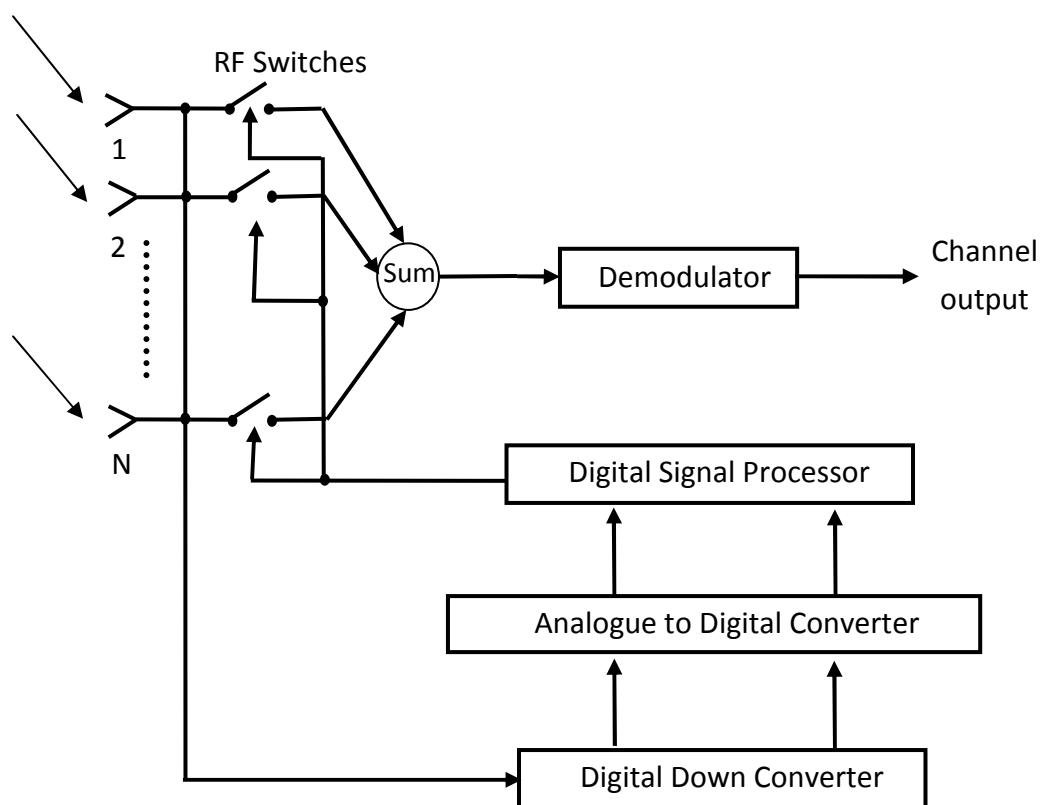
Fig.6.4. A block diagram of a simple adaptive beamforming structure of time

modulated linear array.

Equipped with this background information, now we may begin to investigate the

application of adaptive beamforming applied in a single channel TMLA. First consider

a scenario in which there are only one desired signal and one interference signal with a

signal to interference ratio (SIR) of 0dB impinge the array from the direction of 40° and

-20° respectively. Our primary intention is to compute the conventional elements

amplitude weights by employing adaptive LMS algorithm introduced in equation (6.11).

The next step is to convert the optimum iterative weights into the corresponding

switching sequence necessary to achieve the desired beamforming response at a

specific harmonic component. Here it is chosen to be at the first positive harmonic

(m=1).

In this example, the switching time scheme of one channel output application is presented in Fig.6.5 and the associated beam pattern at the first positive harmonic is shown in Fig.6.6 where it is observed that the first harmonic pattern steers the maximum response towards desired signal while a null has formed in the direction of the interfering signal. The simulated bit error rate graph in Fig.6.7 has shown an excellent agreement with the theoretical result. It should be noted that although equation (6.14) provides an ideal solution for the BPSK modulation scheme, there is no closed form expression for the BER performance in the TMLA considered here. Therefore a numerical way is used to estimate the BER based on a hard decision approach. It is described that the receiver identifies "1" as the originally transmitted signal when the output is greater than 0, and receiver identifies "0" as the originally transmitted signal when the output is less than 0.
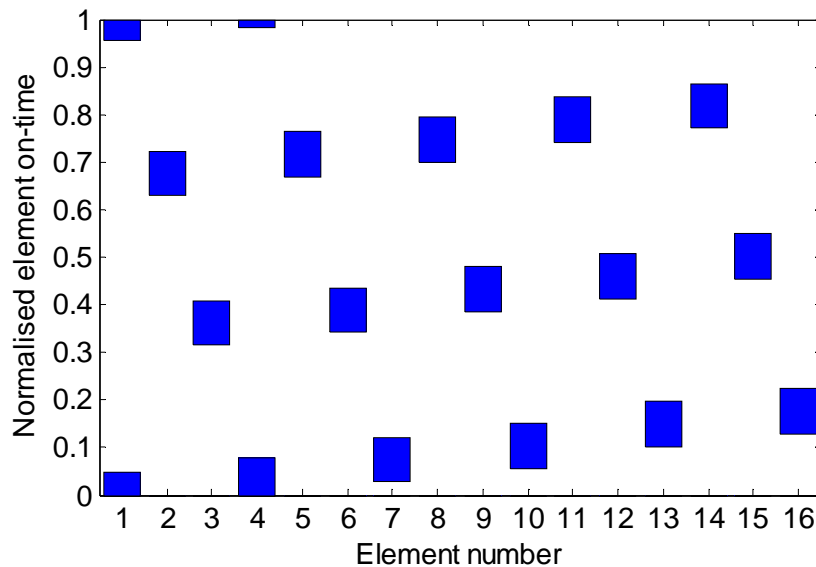

Fig.6.5. Time sequence designed to produce a main beam at 40° and a null formed at

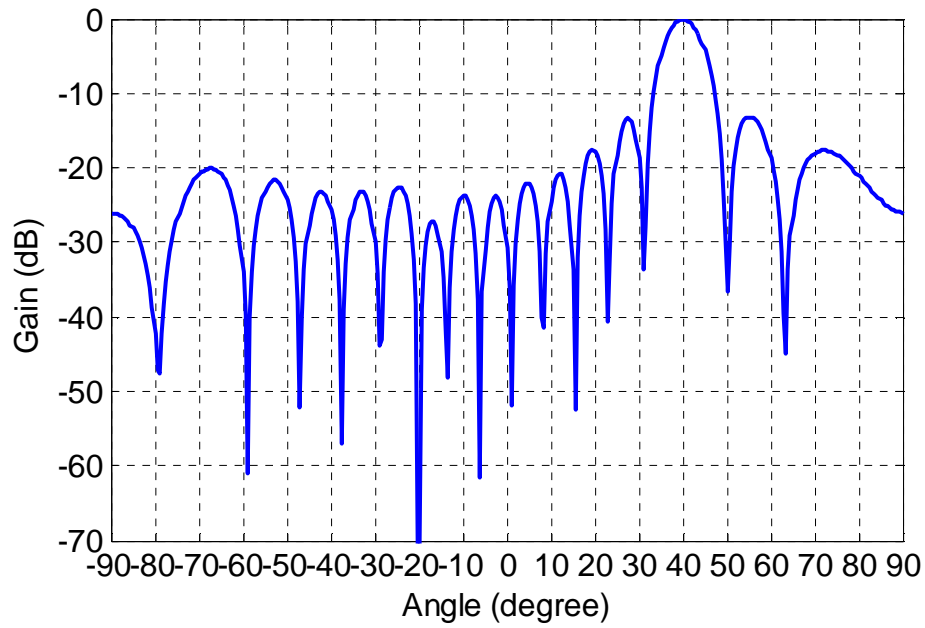-20° for one channel time modulated linear array system.

Fig.6.6. Beampattern at first positive harmonic corresponds to time sequence in Fig.6.5.
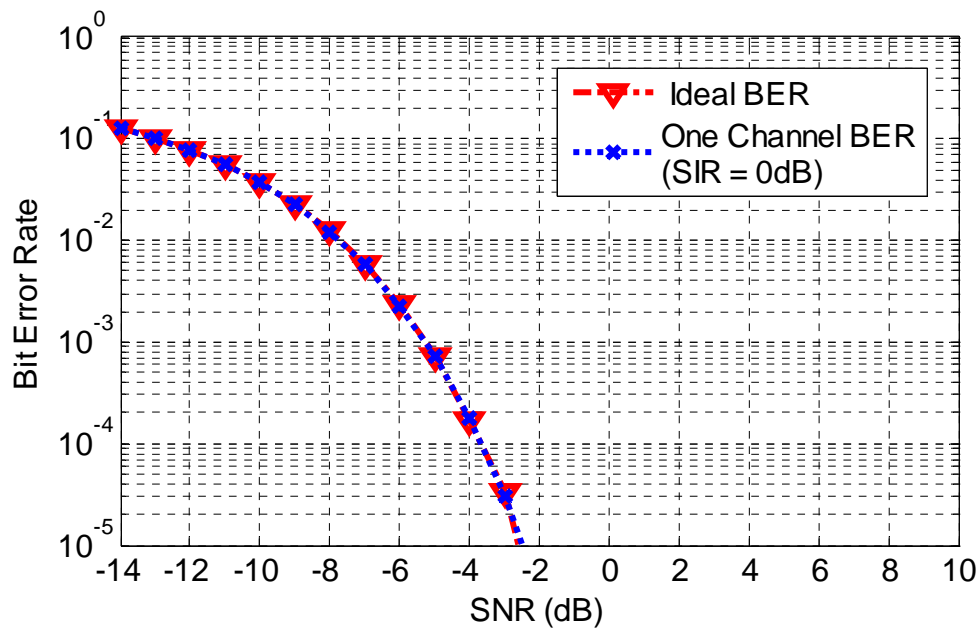

Fig.6.7. BER graph for a one channel adaptive beamforming system against the

theoretical BER.

As a result of periodic time modulation, the array output has a mixture of numerous

beampatterns at different frequencies. In order to exact information from the specific

harmonic component, the output has been down-converted into IR signal and would be properly filtered to reject the fundamental frequency and also other unwanted frequencies (including negative harmonics). Although it may be argued that such an approach is "inefficient" as the power in the remaining harmonic has been discarded, they are not considered to be an important problem for two reasons: firstly the power level of the received signal is very low and hence there is no issue associated with significant power loss. Secondly but most importantly, it is the pattern gain of the array at the desired harmonic frequency which determines the performance of the system. However, for completeness and based on the approach presented in [13], the efficiencies at the fundamental and first 5 positive harmonics of this proposed technique are 9.7%, 9.4%, 8.5%, 7.2%, 5.7% and 4.13% respectively.

Now it is time to examine a more complex circumstance in which there are two desired signals incident on the array from two separate directions. Thus a two-channel adaptive beamforming in TMLA will be employed to extract signals and compute bit error rate from both sources simultaneously. In the scenario where two users (user 1 and user 2) are transmitted useful information to the array from the DOA angles of $40°$ and $-20°$ respectively.

Initially, desired signals from user 1 and user 2 are both assumed to have unit magnitude and hence the power ratio between them in this case is 0dB. As a starting point, consider Channel 1 receives the desired signal from user 1. In this case signal

from user 2 becomes a source of interference and hence may use the previously described procedure to obtain the switching time sequences. The resulting array responses are identical to the patterns shown in Fig.6.6, the main beam steers the maximum response towards the user of interest (user 1) while suppressing the interference signal in the direction of -20°. Subsequently, for another independent channel, user 2 provides the desired signal and user 1 becomes the source of interference. A similar procedure to that described for Channel 1 is then used to acquire the time sequence of Channel 2. A general representation of this application is illustrated in Fig.6.8.
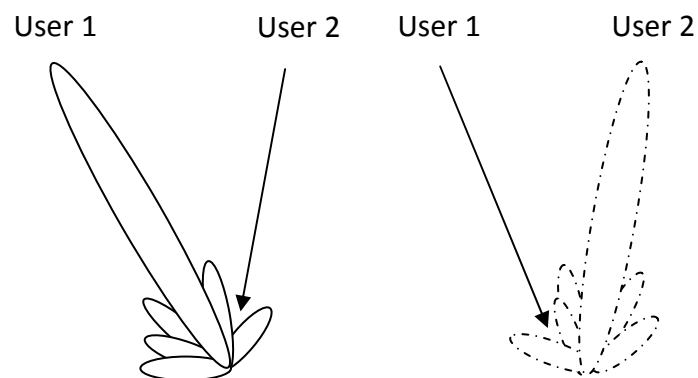

Fig.6.8. A general representation of two-channel time modulated linear array.

The time scheme required for simultaneous operation of both Channel 1 and Channel 2 are presented in Fig.6.9. It is aware that there is a conflict for certain elements of the array since two channels require connections to the same element at the same time. This is shown by the 'overlapping region' in Fig.6.9 and in this example it is applied to elements 1, 3, 5, 7, 9 and 11.

There are many ways to address this problem depending on the particular scenario being considered. For example, if the signal from Channel 1 was deemed to have a higher priority than that of Channel 2, then the time sequence of Channel 1 would take priority and be left unchanged. Channel 2 however would then have a non-optimum time scheme and its performance could be severely degraded. In another situation it may be decided to share the conflicting overlapped region equally between two channels. Adopting this approach has degraded the array response in both Channel 1 and Channel 2 which has been presented in Fig.6.10. It is perceived that although the main beam response in both Channel 1 and Channel 2 is preserved, nulls in the directions of the interfering signals have not been formed as required.
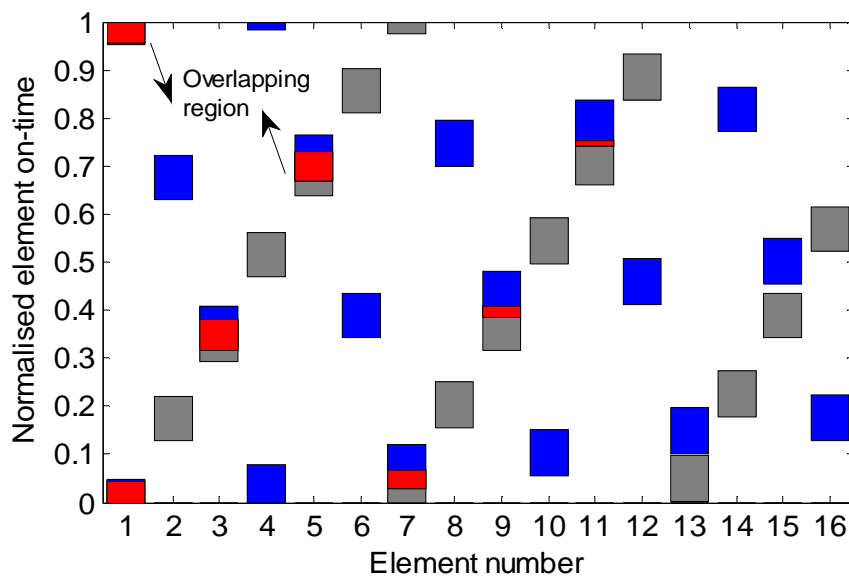

Fig.6.9. Time sequences of a two-channel adaptive beamforming TMLA (Blue– User 1, Gray – User 2, and Red – overlapping region).
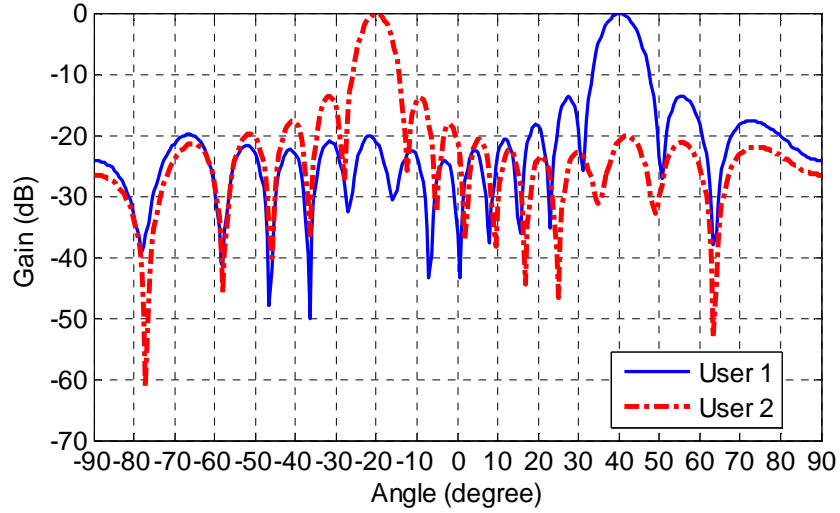
Fig.6.10. Resulting radiation patterns of time sequence in Fig.6.9 when there is no time

offset applied ($\delta = 0$).

Several other time-slot sharing strategies could be examined but an alternative solution

is to introduce a small time offset by adding an arbitrary number less than 1 into the

corresponding switching sequences in both two channels, such that the degree of

mutual overlapping region would be diminished or eliminated. It may therefore modify

the two independent normalised time schemes as follows:

$$\tau 1^{'} = \tau 1 + \delta \tag{6.16}$$

$$\tau 2^{'} = \tau 2 - \delta \tag{6.17}$$

where $\tau 1$ and $\tau 2$ are the original switching time sequences for Channel 1 and Channel 2

when no time offset is applied, $\tau 1$' and $\tau 2$' are the modified time schemes of Channels

1 and 2 respectively and δ indicates the time offset.

To better convey this proposed idea, let us return to the previous mentioned

two-channel TMLA example, desired signals of two independent users are transmitted

from the directions of $40°$ and $-20°$ respectively. Initially consider the case where the

two signals are of equal magnitude so that the corresponding signal to interference ratio

(SIR) for both channels is 0dB. Fig.6.11 and Fig.6.12 have demonstrated the simulated

BER graph under this circumstance at different values of time offsets ranging from $\delta =$

0 to $\delta = 0.03$. For this particular example, the resulting BER for both Channel 1 and

Channel 2 do not deviate significantly from the theoretical value, even there is no time

offset applied ($\delta = 0$). This can be explained by examining Fig.6.10, although no deep

null is produced at the required direction, the sidelobe level of the beampattern is

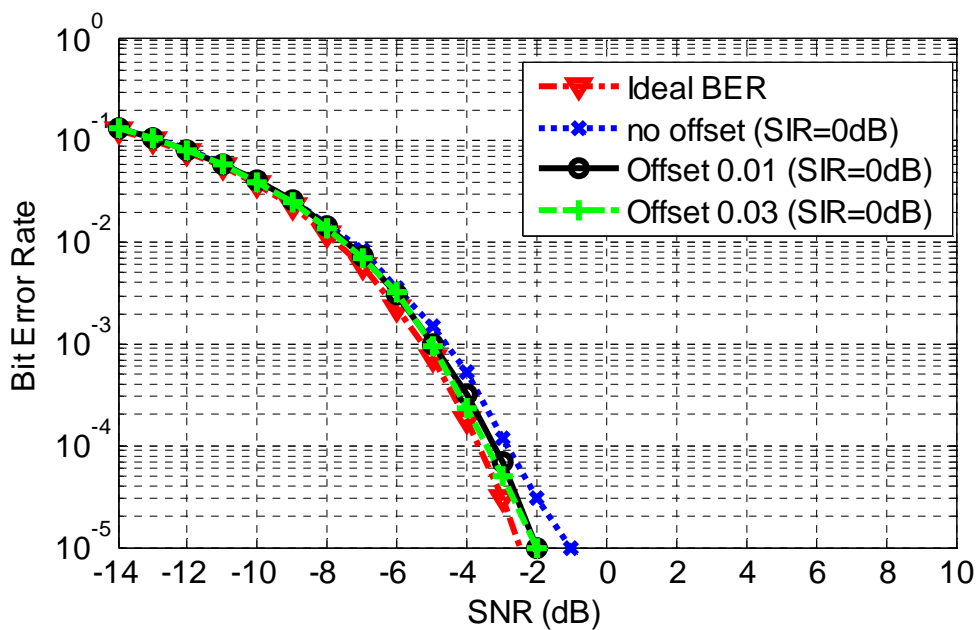sufficient to suppress the interferences when SIR is relatively small.

Fig.6.11. Channel One BER graph at different values of time offset δ when signal to

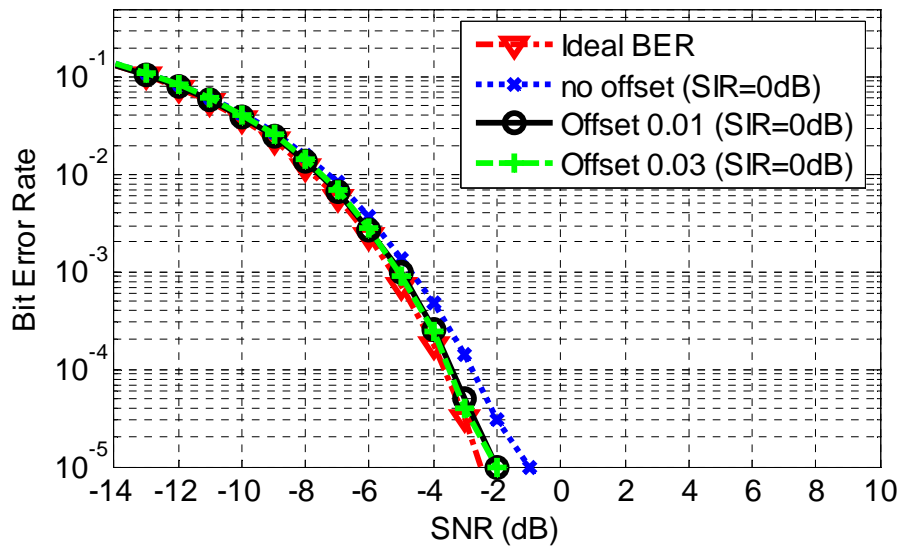interference ratio is 0dB (SIR = 0dB).

Fig.6.12. Channel Two BER graph values of time offset δ when signal to interference

ratio is 0 dB (SIR = 0dB).

Now consider a more demanding environment with much stronger interferences

presented, thus signal to interference ratio has been reduced from 0 dB to -20dB. The

BER estimations for the two independent channels are given in Fig.6.13 and Fig.6.14

respectively.

In this example radiation pattern in Fig.6.10 is no longer able to reject the strong

interference, thus the performance of bit error rate corresponded to the case of no time

offset for both channels have been significantly degraded. However, as the technique of

time offset has been applied, the corrupted beampatterns are gradually restored, which

is plotted in Fig.6.15. It can be noted that the deeper nulls are formed to attenuate

unwanted inferring signals, so a steady improvement of BER is achieved. The

simulation results approaches to the theoretical value when there is no overlapping

region existed between the two time sequences ($\delta = 0.05$ in Fig.6.13 and Fig.6.14).
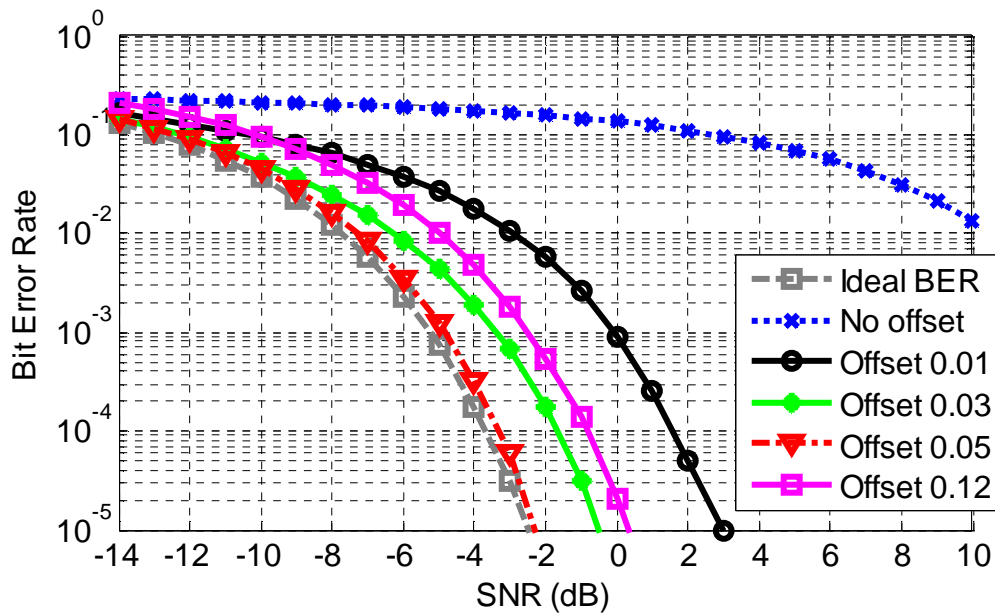

Fig.6.13. Channel One BER plot at various values of time offset when signal to

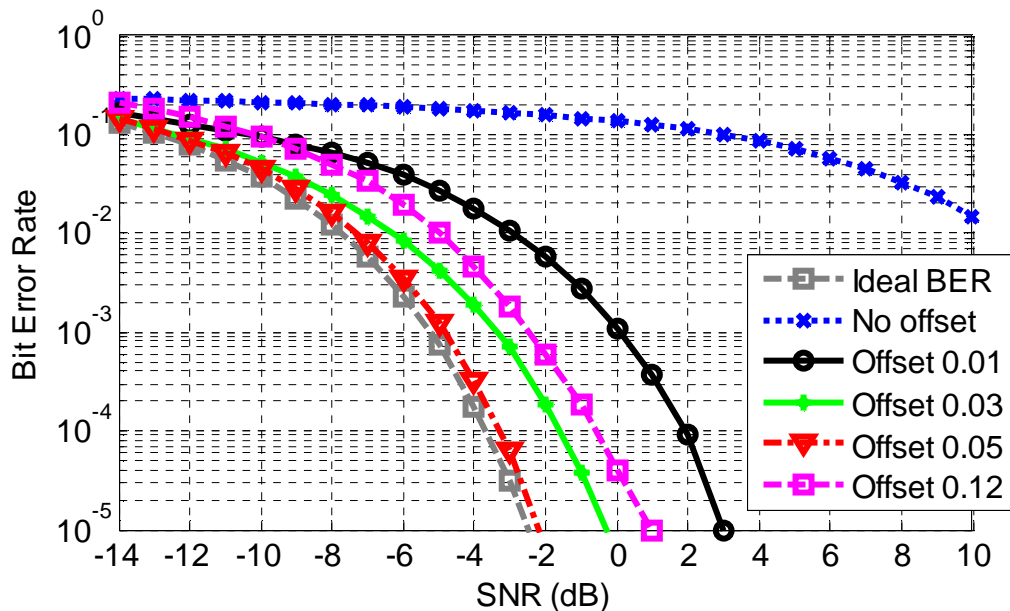interference ratio is -20dB (SIR = -20dB).

Fig.6.14. Channel Two BER plot at various values of time offset when signal to

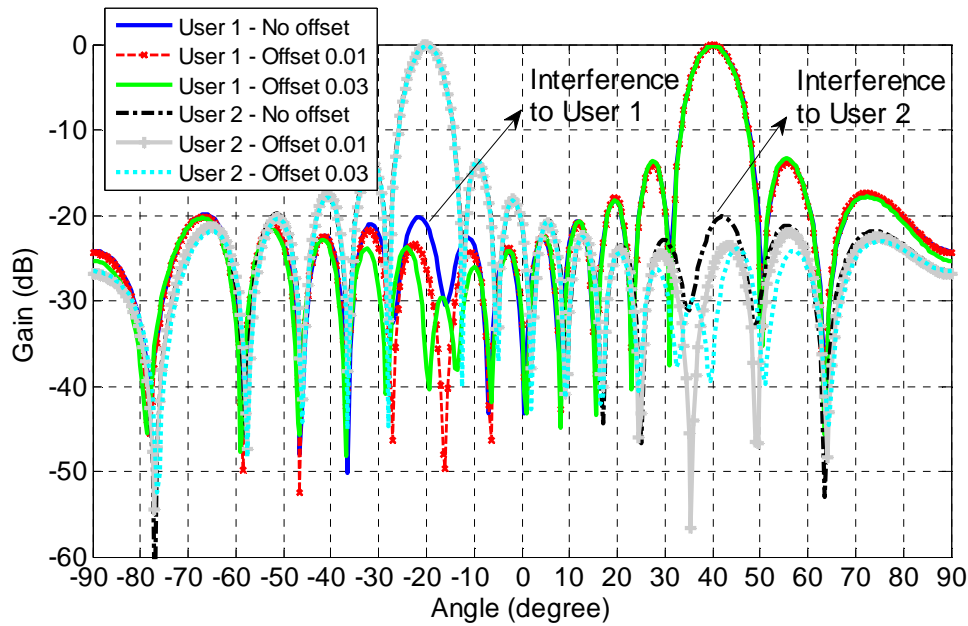interference ratio is -20dB (SIR = -20dB).

Fig.6.15. Beam patterns of User 1 and User 2 at different values of time offset.

The resulting time schemes to implement an offset value of 0.05 for both Channel 1 and Channel 2 are drawn in Fig.6.16 and the associated beampatterns are presented in Fig.6.17. It is now apparent that deep nulls are generated in the direction of the interferences.

For this example an offset value of 0.05 is sufficient to modify the time sequence in such way that they do not overlap. However, any time adjustment applied to the original switching schemes will inevitably compromise the performance of the system. In particular by shifting the entire time sequence will modify the array weights and hence corrupt the bit error rate performance. To illustrate this, Fig.6.13 and Fig.6.14 illustrate the simulation results when the time offset is increased to 0.12. Under this circumstance, although the two time sequences have no conflicting region, the outputs

of the system have shown a severe degradation for both two independent channels. This

is because array weights would be completely distorted after a certain threshold. So by

adjusting the value of time offset within a proper range is still acceptable and it will
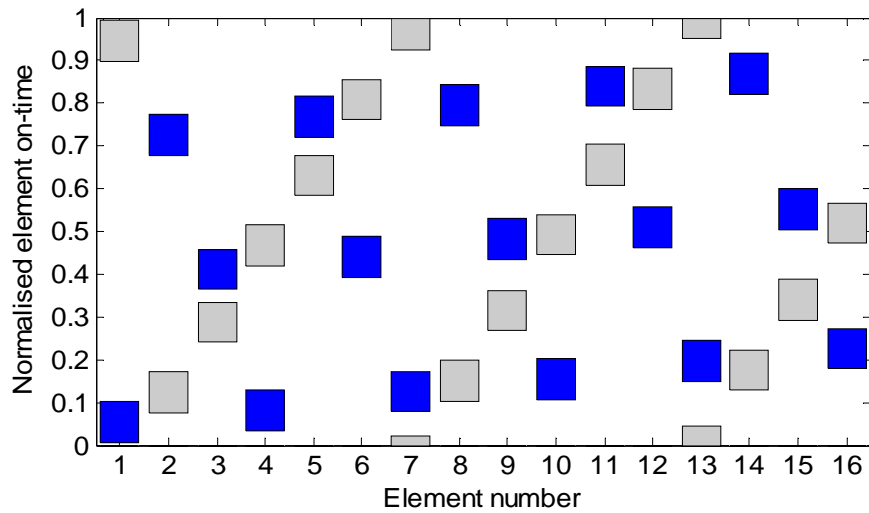
improve the quality of signal received.

Fig.6.16. Time sequences for two-channel adaptive beamforming application when

time offset δ = 0.05 (Black – User 1, Gray – User 2).
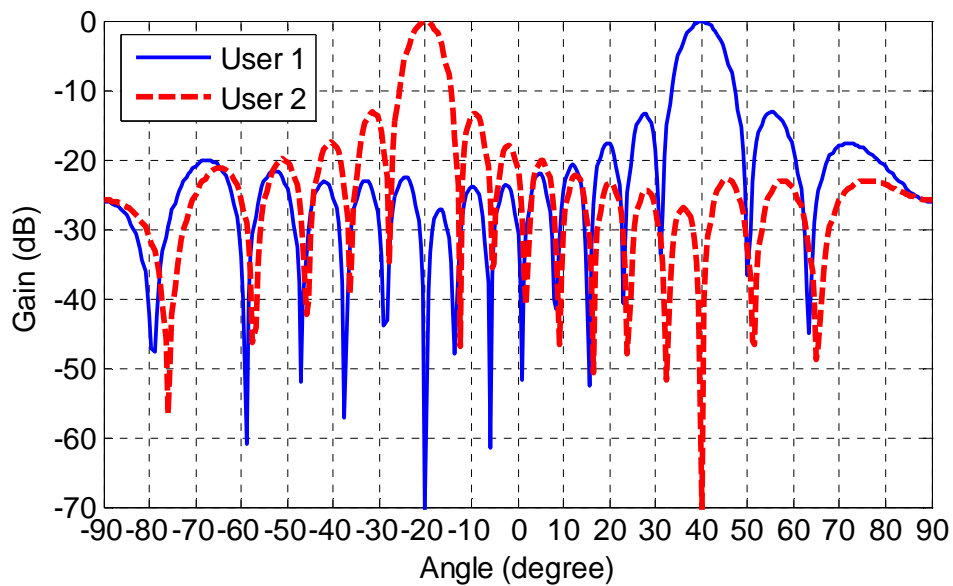

Fig.6.17. Beam patterns of Channel 1 and Channel 2 corresponds to the time sequences

in Fig.6.16 when time offset δ = 0.05.

Although the utilisation of time offset provides a practical solution to resolve the mutual overlapping region, this is not always the case. An example where this issue cannot be effectively solved will start to emerge if the direction of transmitting signals are close to each other. With this respect the proposed approach for a two-channel TMLA application is subject to the general constraints of beamforming as is applied to any array system.

6.4 Conclusion

A new approach for a time-modulated linear array configured for the application in the communication system has been presented. The topology exploits the redundancy in the conventional system designs and allows the beamforming network of the array to be more fully utilised. In an N-element TMLA, each element of the array is only energised for 1/N of the switching period. This redundancy can easily be exploited by modifying the array switching arrangement to incorporate multi-throw switches in an effort to provide several independent output channels. We have illustrated the concept by considering the specific example of a TMLA configured to perform smart antenna technology - switched beam and adaptive beamforming and its application in the BPSK communication channel. The system provides two simultaneous independent outputs at the same harmonic frequency and each channel can perform individual beamforming properties. Such an approach ideally doubles the capacity over a single channel system for minimal increase in system complexity.

6.5 References

[1] Y. Tong and A. Tennant, "Simultaneous control of sidelobe level and harmonic beam steering in time-modulated linear arrays," IET Electronics Letters, vol. 46, no. 3, 2010, pp. 200-202.

[2] A. Tennant and B. Chambers, "A two-element time-modulated array with direction-finding properties," IEEE Antennas Wireless Propagation Letter, vol. 6, 2007, pp. 64–65.

[3] A. Tennant, "Experimental two-element time-modulated direction finding array," IEEE Transactions on Antennas and Propagation, vol. 58, no. 3, March 2010, pp. 986-988.

[4] G. Li, S. Yang and Z. Nie,   "A study on the application of time modulated antenna arrays to airborne pulsed Doppler radar," IEEE Transactions on Antennas and Propagation, vol. 57, no. 5, May 2009, pp. 1578–1582.

[5] G. Li, S. Yang and Z. Nie, "Direction of arrival estimation in time modulated linear arrays with unidirectional phase center motion," IEEE Transactions on Antennas and Propagation, vol. 58, no. 4, April 2010, pp. 1105-1111.

[6] A. Tennant and B. Chambers, "Time-switched array analysis of phase switched screens," IEEE Transactions on Antennas and Propagation, vol. 57, no. 3, March 2009, pp.808–812.

[7] Y. Tong and A. Tennant, "A Two-Channel Time Modulated Linear Array With Adaptive Beamforming", IEEE Transactions on Antenna and Propagation, vol. 60, no. 1, pp.141-147, January, 2012.

[8] W. H. Kummer, A. T. Villeneuve, T. S. Fong, and F. G. Terrio, "Ultra-low sidelobes from time-modulated arrays," IEEE Transactions on Antenna and Propagation, vol. 11, pp. 633-639, Nov, 1963.

[9] B. Widrow, P. E. Mantey, L. J. Griffiths and B. B. Goode, "Adaptive Antenna Systems," Proceedings of the IEEE, vol. 55, no. 12, Dec. 1967, pp 2143 – 2159.

[10] J. G. Proakis, M. Salehi, "Digital Communications", Chapter 5: Optimum Receivers for the Additive White Gaussian Noise Channel, McGraw-Hill, 5th Edition, November, 2007.

[11] R. C. Bernhardt, "The use of multiple-beam directional antennas in wireless messaging systems", IEEE Vehicular Technology Conference, 1995, pp. 858–861.

[12] B. Allen and M. Ghavami, Adaptive Array Systems: Fundamental and Applications, Chapter 4: Adaptive Arrays, John Wiley & Sons, Inc., Chichester, UK, 2005.

[13] J. C. Bregains, J. Fondevila, G. Franceschetti, and F. Ares, "Signal radiation and power losses of time-modulated arrays", IEEE Transactions on Antenna and Propagation, vol. 56, no.6, June 2008, pp. 1799-1804.

Chapter 7 Conclusions and Future Work

7.1 Conclusions

There has been an increasing demanding for developing a low cost system based on phased array technology over the past few decades. This dissertation advances the research of time modulation by using simple and low cost RF switches in the antenna array combined with external electronic circuits. Two most significant characteristics of the time modulated antenna array – pattern synthesis and real time electronic beam scanning were studied, as well as its potential applications in the wireless communication system. Numerical results presented in this thesis have shown that this research work is able to provide an alternative approach to a low cost antenna array system and would bring benefit to the commercial sectors.

Pattern synthesis in the time modulated linear array

Time modulation technique allows conventional array amplitude patterns to be synthesised in a time-average sense by switching the array elements for a period that corresponds to the relative amplitude weight of the array element. However, periodic time modulation generates harmonics or sideband at the multiples of switching frequency. In Chapter 3, two novel approaches have been proposed to reduce sideband levels and improve radiation efficiency at the fundamental frequency. The first methodology was based on concept of employing simple 3dB power dividers to decrease the static weights of the outer elements of a linear array. With this respect, it

increases the relative switch-on times of the outer array elements, which decreases the transients in the time-domain output from the array. This proposed technique has exhibited a better performance compared with the conventional time switching scheme, since the maximum sideband levels at the harmonic patterns have been reduced from -12.0dB to -18.0dB. More importantly, the sidebands radiation has been decreased from 25.5% to 13.1% and the directivity has increased from 9.1 to 10.3.

The other approach in this chapter investigated a way of dividing a continuous time sequence into multiple equal steps in order to redistribute sideband energy into higher harmonic frequencies. Based on this idea then it combined the new switching scheme with a directive element of the array with fixed bandwidth to filter out out-of-band harmonics. Numerical examples have illustrated that the maximum sideband levels of all the harmonics have been successfully reduced to -28.7dB. This technique proves to have a better performance compared with the conventional method. In addition, the proposed approach combined with the half power technique have shown that sideband levels can be further reduced to -31.7dB and minimised the sideband radiation from 24.2% to 15.6%.

Electronic beam scanning based on time modulated antenna array

Chapter 4 concentrates on another important characteristic of the time modulated antenna array, which is the capability to perform electronic beam scanning without the use of phase shifters. In the first part of this chapter, an example of 16 isotropic

elements with uniform amplitude weights was presented to show that multiple harmonics are generated to scan in angle with the increase of positive harmonic number at 7.2°, 14.5° and 38.7° as well as in the negative harmonic frequency. Later based on this analysis, a new time switching sequence was developed to realise harmonic beam steering with controlled low sidelobe levels. The first example was given to show that a -30dB Chebyshev sidelobe level has been achieved at both fundamental and the first positive harmonic frequency. The first positive harmonic pattern steers the main beam at the direction 7.2° as required. Another simulation results was demonstrated that a beampattern with a -40dB Taylor amplitude weights with a scanning angle of 15° at the second positive harmonic frequency can also be achieved by using simple time sequence without the use of phase shifter.

The second part of Chapter 4 investigated the feasibility of implementing null steering technique in the time modulated antenna array by using Linearly Constrained Minimum Variance (LCMV) algorithms. In the presence of interference, the LCMV algorithm can be used to preserve the main beam response to extract desired signal while minimising the contribution from the interferences. In an example of 16-element time modulated linear array, the first positive harmonic produces a beampattern that directs the maximum radiation towards the desired angle of 15.0° and forms a deep null in the direction of the interfering signal at a direction of -20.0°. Another scenario was examined to show the capability of the proposed approach to deal with one desired signal at $\theta_d = -25^{\circ}$ and three interferences coming from $\theta_{I1} =$

-10$^{°}$ at $\theta_{I2} = 10^{°}$ and $\theta_{I3} = 20^{°}$.

Application of time modulated antenna array in the communication system

For an N-element time modulated linear array, the conventional time sequence to realise harmonic beam scanning is inefficient in terms of time utilisation as each array element is only switched on for 1/N of the modulation period. Chapter 5 proposed a simple structure with two output channels based on the time modulated linear array and it exploits the time redundancy of the conventional systems.

The smart antenna application of time modulated antenna array in the wireless communication system was investigated in Chapter 6. Firstly, the switched beam system based on time modulated linear array was examined and an example of 16-elements linear array is used to produce multiple fixed beams pointing at angles in interval of 10$^{°}$. Three different cases - one desired signal at the direction of 10$^{°}$, one desired signal at the direction of 7$^{°}$ and one desired signal at the direction of 7$^{°}$ and interference from the direction of -6$^{°}$ were studied. It can be noticed that the bit error rate performance was getting worse and worse as the intended user moves out the centre of the selected main beam. Another drawback by using the switched beam system is that it would not able to perform real time tracking operation.

In the case of adaptive array system, adaptive beamforming for conventional one channel time modulated linear array was firstly introduced. The results have shown

that bit error rate agrees well with the theoretical result. However, the traditional system only utilises 1/N of the modulation period. Based on the model developed in Chapter 5, a new topology was proposed to apply adaptive beamforming in two independent channels. A problem has occurred when both two channels require connections to the same element at the same time. With this respect, shifting the time sequence by an arbitrary constant was able to resolve the overlapping region problem. Numerical examples have shown that the bit error rate at the two independent outputs agrees well to the theoretical curve, so this approach ideally doubles the capacity over a single channel system.

7.2 Future Work

On the basis of the research works in this thesis, there are still many aspects can be done in the future:

Firstly but an important part is to design a real prototype of a time modulated linear array. A good attempt will be starting of designing an 8 or 16 elements linear array of dipole antennas with a simple feed network, and each array element could be switched on and off by the off-the-shelf RF switches that are controlled by an external FPGA board.

Secondly, Chapter 4 has proposed a new switching scheme by dividing a continuous time sequence into multiple equal steps. This technique redistributes sideband energy

into higher harmonic frequency and is not yet well optimised. New time schemes could possibility be investigated by dividing the entire time sequence into unequal steps and this approach may further reduce the sideband levels.

Thirdly we have already known that harmonic beam scanning based on the time modulated antenna array can be achieved by applying a progressive time delay into each element across the array without the use of phase shifter, but the tradeoff is the gain of the antenna array would be low as only one element is switched on at one time. Future researches could be done to increase the gain of the harmonic pattern.

Finally, a two-channel adaptive beamforming based on time modulated linear array technique was studied in Chapter 6, but in this example we only consider the signal received are uncorrelated with each other under a single path propagation scenario. However, in a more practical environment where multiple propagation and coherent signals may be presented, these factors could severely degrade the BER performance of adaptive beamforming. Moreover, the direction of arrival angle may not always be known at any time, so a more generalised and robust approach needs to be developed in order to combat the multipath fading environment and to estimate the direction of arrival of the desired signal.

Appendix – MATLAB code

1）Conventional array factor

```
lamada=c/f;          % According to the wavelength formula, wavelength =
speed of light/ frequency
k = 2*pi/lamada;     % We know that the constant k = 2*pi/namada
theta=-pi:pi/1800:pi;   % Sample the angle theta in the interval of
pi/1800 from the range -pi to pi
theta_degree= theta*180/pi;   % Convert radians into degree
d=d*lamada;        % Vary the value of d from namada/2, namada, 2*namada
etc
for n = 1:length(theta)  % The start of for loop, setting up n begins with
1 to the value of 1801
    y(n) =sum(exp(([0:N-1]*j*(k*d*cos(theta(n))+P))));
end
rho = abs(y);                                              %
gn1 = 20*log10(rho/min(rho));
```

2）Binomial Array coefficient

```
a =sym2poly((1+x)^(m-1));
for n = 1:length(theta)   ;
   if   rem(m,2) ==0;
       A = a((m/2+1):m);
       y(n)=
sum(A.*exp(([1:2:(m-1)]*j/2*(k*d*sin(theta(n))+P))))+sum(A.*exp(([1:2
:(m-1)]*(-j)/2*(k*d*sin(theta(n))+P)))) ;
   else A = a((m+1)/2:m);
       y(n) =2*A(1)/2 +
sum(a(((m+1)/2+1):m).*(exp([1:(m-1)/2]*j*(k*d*sin(theta(n))+P))))+sum
(a(((m+1)/2+1):m).*exp(([1:(m-1)/2]*(-j)*(k*d*sin(theta(n))+P))));
   end
end
```

3）Chebyshev Array coefficient

```
if rem(m,2)==0;
   M = m/2;
   for n = 1:M;
      a = 0;
      for q = n:M
         a(q)
=(-1)^(M-q)*zo^(2*q-1)*prod(1:(q+M-2))*(2*M-1)/(prod(1:(q-n))*prod(1:
(q+n-1))*prod(1:(M-q)));
```

```
            A(n) = sum(a);
        end
    end
else  M = (m+1)/2-1;
    for n = 1:(M+1);
         a= 0;
         for q = n:(M+1);
             if   n == 1;
                  e = 2;
             else e = 1;
             end
             a(q)
=(-1)^(M-q+1)*zo^(2*(q-1))*prod(1:(q+M-2))*(2*M)/(e*prod(1:(q-n))*pro
d(1:(q+n-2))*prod(1:(M-q+1)));
             A(n) =sum (a);
         end
    end
end
A1 = A/min(A);


4）Numerical way to find maximum sidelobe level
a=[];
g=[];
i = 1;
for g = 2:length(theta)-1
%    a=[];g=[];
   if ph(g) > ph(g+1) & ph(g) > ph(g-1)
      a(i) = ph(g);
%        h(i)= g;
      i = i+1;
   end
end
Z = 20*log10(a);
Z1 = find(Z<0);
Z2 = Z(Z1);
directr_reading_maximum_sidelobe_level(m+1) = max(Z2);
```

5）Fourier coefficient
```
An=(j/(m*2*pi)) * ((exp(-j*m*2*pi*tend)-exp(-j*m*2*pi*tstr)));
```

6）TMLA directivity calculation
```
a0=1; a1=1; a2=0;

for s=1:N
```

```
   x2(s)=A(s)*wt(s);
end


x1=abs(sum(x2))^2;

%  Calculation of I1
for s=1:N
   for m=1:1000
       x3(m)=(sin(pi*m*wt(s))/(pi*m*wt(s)))^2;
   end
   x4=sum(x3);
   x_3(s)=((A(s)*wt(s))^2)*(1+2*x4);
end
x5=a0*sum(x_3);


7）Power loss calculation
for i=1:N
for q=1:1000
x4(q,i)=(A(i)^2)*abs(An1(q,i))^2;
end
end
%
for k=1:1000
x5(k)=sum(x4(k,:));
end
%
power_loss=(2*sum(x5(2:end)))/ (2*sum(x5(2:end))+x5(1))


8）LCMV
wt=ones(1,N);
for u = 1:o
   for m = 1:N
       A(m,u) = wt(m)*exp(j*pi*sin(theta1(u)/180*pi)*(m-1));
   end
end

C=A;
w=inv(Rxx)*C*inv(C'inv*(Rxx)*C)*F;


9）LMS
error = d - w' * x;
w = w + 2 * Mu * x * conj(error);
```